ISBN: 978-93-48620-73-6

Innovations and Research in Science and Technology

Volume I

Editors:
Dr. P. Gajalakshmi
Dr. Poonam Panaskar
Dr. R. Elavarasi
Mrs. N. Priya

BHUMI PUBLISHING, INDIA
FIRST EDITION: NOVEMBER 2025

Innovations and Research in Science and Technology Volume I

(ISBN: 978-93-48620-73-6)

DOI: https://doi.org/10.5281/zenodo.17832321

Editors

Dr. P. Gajalakshmi

Department of Electrical and Electronics Engineering, University College of Engineering, Tindivanam, Tamil Nadu

Dr. Poonam Panaskar

Department of Botany, Dapoli Urban Bank Senior Science College, Dapoli, Maharashtra

Dr. R. Elavarasi

Department of Electrical and Electronics Engineering, AMET Deemed to be University, Chennai, Tamil Nadu

Mrs. N. Priya

Department of Electrical and Electronics Engineering, Easwari Engineering College, Chennai, Tamil Nadu

Bhumi Publishing

November 2025

Copyright © Editors

Title: Innovations and Research in Science and Technology Volume I

Editors: Dr. P. Gajalakshmi, Dr. Poonam Panaskar, Dr. R. Elavarasi, Mrs. N. Priya

First Edition: November 2025

ISBN: 978-93-48620-73-6

DOI: https://doi.org/10.5281/zenodo.17832321

All rights reserved. No part of this publication may be reproduced or transmitted, in any form or by any means, without permission. Any person who does any unauthorized act in relation to this publication may be liable to criminal prosecution and civil claims for damages.

Published by Bhumi Publishing,

a publishing unit of Bhumi Gramin Vikas Sanstha

Bhumi Publishing

Nigave Khalasa, Tal – Karveer, Dist – Kolhapur, Maharashtra, INDIA 416 207

E-mail: bhumipublishing@gmail.com

Disclaimer: The views expressed in the book are of the authors and not necessarily of the publisher and editors. Authors themselves are responsible for any kind of plagiarism found in their chapters and any related issues found with the book.

PREFACE

The rapid transformations in the global scientific landscape are driven by relentless innovation, interdisciplinary collaboration, and a shared commitment to advancing human knowledge. *Innovations and Research in Science and Technology* is a collective effort to present contemporary developments, emerging trends, and progressive ideas from diverse scientific fields. This volume brings together researchers, academicians, and practitioners who contribute valuable insights and novel perspectives that have the potential to influence future scientific inquiry and technological advancement.

Science and technology today are no longer confined to isolated domains; major breakthroughs emerge at the interface of disciplines. From materials science, biotechnology, environmental studies, and computational modeling to applied physics, chemistry, and engineering, this book reflects a broad spectrum of ongoing research. Each chapter aims to bridge theoretical concepts with practical applications, highlighting how innovative thinking and experimental approaches are shaping solutions for complex real-world challenges.

The contributors have undertaken significant efforts to present current research trends, well-supported analyses, and meaningful interpretations. This compilation will serve as a useful reference not only for students and researchers but also for industry professionals and policymakers seeking to understand the expanding horizons of science and technology. We hope that the ideas presented here will inspire further exploration, foster academic dialogue, and encourage collaborative endeavors across institutional and geographical boundaries.

We express our sincere appreciation to all the authors for their dedication and timely contributions. We also extend our thanks to our editorial team, reviewers, and all those who supported the publication of this volume. Their collective efforts have made this book possible.

It is our sincere belief that *Innovations and Research in Science and Technology* will stimulate curiosity, promote research culture, and serve as a platform for intellectual growth in the scientific community.

- Editors

TABLE OF CONTENT

BIOENERGY CROPS: AN OPTION FOR THE FUTURE ENERGY

S. Mobeena

Regional Agricultural Research Station (RARS), Tirupati – 517 502

Corresponding author E-mail: mobeena.shaik2693@gmail.com

Introduction:

Energy is a fundamental prerequisite for the progress of practically every part of a society in the globe, and it is also necessary for the existence of ecosystems, life itself, and human civilizations. Electricity, transportation, cooking, and heating are the primary areas of energy-consumption. The main sources of energy are divided into two types

1. **Non-renewable energy**: Non-renewable energy is finite resources that will ultimately run out over the time frame. It is one that does not regenerate itself quickly enough to allow for sustained economic exploitation across timescales that are relevant to people. It is energy derived from fossil fuels like uranium, coal, crude oil, and natural gas. Non-renewable energy requires human intervention to make it appropriate for use, as contrast to renewable energy. Carbon is the major component of fossil fuels. Fossil fuels are thought to have developed more than 300 million years ago, when the earth's surface looked very different.
2. **Renewable energy:** Renewable energy comes from naturally regenerating sources that are virtually infinite in terms of duration but have a finite amount of energy accessible per unit of time. Biomass, hydropower, geothermal, wind, and solar energy are the main categories of renewable energy.

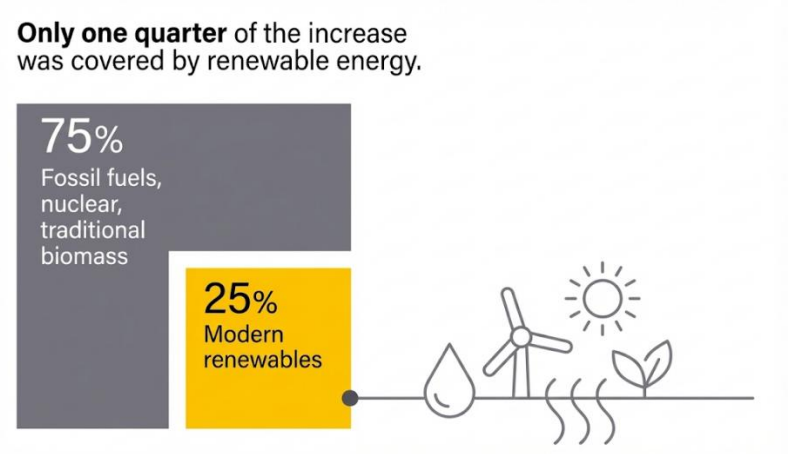

Figure 1: Growth in modern renewables as share of total final energy consumption (Renewables 2021, Global status report).

The world's population is rapidly expanding which urges a steep surge for energy demands that has to be fulfilled by the non-renewable and renewable energy sources. In the

current situation of the world, the most part of the energy *i.e.* 75% is met through non-renewables energy sources and only 25 % is met through renewable sources (Renewables 2021, Global status report). Despite phenomenal growth in certain renewable energy industries, the percentage of renewable energy has only slightly grown each year. This gradual progress highlights the crucial and complementary roles that renewable energy, energy efficiency, and energy conservation play in lowering the share of fossil fuels to supplying the world's energy demands and lowering emissions.

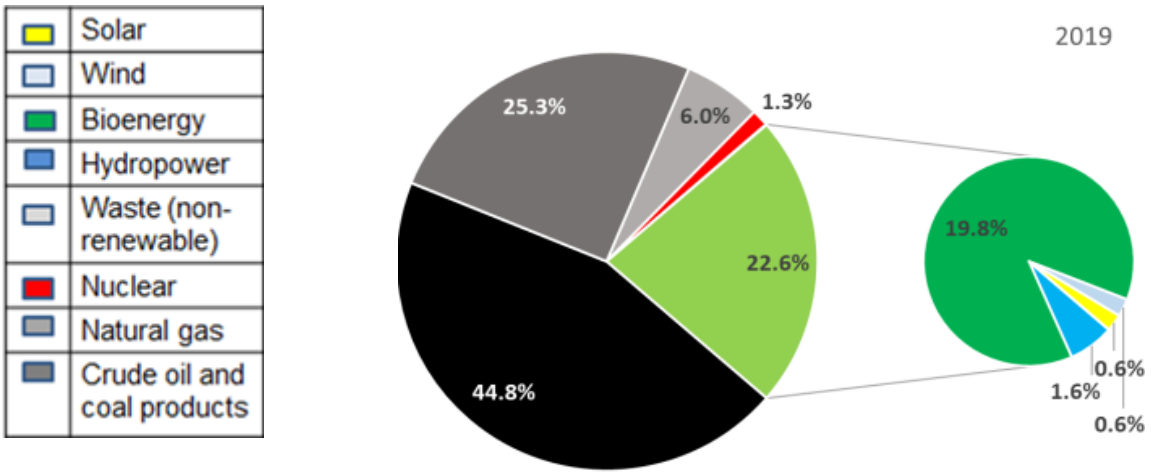

Figure 2: Total energy supply and the contribution of different energy sources in India (IEA, 2021)

In the past few decades, the world has seen an uncontrolled use of fossil fuels. It is undeniably true that fossil fuels hold the credit of shaping our world, but at the cost of environmental and related hazards. The primary sources of fossil fuels in India today are coal, petroleum, and natural gas, followed by renewable energy sources including bioenergy, wind, solar, and hydropower. In order to maintain the environment and lessen our long-term reliance on fossil fuels, it is necessary to diversify the present energy supply with more renewable energy sources as non-renewable energy sources diminish over time. One of the finest options is usage of renewable energy. Among the renewable sources, bioenergy has emerged as one of the most promising renewable energy sources globally. Renewable energy sources such as energy from biomass (bioenergy) is a key to address concerns for energy security and climate change.

Bioenergy is defined as “renewable energy that is manufactured from biomass (biological commodity)”. It is equal to the total of municipal trash, industrial waste, primary solid biofuels, biogas, bioethanol, and other liquid biofuels, as well as charcoal and other fuels. The biodegradable portion of agricultural products, trash, and leftovers are referred to as biomass.

Any plant material utilized to create energy is referred to as a bioenergy crop. The raw materials used to create another product are known as feedstock. Biomass feedstocks can be obtained from a variety of sources, including waste fuels, energy or agricultural products, etc. Bio-ethanol, biodiesel, and biogas are the main end products of bioenergy crops.

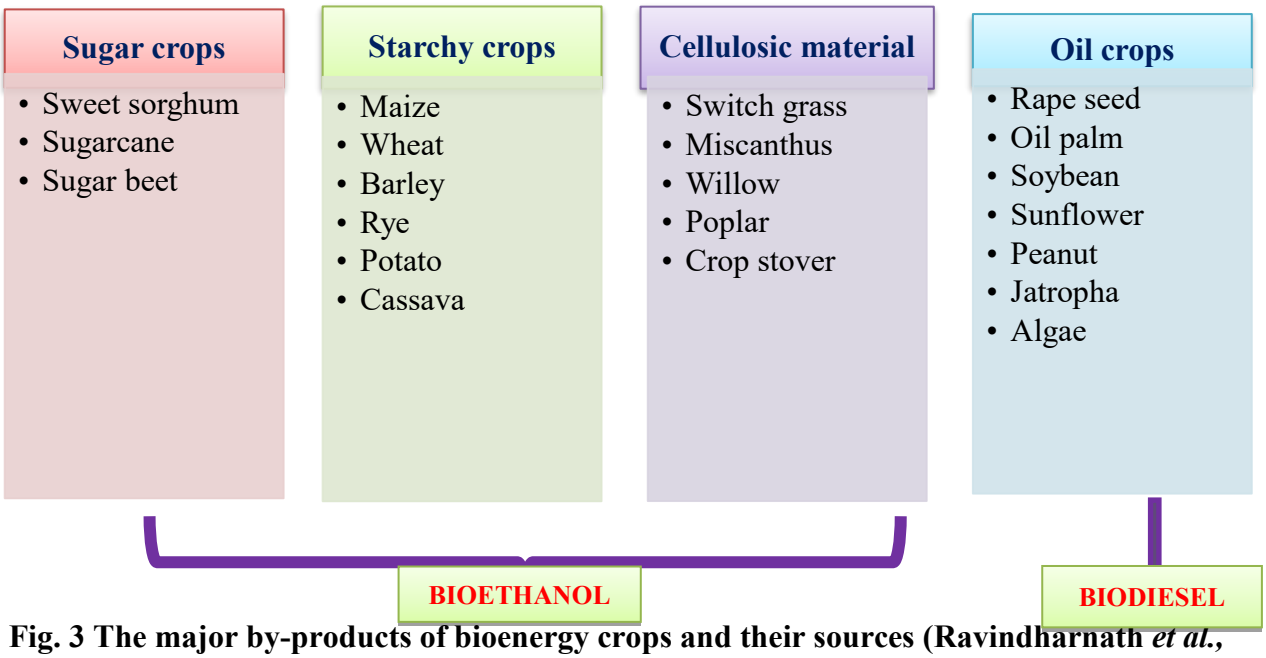

Fig. 3 The major by-products of bioenergy crops and their sources (Ravindharnath *et al.*, 2011)

Taking modern bioenergy into account, the two main byproducts of bioenergy are biodiesel and bioethanol. These two products can be used as a replacement for the traditional transportation fuels, hence are referred to as biofuels.

Bioethanol: It can be produced from variety of sources including sugar crops (sweet sorghum, sugarcane, sugarbeet etc), starchy crops (maize, wheat, barley, rye, potato, cassava etc), and cellulosic material (switch grass, miscanthus, willow, poplar, crop stover etc). Due to its potential to replace conventional fossil fuels, ethanol has received a lot of attention recently. In addition to these applications, ethanol is a critical component of many chemical processes, serving as a raw material in the process. Moreover, ethanol can help in reducing environmental pollution and is a renewable fuel, thus is advantageous over fossil fuels in various aspects. It can be blended with gasoline to produce gasohol that can serve as an alternative to petroleum-based fuels. Furthermore, ethanol can aid in reducing greenhouse gas emissions, particularly CO_2 emissions.

Biodiesel: It can be produced using oil crops such rapeseed, oil palm, soybeans, sunflower, peanuts, jatropha, and algae. In recent years, biodiesel has also drawn increased attention due to the depletion of fossil fuels and the need to discover alternative fuel sources in order to protect

the environment and guarantee energy security. As a non-toxic, renewable, and biodegradable fuel for diesel engines, biodiesel is one of the most environmentally friendly options available.

Key factors for driving interests in bioenergy

Bioenergy has received a great interest during the recent times because of the following:

- **Rising world fuel prices:** The most part of the world is dependent on the fossil fuels, when the supply of the product decreases and demand increases, obviously the price of the product will increase.
- **Growing demand for energy:** Due to rapid growth of population, industrialization and urbanization and luxurious nature of people there is an increase in demand for the energy.
- **Concerns about global warming**: Now-a-days the buzz word is climate change. One of the main reasons of the climate change is rapid usage of fossil fuels. The use of traditional fuels is associated with an environmental surge in the intensity of harmful gases like carbon dioxide, greenhouse gases and nitrogen oxide. For example, coal emits greenhouse gases like carbon dioxide, particulate soot and sulphur-containing compounds, leading to soil acidification.

With growing energy prices, demand, environmental pollution, and uncertainty about fossil fuel reserves, it is critical to consider more affordable, safe, and renewable energy sources, such as bioenergy, which is crucial for environmental sustainability.

Characteristics of bioenergy crops

As potential bioenergy crops, researchers are looking at plant species with quick growth, tolerance to biotic and abiotic stresses, and little requirement for biological, chemical, or physical pretreatments. They currently possess improved phenotypic, architectural, biochemical, and physiological traits that are all beneficial for the production of biofuels. These are a few characteristics of bio-energy crops.

Agronomic and metabolic traits

Bioenergy crops have good adaptation to marginal lands, use little energy to develop, and have higher biomass levels. These plants help to slow down global warming and lessen the impact of climate change. According to agronomic characters, bioenergy crop should exhibit properties such as long canopy duration, perennial growth, sterility, lower dry matter to reproductive structures, and lower moisture content at harvest. A C_4 perennial grass, *Miscanthus* spp., holds most such agronomic traits. The metabolic architecture of a crop grown specifically for energy reduces competition from other plants and weeds. The alteration in plant metabolism

also lessens radiation absorption, improves water use effectiveness, and speeds up field drying. Such plants are water-resistant, straight, and thick with upright stem branching.

Physiological and eco-physiological traits

In a variety of biochemical forms, bioenergy plants store solar and thermochemical energy. For such plants to maximize radiation absorption, water efficiency, nutrient utilization, and environmental sustainability, numerous physiological and eco-physiological features are required. These physiological characteristics include effective light capturing, efficient C_4 or CAM photosynthetic pathway, minimal nutritional need, carbon sequestration, limited competition among plan groups, long canopy duration, and efficient nutrient cycling. All of these physiological characteristics help plants produce more above-ground biomass during the growing season. Carbon and nitrogen ratio is the deciding factor in bioenergy production from plant biomass. Bioenergy crops with higher C:N ratios produce more bioenergy in the form of methane (Long *et al.,* 2006).

Biochemical composition

The biochemical makeup of carbohydrates, proteins, lipids, and organic acids varies among plants. The specificity of their biochemical makeup determines how they are used in the bioenergy industry. A key quality in bioenergy crops is the ability to produce carbohydrates. In order to produce biofuel, the carbohydrates are used in the fermentation process. Since the breakdown of cellulosic crops releases a significant number of glucose units, they have a greater potential for producing bioenergy. An increase in the bioenergy crop's structure and biochemical composition raises its caloric value, increasing the amount of energy produced per tonne of biomass.

Classification of bioenergy crops

The concept of bioenergy crops is drawing attention in the scientific community for its renewability and eco-friendly nature. Bioenergy crops are categorized on the basis of specific characters like oil yields, oil quality in to 5 types (Meghwanshi and Vashishtha, 2014). They are

1. First generation bioenergy crops
2. Second generation bioenergy crops
3. Third generation bioenergy crops
4. Dedicated bioenergy crops
5. Halophytes

First generation bioenergy crops:

The bio-energy is mainly produced from food crops which includes starch and sugar-based biomass. Wheat, corn, sugarcane, sugar beet, barley, potatoes, and other similar crops are

the most often utilized feedstock for the production of bioenergy. First-generation bioenergy crops served as the foundation for the production of biofuel. Large levels of saccharose are present in sugar crops like sugarcane and sugar beet, which can be extracted and fermented to produce bioethanol. First generation bioenergy crops are used to make bioethanol through the fermentation of starch and sugar-based biomass.

As the global and country population is increasing tremendously, to feed that amount of population we need to increase the productivity of the crops. If the food produce is utilized for the production of bioenergy, then the demand of food crops will increase which substantially increase the food prices. The utilization of food crops for biofuel production raises the debate known as food versus fuel. This raises issues such as food security, change in land use, reduced supply of food crops, and increasing prices of food. The problem was particularly large in the developing countries that are major net food importers. The issue was particularly severe in developing nations that import a significant amount of food on a net basis. Additionally, it will be extremely challenging to meet global need for both food and biofuels due to rising food consumption and demand. Due to their higher production costs, first generation bioenergy crops, however, have a limited capacity to replace petroleum-based products.

Second generation bioenergy crops:

The bioenergy is derived from ligno-cellulosic biomass such as crop residues (paddy straw, wheat straw, corn straw etc), perennial grasses (switch grass, miscanthus, berseem etc) and non-edible oils (neem oil, mahua oil, jatropa oil, karanj oil etc). The term "ligno-cellulosic" describes plant biomass made up of cellulose, hemicellulose, and lignin polymers. When biomass is hydrolyzed, the resultant sugars can be used to make ethanol and possibly other biofuels. These can be produced on marginal crop land where it is not profitable to grow crops. When compared to first generation bioenergy crops, the production of biofuel from cellulosic biomass is more energy efficient.

The bio-fuel that is generated from second generation bio-energy is non-oxygenated and pure hydrocarbon fuel. The main challenge associated with the cellulosic biofuels is the efficiency of the cellulose conversion. While enzymes can convert sugar to ethanol with 90% efficiency, they can only convert cellulose with a 40% efficiency since the cellulose must first be broken down. In order to create the same amount of biofuel, more feedstock is therefore required. The cost of producing second-generation biofuel is significantly higher than that of first-generation biofuel (Sims and Taylor, 2008). So, the second-generation biofuel has not been achieved commercial production yet.

Major non-edible tree borne oilseeds in India

1. Mahua (*Madhuca indica)*: It is commonly known as 'Indian butter tree'. In India's tribal regions, it is widely distributed. This plant's seeds contain mahua oil, which has 30%-40% oil content. It is primarily present in the Indian states of Orissa, Chhattisgarh, Jharkhand, Bihar, Madhya Pradesh, and Tamil Nadu.

2. Jatropha (*Jatropha curcas* L.) In marginal or poor soils, it can be grown successfully. It has been studied as a semi-evergreen, drought-resistant shrub that produces seeds with a 37% oil content. Jatropha oil, which is made from jatropha seeds, may be used as fuel right away and doesn't need to be refined. Jatropha oil has been successfully tested as a fuel for basic diesel engines, and it produces a clear, smokeless flame

3. Karanj (*Millettia pinnata* L.): It is a non-edible oil plant that originated in India. In Asia's tropical regions, it is extensively dispersed. It can be found in some parts of Eastern Asia as well as the Western Ghats of India, northern Australia, and Fiji. This tree produces pods that, over the course of roughly ten months, turn from green to tan. The pods are filled with kidney-shaped brown and red kernels. These kernels can yield an oil content of about 27.5% when they are air-dried.

4. Neem (*Melia azadirachta* L.).: It is indigenous to India and Burma and thrives in tropical and semi-tropical climates. This tree grows quickly and can reach heights of 15 to 40 meters. Neem tree seed kernels have a healthy amount of fat, ranging from 33% to 45%. Other uses for neem oil include soaps, medications, and insecticides.

Table 1: Comparison on properties of biodiesel (Parthasarathy *et al.,* 2013)

Properties	**Pongamia**	**Tamanu**	**Mahua**	**Diesel**
Density @15.56ºC (Kg/m^3)	960	880	920	850
Viscosity @ 40ºC (mm^{2}s)	8.9	5.3	6.2	2.6
Flash Point (ºC)	205	108	164	65
Calorific Value (MJ/Kg)	36.8	41.5	38.96	44
Pour point (ºC)	13.2	11.3	14	12
Cetane Number	45.5	50	47	45

These parameters influence the efficiency of atomization of the fuel, flow, distribution and lubrication of the fuel. All the values of above mentioned parameters are very close to

traditional diesel which concludes that these oils can be used in diesel based engines in the form of pure or blended oils.

Third generation bioenergy crops

Utilizing third generation bioenergy crops can help to mitigate the main drawbacks of first and second generation bioenergy crops. Microalgae are an important source of the bioenergy. Microalgae biodiesel is often known as "green diesel" because to its exceptional environmental qualities (Azad *et al.,* 2014). Microalgae are the oldest living microorganism survived over 2.5 billion years. These are unicellular and reproduce incredibly quickly by using sugar, sunlight, and CO_2 from the environment to make enormous quantities of lipids, proteins, and carbohydrates in a short amount of time.

The microalgae have some remarkable advantages to be used as a biodiesel feedstock such as these are cultured to act as a low-cost raw material (feedstock), contain high energy per unit mass, renewable, environmentally friendly and can contribute to reduce CO_2 levels in the atmosphere by consuming for its own reproduction. By consuming extremely basic nourishment, it may thrive in a range of environments including fresh water, marine water, and treated industrial waste water. In this, the oil is extracted from the complete cell mass. Microalgae have an oil content that ranges from 20 to 50 percent of their dry biomass weight. Microalgal oil production is higher than that of conventional crops. While corn only produces 60 gal/acre (560 l/ha), algae may produce 10,000 gal/acre (94,000 l/ha) of biofuel annually. On an area basis, microalgae produce 15-300 times more oil for the generation of biodiesel than traditional crops.

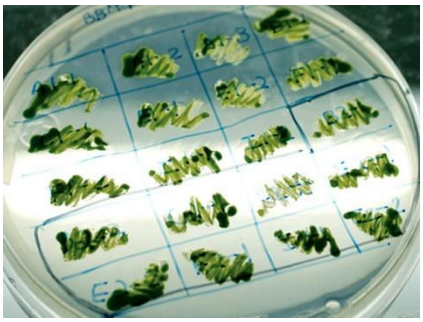

Microalgae can be used to make biodiesel, bio-methane, bio-hydrogen, and bioethanol as by-products (Ahmad *et al.,* 2011). The micro-algae have high lipids accumulation which is about 70%. Algal-derived biodiesel is non-toxic and has a high biodegradability. Additionally, compared to terrestrial plants, it has a greater photon conversion efficiency that ranges from 3-8%, as opposed to 0.5% (Williams *et al.,* 2007). By using microalgae as an alternative fuel feedstock, the conflict between fuel and food can be avoided.

Historic evolution of microalgae production systems

Over the past 50 years, there has been much study on the use of microalgae, and Nihon chlorella launched the first large-scale microalgae culture in the early 1960s with the cultivation of chlorella. The interest in using microalgae for the manufacture of biofuels developed during the first oil crisis in the 1970s.

From the year 1978-1996, the U.S. National Renewable Energy Laboratory through the Aquatic Species Program, started a specific research and development program dedicated to alternative renewable fuels, including biodiesel from microalgae. Studying the biochemistry and physiology of lipid synthesis in microalgae was one of this program's key goals (Teresa *et al.,* 2010). The utilization of microalgae for the low-cost synthesis of biodiesel was shown to be technically viable, although high productivity still requires extensive long-term R&D.

A renewed interest in the production of biodiesel has been sparked by the recent price volatility of crude oil and the anticipated future price increase, coupled with the need to reduce greenhouse gas emissions and pollutant emissions. Today, a large number of consortiums, private organisations, and public organisations are investing in R&D on microalgae with the goal of using the most efficient and affordable technology to produce significant amounts of oil. Microalgae are seen as an alternative feedstock for the production of biodiesel.

Biodiesel production from micro-algae

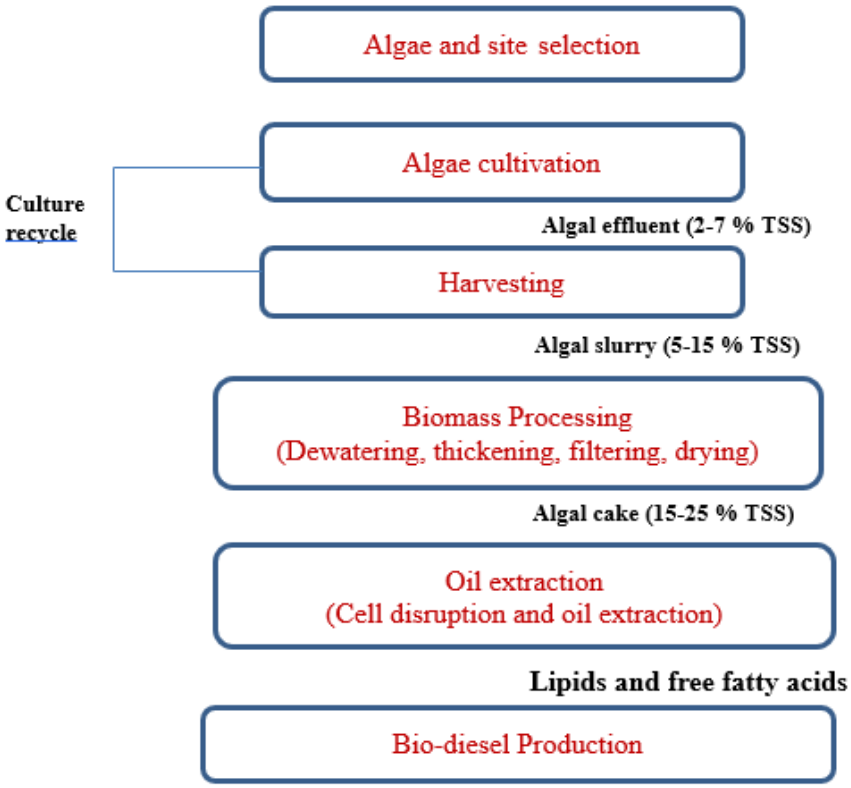

Figure 4: Process of micro-algae based biodiesel production (Teresa *et al.*, 2010)

Algae and site selection

It is regarded as the crucial step that ultimately decides the process's economic viability. Topography, geography, water availability, and climatic factors like temperature, insulation, evaporation, and precipitation should all be taken into consideration while choosing a site. In addition to choosing the best location for microalgae development, it is critical to carefully

consider the choice of the best species and strains, growing conditions, and nutrients accessible for their growth.

Microalgae cultivation

Microalgae have developed adaptations that allow them to gather materials from their surroundings, store them, or use them more effectively. These typically require a sufficient amount of a carbon source and light to perform photosynthesis in order to grow biomass. Microalgae may grow rapidly in the right climatic conditions and with enough nutrients. At present, the cultivation methods of the microalgae production are commonly using in these two ways:

1. The open pond system
2. Close photo bioreactors system

Open pond system:

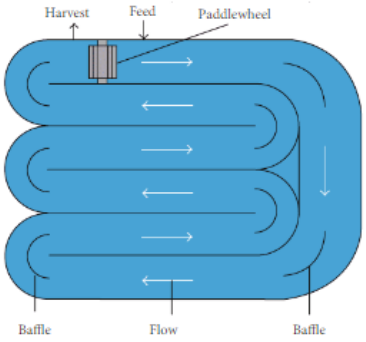

It is the earliest and most straight forward method of growing microalgae. In this method, the microalgae are grown in an open setting, such as ponds, lakes, rivers, oceans, and waste water. It is the most established, simple to maintain, affordable, and cutting-edge method of cultivation. The key benefit of this system is the lack of additional equipment needed to maintain the temperature and light source.

The open pond system contains a paddle wheel to mix and cycle the algae cell and is shaped like a raceway. It is designed to operate in a cycle mode so that fresh feeds can be supplied to the pond from the direction of the paddle wheel and harvested throughout the circulation process. The majority of open pond systems consist of small ponds. The raceway is around 15 cm to 30 cm deep to allow enough sunshine to reach the pond's bottom. In this, the CO_2 can be absorbed from the environment, but the nutrients must be artificially supplied. The open pond system is used to develop species like *Dunaliella, Chlorella, and Spirulina.* The only dis-advantage associated with this system is it will get easily contaminated by other algal species.

Close photo bioreactors system:

Algae can be grown under regulated conditions in this system. The environment can be changed to suit a species needs. You can regulate every variable, including the temperature, water supply, and carbon dioxide level. There are various varieties of close photo bioreactor systems, such as fermentation tank photobioreactors, tubular photobioreactors, and plate photobioreactors (Faried *et al.,* 2017). The tubular photobioreactor system is the one that is best

suited for growing microalgae. Typically, clear plastic or glass tubing are used to construct photo bioreactors. With the use of a pump or an airlift system, the microalgae can be pumped into the tubes. In comparison to open pond systems, the biomass productivity with near photo-bioreactors is 13 times higher. The dis-advantage by using this system includes fouling smell, some degree of wall growth.

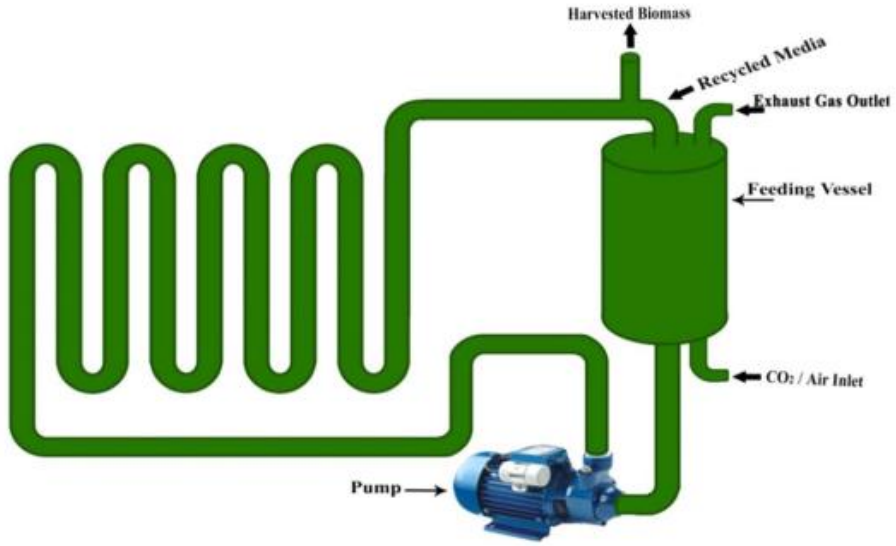

Figure 5: Tubular photo-bioreactor with parallel run vertical tubes (Faried *et al.,* 2017)

These bioreactors are constructed from glass or plastic tubing, respectively. Tubes could be near-horizontal, horizontal, or vertical. Algal culture is added to the feeding vessel in this process, and a pump is used to force the culture into the tubes. Aeration and mixing are typically carried out *via* an airlift system or air pump. The easy passage of light necessary for photosynthesis is made possible by the use of transparent materials like plastic or glass. The CO_2 must be supplied as gas CO_2 through the inlet because it cannot be taken as in an open system. Additionally, it makes sure that the oxygen created during photosynthesis can be removed quickly. Finally, the top of the bioreactor can be used to collect the biomass of the algal culture.

Factors influencing the algal growth

A growth medium with a supply of solar energy for photosynthesis, suitable nutrients, and CO_2 or air flow are essential elements for algae growth. Other factors that affect algae include processing factors like mixing and light intensity as well as environmental factors like temperature, pH, salinity, and oxygen content. All of these growth variables must be specified for successful microalgae production for a particular application because the culture conditions vary depending on the species.

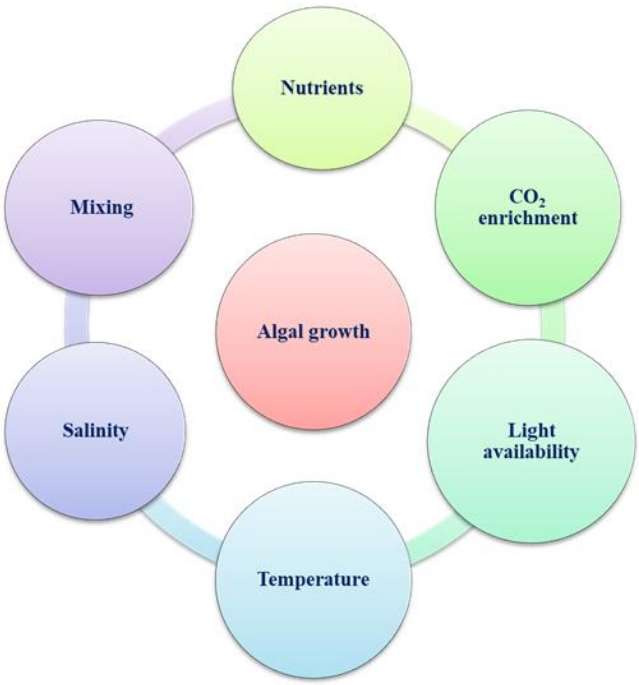

Figure 6: Factors affecting the growth of algal culture (Chowdury *et al.*, 2020)

Light availability: The presence of light is crucial for the development and productivity of photosynthesis in microorganisms. Light must be harnessed to its full potential because it is the primary energy source for photosynthetic bacteria. However, too much light, especially when combined with an unfavourable temperature or high oxygen content, might harm the photosynthetic apparatus. Microalgae experience an increase in photosynthesis as light intensity rises, reaching a maximum rate at the saturation point. Photo inhibition is a phenomenon that occurs when there is too much light over the saturation point.

Temperature: One of the most important environmental elements that affect algal growth rate, cell size, metabolic makeup, and nutrient requirements is temperature. Although some mesophilic species can withstand temperatures as high as 40 °C, the ideal temperature range for microalgae growth is 20 °C to 35 °C. The strain's yield decreases below the ideal temperature, although over heating of the cultures has been found to be dangerous since it can harm the cells.

Nutrients: Inorganic components including phosphorus (P), nitrogen (N), and iron (Fe), among others, must be present in an ideal microalga growing medium; these components may differ depending on the farmed species. The approximate chemical formula CO0.48H1.83N0.11P0.01 can be used to calculate the minimal nutritional requirements needed for microalgal development. So, the three macronutrients of carbon (C), nitrogen (N), and phosphorus (P) are crucial for autotrophic development. These nutrients must be present in the culture medium for the cultures to function at their best, based on the biomass composition.

Mixing: It is yet another crucial growth factor since it uniformizes the distribution of cells, metabolites, and gases. Additionally, some turbulence is preferred, particularly in large-scale production, to encourage the quick movement of microalgae cells from the dark to the light zone of the reactor.

Salinity: During the cultivation of microalgae, it is another aspect that needs consideration. Both in open and closed settings, salinity can have an impact on the development and cellular makeup of microalgae. Each alga has a distinct range of optimal salinity that might rise in hot weather because of increased evaporation. Adding salt or fresh water as needed is the simplest approach to control saltiness.

Carbon dioxide: The production of microalgae is influenced by carbon dioxide (CO_2), another significant component. In closed systems, it can be given as gas CO_2, but only the portion that is effectively transported to the liquid phase is actually available for the cells. This is different from open pond cultivation, where it can be directly obtained from sunlight. Microalgae require 1.8-2.0 kg of CO_2 to create 1 kilo gram of biomass (Chowdury *et al.,* 2020).

Harvesting methods

From the cultivation system, slurry of water and algae are produced. The oil from the algae must be removed from this slurry by dewatering it. Harvesting of algal biomass and further drying is important prior to mechanical and solvent extraction for the recovery of oil. The cost of biomass recovery from the broth can make up to 20-30% of the total cost of producing the biomass. Microalgae harvesting is a two-stage process, involving

1. **Bulk harvesting**: It seeks to separate the biomass from the bulk suspension. To achieve a 2-7% total solid matter, the concentration factors for this technique are typically 100-800 times. This will depend on the initial biomass content and any methods used, such as flocculation, flotation, or gravity sedimentation.
2. **Thickening:** It often requires more energy than bulk harvesting because the main goal is to concentrate the slurry by methods including centrifugation, filtration, and ultrasonic aggregation.

Some of the important methods of harvesting of algal culture:

Flocculation: In order to facilitate the quick and efficient removal of the biomass, it causes the micro-algal cells to aggregate and produce large floccules. In order to facilitate the aggregation of microalgae cells, salts like ferric chloride, aluminium sulphate, and ferric sulphate are typically employed to neutralize charges on the surface of the cells.

Floatation: This technique involves dispersing tiny air bubbles into the media, which causes the tiny algae cells to float on their own. Unlike flocculation, this process doesn't require for the

addition of any chemicals. Due to their high lipid content, certain microalgae float at the water's surface naturally.

Sedimentation: This is the most popular technique for collecting algal cells made from waste water from waste treatment facilities. However, only large microalgae greater than 70 µm are acceptable for this approach.

Centrifugation: For harvesting biomass containing high-value metabolites and products, this is the preferable technique. Although the procedure is quick, a lot of electrical energy is used. The biomass recovery depends on the factors *viz.* density of the cells and residence time of slurry in the centrifuge. On the other hand, centrifugation is more cost-effective than micro and ultra-filtration for extracting biomass from larger scale enterprises.

Filtration: It is an appropriate technique for harvesting somewhat large (>70 m) microalgae, like *Spirulina* and *Coelastrum*. Small algae like *Chlorella* and *Dunaliella* cannot be harvested using this method.

Microfiltration and ultrafiltration procedures can be used to recover algal cells that are smaller than 30 µm.

Process of energy conversion

The collected biomass must be transformed into bioenergy products. There are specific technologies for such, including the following

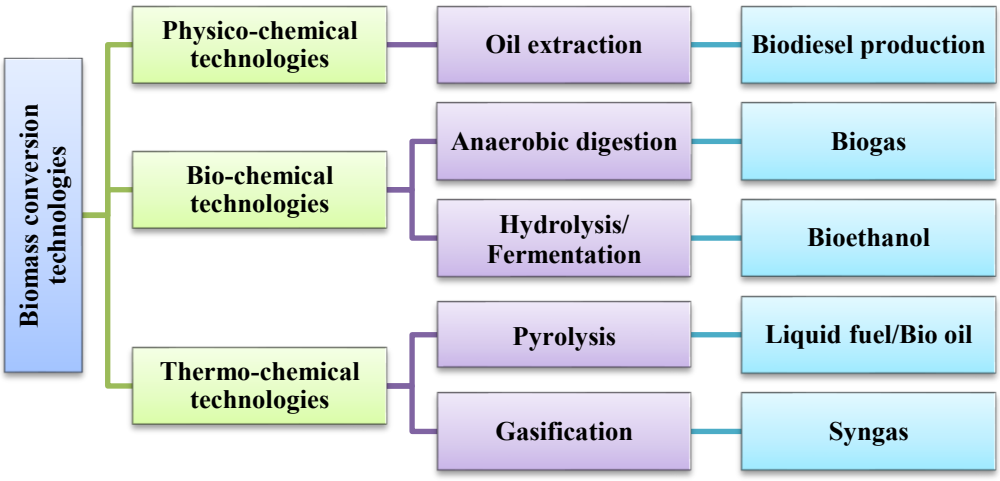

Figure 7: Biomass conversion processes (Behra *et al.*, 2015)

Physico-chemical technologies: Chemicals are employed in this procedure to extract the oil through transesterification. A chemical reaction called transesterification creates glycerin and biodiesel by reacting an alcohol with the triglycerides found in animal and vegetable fats. This method is frequently employed to create B100 biodiesel with petroleum diesel.

Bio-chemical technologies: The ingredients, such as sugars and proteins, are fermented in this process to create usable alcohols or other liquid fuels.

I. **Anaerobic digestion**: Methane and other gases and by-products that are helpful on the farm are created as a result of the anaerobic breakdown of organic matter. This mixture of gases is frequently referred to as digester gas or biogas. Biogas burns easily and often contains between 50% - 60% methane.

II. **Fermentation**: Bioethanol can be produced in this process by anaerobically digesting biomass using yeast.

Thermo-chemical technologies: This allows for the heating of the produced biomass to produce valuable bioenergy products including heat, gases, and liquids.

I. **Pyrolysis:** The biomass is transformed into bio-oil anaerobically at temperatures between 350 and 700 ^{o}C.

II. **Gasification:** This process involves heating up algal biomass to extremely high temperatures (800–1000 ^{O}C) in order to produce a mixture of combustible gases *i.e* syngas.

Table 2: Comparison of microalgae with other feedstocks (Arif *et al.,* 2019)

Oil feedstocks	Oil content (% dry wt. Biomass)	Oil Yield (L oil/ha/year)	Biodiesel Productivity (L biodisel/ha/year))
Microalgae	70	136,900	142,475
Corn	44	172	179
Soybean	18	636	661
Sunflower	40	1,070	1,113
Castor	40	1,307	1,360
Palm oil	36	5,366	5,585

The productivity of biodiesel has been assessed by using different feedstocks. The highest oil content, oil yield and productivity of biodiesel has recorded with micro-algae when compared to other feedstocks.

Dedicated bioenergy crops

Bioenergy is produced from perennial herbaceous and woody plant species (eucalyptus, poplar, willow and birch, etc). For the formation of biomass, these crops require fewer biological, chemical, or physical treatments. Additionally, they have the capacity to address environmental issues by lowering salinity, capturing carbon, enhancing biodiversity, and enhancing the quality of the soil and water. The most promising crop specifically designed for

the generation of bioenergy is short rotation coppice (SRC). Pioneers in the large-scale planting of specific bioenergy crops include Sweden and the UK.

Halophytes

These are certain plants that flourish on soils that are salty, semi-desert, and swampy. Halophytes could phytoremediate soils contaminated with heavy metals and quickly colonise salt-degraded fields. *Acacia, Eucalyptus, Casuarina, Melaleuca, Prosopis, Rhizophora* and *Tamarix* halophytes are frequently employed in the production of biofuel. It has been demonstrated that perennial halophyte (*Kosteletzkya pentacarpos*) seeds can be used to produce biodiesel. Due to increased concentrations of secondary metabolites, halophytes have a higher efficiency rate of biofuel conversion.

Genetic improvement of bioenergy crops

Plant varieties with desired morphological, phenotypic, and biochemical characteristics have been developed with the help of traditional breeding procedures. Additionally, food crops could be genetically altered to produce more starch and a higher C:N ratio in order to modify them for bioenergy production. Bioenergy crops that have undergone genetic modification are more tolerant to unfavourable environmental conditions, grow faster, and contain more calories. Due to its quick growth and simple propagation, willow has been deemed a promising biomass crop. Through genetic engineering, willow yields can be increased without noticeably requiring more water or fertilizer.

Environmental impact of bioenergy crops

1. **Water and minerals:** The water needs of first-generation biofuel crops are relatively high. The area hydrologic cycle and water quality will be severely impacted by the large-scale production of second-generation biofuel feed stocks, which have the potential to replace conventional crops. *Miscanthus* and S*witchgrass* are significantly more effective than corn at removing nitrates from deeper soil levels
2. **Phytoremediation:** Phytoremediation entails using plants to clean up polluted groundwater, sediments, and soil. Heavy metals could be eliminated from soil using phytoremediation at bioenergy facilities to enhance soil quality. The approach also has the benefit of not requiring excavation to treat contaminated sites. Phytostabilization and phytoextraction are the two main phytoremediation techniques used to clean up heavy metal-contaminated land.

   Phytostabilization: It involves the utilization of root accumulating plants which lowers the bioavailability of metals stabilized in the substrate.

   Phytoextraction: It includes the use of plants with the ability of high shoot accumulation of heavy metals from soils, sediments and water.

3. **Carbon sequestration:** Removing CO_2 from the atmosphere through the action of plants is known as carbon sequestration. Through a high biomass accumulation, bioenergy crops reduce atmospheric CO_2. Perennial crops have the potential to enhance soil quality by boosting carbon sequestration through high biomass production and extensive root systems. Bioenergy crops are known to capture ambient CO_2 and increase biomass productivity for bioenergy production.
4. **GHG emissions:** The most crucial criteria for producing bioenergy crops now center on reducing GHG emissions. By absorbing CO_2 and storing it in the crop biomass, bioenergy crops can lower GHG emissions. Among the GHGs, CO_2 and N_2O are two primary components because of their large quantity and multi approaches of production. Algal bio-diesel production on a large scale has the potential to replace diesel and reduce world GHG emissions by 13-14%.

Policies to promote bioenergy in India:

India has implemented a number of measures to promote bioenergy in the nation in an effort to combat climate change and minimize GHG emissions. Numerous policy measures, capacity building, and public-private partnerships are all part of the bioenergy strategy.

- The Electricity Act of 2003, helps State Electricity Regulatory Commissions to encourage cogeneration and generation of electricity from non-conventional sources.
- The Government of India in November 2017, introduced Policy on Biomass utilization for power generation through co-firing in coal based power plants.
- In June 2015, the Government of India (GoI) revised the Central Motor Vehicles Rules, 1989 to incorporate provisions for the use of biogas in the form of bio-CNG in motor vehicles manufactured from waste.
- The Indian government announced its National Policy on Biofuels (NPB) in June 2018. Since the implementation of Policy, the amount of ethanol in gasoline has increased from 2% to about 8.0%. By 2030, the Indian government wants to blend 5% biodiesel and 20% ethanol into regular gasoline (NPB, 2018).

Conclusion:

Use of bioenergy crops for energy generation could aid in utilizing this alternative source of renewable energy. Using current engine technologies, the commercial production of bioenergy crops could lessen our reliance on non-renewable fossil fuels. These can play a significant part in the production of ethanol and biodiesel to support the rural economy, offer higher energy efficiency, and utilize environmentally damaged lands in a useful way. In compared to

conventional crops, research has revealed that energy crops have higher soil moisture and stability, lower surface water runoff, and less sediment and nutrient transport. A reduction in emissions is another advantage of using energy crops for the environment. With increasing population and food demand, food versus fuel debate needs to be seriously addressed at the global scale, and the third and fourth generation biofuel production bring hope in this regard.

References:

1. Ahmad, A., Yasin, N. M., & Derek, C. L. (2011). Microalgae as a sustainable energy source for biodiesel production: A review. *Renewable and Sustainable Energy Reviews, 15*, 584–593.
2. Arif, R., Nining, B. P., & Nasruddin, N. (2019). Fatty acid of microalgae as a potential feedstock for biodiesel production in Indonesia. *AIP Conference Proceedings, 2062*(1), 020059.
3. Azad, A. K., Rasul, M. G., Khan, M. K., & Subhash, C. S. (2014). Review of biodiesel production from microalgae: A novel source of green energy. *The 9th International Green Energy Conference*, 879–888.
4. Behra, S., Richa, S., Richa, A., Nilesh, K. S., Madhulika, S., & Kumar, S. (2015). Scope of algae as third generation biofuels. *Frontiers in Bioengineering and Biotechnology, 2*, 90.
5. Chowdury, K. H., Nahar, N., & Kumar, U. (2020). The growth factors involved in microalgae cultivation for biofuel production: A review. *Computational Water, Energy, and Environmental Engineering, 9*, 185–215.
6. Farieda, M., Samer, M., Abdelsalam, E., Yousef, R. S., Attia, Y. A., & Ali, A. S. (2017). Biodiesel production from microalgae: Processes, technologies and recent advancements. *Renewable and Sustainable Energy Reviews, 79*, 893–913.
7. IEA. (2021). *World energy statistics and balances*. IEA, Paris. https://www.iea.org/subscribe-to-data-services/world-energy-balances-and-statistics
8. Long, S. P., Zhu, X. G., Naidu, S. L., & DR, D. R. (2006). Can improvement in photosynthesis increase crop yields. *Plant Cell Environment, 29*, 315–330.
9. Meghwanshi, G. K., & Vashishtha, A. (2014). Microalgae as potential sources of biofuels. *Journal of Phytological Research*, 41–56.
10. Parthasarathy, M., Lalvani, J. I. J. R., Parthiban, B., & Annamalai, K. (2013). Comparison of performance and emission characteristic of tamanu, mahua and pongamia biodiesel in a DI diesel engine. *Advanced Materials Research, 768*, 218–225.

11. Ravindranath, N., Lakshmi, H., Manuvie, C. S., & Balachandra, P. (2011). Biofuel production and implications for land use, food production and environment in India. *Energy Policy, 39*, 5737–5745.
12. Renewables. (2021). *Global status report: Global overview* (pp. 28–52). https://www.ren21.net/wp-content/uploads/2019/05/GSR2021_Full_Report.pdf
13. Sims, R., Taylor, M., Saddler, J., & Mabee, W. (2008). *From 1st to 2nd generation biofuel technologies: An overview of current industry and RD&D activities extended executive summary*. OECD/IEA, Paris, France.
14. Teresa, M. M., Antonio, A. M., & Caetano, N. S. (2010). Microalgae for biodiesel production and other applications: A review. *Renewable and Sustainable Energy Reviews, 14*, 217–232.
15. Williams, C., Black, I., Biswas, T., & Heading, S. (2007). Pathways to prosperity: Second generation biomass crops for biofuels using saline lands and wastewater. *Agri Sciences, 21*, 28–34.

RECENT AI INNOVATIONS IN FOOD SCIENCE

Jagruti Jankar

Annasaheb Dange College of Engineering and Technology,

Ashta, Sangli, M.S. India

Corresponding author E-mail: jankjagruti@gmail.com

Abstract:

Artificial Intelligence (AI) has emerged as a transformative force in food science, significantly advancing food quality assessment, safety monitoring, product development, precision agriculture, and personalized nutrition. Modern AI methods—including deep learning, generative models, reinforcement learning, predictive analytics, and digital twin systems—have enabled unprecedented accuracy, efficiency, and innovation across the food system. This chapter presents an in-depth examination of recent advancements (2022–2025) in the integration of AI into food science, supported by contemporary research literature. Key breakthroughs in hyperspectral imaging, sensor-driven quality control, protein design, automated processing, spoilage detection, and dietary personalization are discussed alongside current challenges and future research directions. The chapter concludes by emphasizing the pivotal role of AI in shaping sustainable, datadriven, and consumer-centric food landscapes.

Keywords: Artificial Intelligence, Food Science, Machine Learning, Food Safety, Computer Vision, Predictive Modeling, Generative AI, Personalized Nutrition

1. Introduction:

The global food sector is undergoing a technological revolution driven by Artificial Intelligence (AI). Rising consumer demands for safety, transparency, nutrition, and sustainability have pushed food science toward adopting advanced computational methods. AI has become critical across the farm-to-fork chain, from yield prediction and disease detection to automated quality control and novel food formulation (Galanakis, 2021).

The integration of AI offers key advantages: rapid pattern recognition, early spoilage prediction, real-time decision-making, and autonomous system optimization. Recent years (2022–2025) have seen explosive growth in AI systems powered by deep learning, reinforcement learning, and generative modelling. These technologies are now embedded in precision agriculture, food processing, supply chain management, and consumer nutrition platforms (Misra & Schmidt, 2023).

This chapter highlights the most recent AI-driven innovations in food science, offering a detailed analysis backed by scholarly studies and industrial applications.

2. AI techniques applied in food science

2.1 Deep learning

Deep learning architectures such as convolutional neural networks (CNNs) and transformer-based models have become standard tools for classification, segmentation, and prediction tasks in food science. CNNs are extensively applied for image-based quality analysis, including fruit ripeness, meat freshness, and microbial contamination (Zhang *et al.,* 2024).

2.2 Computer vision

Modern food inspection systems use RGB, hyperspectral, multispectral, and thermal imaging combined with AI for non-destructive evaluation. Computer vision performs:

- Defect detection
- Foreign object identification
- Shelf-life estimation
- Texture and color grading

(Jayawardena & Ampitiyawatta, 2022)

2.3 Reinforcement Learning (RL)

RL algorithms autonomously learn optimal control strategies. In food processing, RL optimizes:

- Baking temperature and time
- Fermentation conditions
- Energy usage in thermal processes

This leads to improved efficiency and consistent product quality (Singh & Raghavan, 2023).

2.4 Generative models (GANs, VAEs, LLMs)

Generative AI has become crucial in designing new food ingredients, predicting flavor trends, modelling textures, and accelerating formulation research. GANs simulate food images for training datasets, while VAEs and LLMs design protein structures and food recipes (Kim *et al.,* 2024).

2.5 Predictive analytics and machine learning

These models support:

- Yield prediction
- Food fraud detection
- Shelf-life modelling
- Risk assessment (Mishra *et al.,* 2023)

2.6 Digital twins

Digital twins create virtual replicas of food processing plants to simulate outcomes before physical implementation (Pavlović *et al.,* 2024).

3. Applications of AI in modern food science

3.1 AI in precision agriculture

AI-powered systems use sensors, drones, and satellite imagery for:

- Disease & pest detection using CNNs
- Soil nutrient analysis
- Irrigation optimization
- Harvest prediction (Mahesh *et al.,* 2023)

Deep learning models have achieved over 95% accuracy in classifying crop diseases in various studies (Li *et al.,* 2024).

3.2 Food spoilage prediction and safety monitoring

AI + hyperspectral imaging enables early detection of spoilage patterns based on spectral fingerprints that precede visible changes. Recent studies show that AI models can detect microbial spoilage in berries, meat, and dairy products with high accuracy (Feng & Wu, 2023). Computer vision systems now identify Salmonella contamination zones, fungal growth, and toxin-producing microorganisms.

3.3 Food quality control and automated sorting

AI-driven systems in food factories perform high-speed grading of fruits, vegetables, grains, and nuts. For example, almond-processing industries use CNNs for defect classification at industrial conveyor speeds (Nguyen *et al.,* 2023).

3.4 Novel food formulation using AI

Generative AI accelerates R&D of:

- Plant-based meats
- Alternative dairy proteins
- Low-sugar snack foods
- Flavor mimetics

AI models predict chemical interactions between ingredients, simulate textures, and identify optimal formulations (Kim *et al.,* 2024).

3.5 Personalized nutrition

Wearable devices + AI generate individualized meal recommendations using:

- Blood glucose data
- Gut microbiome profiles

- Genetic markers
- Food preferences

An RL-based model developed by a health tech startup improved dietary adherence by 30% (Rahman *et al.,* 2024).

3.6 Optimization of food processing

AI optimizes unit operations such as:

- Drying
- Extrusion
- Fermentation
- Baking

For example, reinforcement learning algorithms optimized bread crust color and reduced baking energy consumption by 15% (Singh & Raghavan, 2023).

3.7 Supply chain and food waste reduction

Predictive models identify potential bottlenecks, forecast demand, and optimize routing. AI-driven cold chain monitoring has reduced spoilage rates by up to 25% in some pilot studies (O'Reilly *et al.,* 2023).

4. Case studies

Case study 1: AI-based spoilage prediction in strawberries

A study by Feng & Wu (2023) used hyperspectral imaging + CNNs to detect spoilage up to 48 hours earlier than human inspection.

Case study 2: Generative AI for designing plant proteins

Kim *et al.* (2024) developed a VAE-based model to design novel protein sequences that mimic chicken texture, improving sensory scores significantly.

Case study 3: RL-optimized baking lines

Singh & Raghavan (2023) demonstrated how reinforcement learning improved baking consistency in industrial ovens by continuously adjusting heating profiles.

Case study 4: Personalized diabetes diet platform

Rahman *et al.* (2024) reported a 22–35% reduction in glycemic variability using RLdriven meal recommendations integrated with real-time glucose monitoring.

5. Challenges and limitations

5.1 Data quality and availability

Food systems are diverse; limited high-quality datasets hinder model training (Misra & Schmidt, 2023).

5.2 Model interpretability

Black-box models limit trust in safety-critical applications such as contamination detection.

5.3 Regulatory and ethical issues

AI-generated foods require transparent evaluation for safety and compliance with food laws (Galanakis, 2021).

5.4 Scalability

AI models developed in controlled lab conditions may fail in industrial settings due to variability in raw materials (Pavlović *et al.,* 2024).

5.5 High implementation costs

Upfront cost of sensors, robotics, and data infrastructure remains a barrier.

6. Future directions

- **Federated learning for food systems:** Allows data sharing without exposing sensitive information.
- **Explainable AI (XAI):** Critical for ensuring safety, transparency, and regulatory acceptance.
- **Advanced digital twins:** More accurate virtual simulations will reduce trial-and-error in food processing.
- **AI in waste valorization:** Optimizing conversion of food waste into value-added products.
- **AI-driven flavor prediction:** Combining neural networks with metabolomics to model taste and aroma.
- **Integration of AI + synthetic biology:** Design microbes for novel food production, such as alternative proteins.

Conclusion:

AI has become essential in building modern, efficient, and sustainable food systems. From precision agriculture and spoilage prediction to personalized nutrition and novel ingredient design, AI has dramatically advanced the capabilities of food science. However, challenges such as data scarcity, regulatory constraints, and scalability must be addressed. With advancements in federated learning, digital twins, and generative models, AI will continue to revolutionize the global food landscape in the coming decade.

References:

1. Feng, Y., & Wu, T. (2023). Early detection of fruit spoilage using hyperspectral imaging and deep learning. *Journal of Food Engineering*, 345, 110–125.

2. Galanakis, C. (2021). The food systems in the era of the Fourth Industrial Revolution. *Food Science and Human Wellness*, 10(1), 1–12.
3. Jayawardena, C., & Ampitiyawatta, A. (2022). Computer vision as a tool in food quality assessment. *Food Analytical Methods*, 15(6), 1423–1435.
4. Kim, S. J., Patel, V., & Romano, L. (2024). Generative AI for plant-based protein structuring. *Innovative Food Science & Emerging Technologies*, 86, 102–118.
5. Li, X., Huang, Z., & Chang, Y. (2024). Deep learning models for precision crop disease diagnosis. *Computers and Electronics in Agriculture*, 212, 108–120.
6. Mahesh, N., Kumar, R., & Jadhav, M. (2023). AI-enabled precision farming: A review. *Agricultural Systems*, 206, 103–145.
7. Misra, N., & Schmidt, C. (2023). Machine learning applications in food safety and traceability. *Trends in Food Science & Technology*, 140, 499–517.
8. Mishra, S., Dwivedi, P., & Roy, R. (2023). Predictive analytics for shelf-life estimation of packaged foods. *Journal of Food Processing & Preservation*, 47(1), e16590.
9. Nguyen, P. T., Silva, S., & Almeida, A. (2023). AI-driven defect detection during nut processing. *Food Control*, 150, 109–214.
10. O'Reilly, M., Gupta, P., & Larson, D. (2023). AI in food logistics: Reducing waste through predictive analytics. *Sustainable Food Systems*, 5(2), 102–119.
11. Pavlović, M., Savić, A., & Han, Z. (2024). Digital twins in food processing: Current advancements and future perspectives. *Journal of Food Engineering*, 380, 111–133.
12. Rahman, F., Choi, D., & Ahmed, H. (2024). AI-driven personalized nutrition for glucose management. *Nutrition & Digital Health*, 2(1), 45–60.
13. Singh, A., & Raghavan, G. S. V. (2023). Reinforcement learning for industrial baking optimization. *Journal of Food Process Engineering*, 46(4), e14160.
14. Zhang, T., Liu, J., & Wang, P. (2024). Deep learning for meat freshness detection. *Meat Science*, 197, 109–131.

Bhumi Publishing, India
November 2025

THE MOLECULAR BIOLOGY OF CANCER

Pratima Sharma[1] and Farah Khan[2]

[1]Faculty of Biotechnology, Institute for Excellence in Higher Education, Bhopal, M.P.

[2]Department of Biotechnology, Technocrats Institute of Commerce & Sciences, Bhopal, M.P.

Abstract:

Cancer is a multifactorial disease arising from complex interactions among genetic mutations, epigenetic modifications, and environmental influences that disrupt normal cellular regulation. This chapter explores the molecular underpinnings of cancer development, progression, and therapeutic targeting. It begins with an overview of genetic alterations, distinguishing between oncogene activation and tumor suppressor gene inactivation. The discussion extends to key signal transduction pathways, including MAPK/ERK, PI3K/AKT/mTOR, and Wnt/β-catenin, which govern proliferation and survival. Epigenetic regulation, genomic instability, and the tumor microenvironment are examined as integral components of tumor evolution and heterogeneity. The chapter also highlights recent advances in molecular diagnostics, targeted therapy, and immunotherapy that have transformed cancer management through precision medicine. By integrating classical concepts with modern molecular insights, this chapter underscores how understanding cancer biology at the molecular level informs prevention, diagnosis, and treatment strategies for the future of oncology.

Keywords: Oncogenes, Tumor Suppressor Genes, Signal Transduction Pathways, Epigenetic Regulation, Molecular Oncology

1. Introduction:

Cancer is a disease characterized by uncontrolled cell growth and division caused by accumulated genetic and epigenetic alterations. At its molecular core, cancer represents the breakdown of cellular regulatory mechanisms that control proliferation, differentiation, and apoptosis (Weinberg, 2013). The molecular biology of cancer explores how mutations, chromosomal rearrangements, and changes in gene regulation drive the transformation of normal cells into malignant ones (Hanahan & Weinberg, 2011).

2. The Genetic Basis of Cancer

2.1 Somatic vs. Germline Mutations

Most cancers arise due to somatic mutations—genetic changes acquired during an individual's lifetime. However, some individuals inherit germline mutations that predispose them

to cancer, such as mutations in *BRCA1* and *BRCA2* associated with breast and ovarian cancers, or *APC* mutations linked to familial adenomatous polyposis (Knudson, 1971; Miki *et al.,* 1994).

2.2 Driver and Passenger Mutations

Driver mutations confer a selective advantage by promoting proliferation or survival, whereas passenger mutations are neutral by-products of genomic instability (Vogelstein *et al.,* 2013). Identifying driver mutations is essential for developing molecularly targeted therapies.

3. Oncogenes and Proto-Oncogenes

3.1 Activation of Oncogenes

Proto-oncogenes normally promote cell growth and differentiation. When mutated or overexpressed, they become oncogenes that drive malignant transformation. Mechanisms include point mutations, gene amplification, or chromosomal translocations (Bishop, 1983).

3.2 Examples of Oncogenes

Oncogene	Normal Function	Activation Mechanism	Associated Cancer
RAS	GTP-binding protein for signaling	Point mutation	Colon, pancreatic
MYC	Transcription factor	Amplification	Burkitt lymphoma
BCR-ABL	Tyrosine kinase	Translocation (t9;22)	CML
HER2/ERBB2	Receptor tyrosine kinase	Amplification	Breast, gastric

These oncogenes disrupt cell signaling pathways, leading to unchecked proliferation (Downward, 2003).

4. Tumor Suppressor Genes

4.1 Loss of Function and the Two-Hit Hypothesis

Tumor suppressor genes (TSGs) inhibit cell division, repair DNA damage, or promote apoptosis. Cancer often arises after both alleles of a TSG are inactivated—a concept described as the "two-hit hypothesis" (Knudson, 1971).

4.2 Key Tumor Suppressors

Gene	Function	Inactivation Mechanism	Associated Cancer
TP53	DNA damage response	Mutation, deletion	Many
RB1	Cell cycle checkpoint	Mutation	Retinoblastoma
APC	Wnt signaling control	Mutation	Colorectal
BRCA1/2	DNA repair	Germline mutation	Breast, ovarian

The *TP53* gene, often termed the "guardian of the genome," is the most frequently mutated gene in human cancers (Levine, 2020).

5. Hallmarks of Cancer

Hanahan and Weinberg (2000, 2011) identified essential biological capabilities that define cancer:

1. Sustaining proliferative signaling
2. Evading growth suppressors
3. Resisting cell death
4. Enabling replicative immortality
5. Inducing angiogenesis
6. Activating invasion and metastasis
7. Reprogramming energy metabolism
8. Avoiding immune destruction

These hallmarks are driven by molecular alterations in oncogenes and tumor suppressor genes, creating a unified framework for understanding cancer progression.

6. Signal Transduction Pathways in Cancer

6.1 MAPK/ERK Pathway

The MAPK/ERK pathway transduces signals from growth factor receptors to the nucleus. Mutations in *RAS* or *BRAF* (e.g., *BRAF V600E*) cause continuous activation, promoting proliferation and survival (Dhillon *et al.,* 2007).

6.2 PI3K/AKT/mTOR Pathway

This pathway regulates cell metabolism and survival. Mutations in *PIK3CA*, *AKT*, or loss of *PTEN* are common in breast, endometrial, and glioblastoma cancers (Vivanco & Sawyers, 2002).

6.3 Wnt/β-Catenin Pathway

The Wnt pathway is crucial for cell fate determination. Loss of *APC* leads to β-catenin accumulation and activation of growth-promoting genes, particularly in colorectal carcinoma (Clevers, 2006).

7. Epigenetic Alterations

Epigenetic changes—such as DNA methylation, histone modification, and noncoding RNA regulation—alter gene expression without changing DNA sequences (Esteller, 2008).

Examples include:

- Promoter hypermethylation of *CDKN2A/p16* leading to loss of cell cycle control
- Histone deacetylation causing chromatin condensation and gene silencing

- MicroRNA (miRNA) dysregulation affecting oncogene and tumor suppressor expression (Calin & Croce, 2006)

8. Genomic Instability

Cancer cells exhibit chromosomal instability (CIN) and microsatellite instability (MSI), resulting from defective DNA repair mechanisms (Negrini *et al.,* 2010). Deficiency in mismatch repair genes (*MLH1*, *MSH2*) is characteristic of Lynch syndrome and MSI-high tumors.

9. Tumor Microenvironment

The tumor microenvironment (TME) includes fibroblasts, immune cells, and extracellular matrix components that interact with cancer cells (Quail & Joyce, 2013).

- Cancer-associated fibroblasts (CAFs) secrete growth factors promoting invasion.
- Tumor-associated macrophages (TAMs) produce VEGF, aiding angiogenesis.
- Hypoxia induces HIF-1α, driving angiogenesis and glycolysis (Semenza, 2003).

10. Mechanisms of Metastasis

Metastasis is a multistep process involving:

1. **Epithelial–mesenchymal transition (EMT)**
2. **Invasion and intravasation**
3. **Circulatory survival**
4. **Extravasation and colonization**

Loss of *E-cadherin*, upregulation of matrix metalloproteinases (MMPs), and activation of chemokine receptors like *CXCR4* facilitate metastasis (Lambert *et al.,* 2017).

11. Molecular Diagnostics and Targeted Therapy

11.1 Diagnostic Tools

Advances in next-generation sequencing (NGS), immunohistochemistry (IHC), and liquid biopsies enable precise molecular profiling (Wan *et al.,* 2017).

11.2 Targeted Therapy Examples

Target	**Drug**	**Mechanism**	**Cancer**
BCR-ABL	Imatinib	Tyrosine kinase inhibitor	CML
EGFR	Erlotinib	RTK inhibitor	NSCLC
HER2	Trastuzumab	Monoclonal antibody	Breast
BRAF V600E	Vemurafenib	Kinase inhibitor	Melanoma

These therapies exemplify precision medicine—tailoring treatment based on molecular profiles (Druker *et al.,* 2001).

12. Immune Evasion and Immunotherapy

Tumors evade immune surveillance by suppressing antigen presentation and upregulating immune checkpoints like PD-L1 and CTLA-4 (Pardoll, 2012).

Checkpoint inhibitors (e.g., pembrolizumab, nivolumab) and CAR-T cells have revolutionized cancer immunotherapy (June *et al.,* 2018).

Future Perspectives:

Emerging tools such as CRISPR-Cas9 gene editing, single-cell sequencing, and multi-omics integration are uncovering mechanisms of tumor heterogeneity and therapy resistance (Lawson *et al.,* 2018). Integrating molecular biology with computational approaches will shape the next generation of personalized oncology.

Summary:

Cancer is fundamentally a molecular disease arising from complex interactions between genetic mutations, epigenetic regulation, and the tumor microenvironment. Molecular biology provides the foundation for understanding these mechanisms and developing targeted interventions that improve patient outcomes.

References:

1. Bishop, J. M. (1983). Cellular oncogenes and retroviruses. *Annual Review of Biochemistry, 52*(1), 301–354.
2. Calin, G. A., & Croce, C. M. (2006). MicroRNA signatures in human cancers. *Nature Reviews Cancer, 6*(11), 857–866.
3. Clevers, H. (2006). Wnt/β-catenin signaling in development and disease. *Cell, 127*(3), 469–480.
4. Dhillon, A. S., Hagan, S., Rath, O., & Kolch, W. (2007). MAP kinase signalling pathways in cancer. *Oncogene, 26*(22), 3279–3290.
5. Druker, B. J., Talpaz, M., Resta, D. J., Peng, B., Buchdunger, E., Ford, J. M., ... & Sawyers, C. L. (2001). Efficacy and safety of a specific inhibitor of the BCR-ABL tyrosine kinase in chronic myeloid leukemia. *New England Journal of Medicine, 344*(14), 1031–1037.
6. Esteller, M. (2008). Epigenetics in cancer. *New England Journal of Medicine, 358*(11), 1148–1159.
7. Hanahan, D., & Weinberg, R. A. (2000). The hallmarks of cancer. *Cell, 100*(1), 57–70.
8. Hanahan, D., & Weinberg, R. A. (2011). Hallmarks of cancer: The next generation. *Cell, 144*(5), 646–674.

9. June, C. H., O'Connor, R. S., Kawalekar, O. U., Ghassemi, S., & Milone, M. C. (2018). CAR T cell immunotherapy for human cancer. *Science, 359*(6382), 1361–1365.
10. Knudson, A. G. (1971). Mutation and cancer: Statistical study of retinoblastoma. *Proceedings of the National Academy of Sciences, 68*(4), 820–823.
11. Lambert, A. W., Pattabiraman, D. R., & Weinberg, R. A. (2017). Emerging biological principles of metastasis. *Cell, 168*(4), 670–691.
12. Lawson, D. A., Kessenbrock, K., Davis, R. T., Pervolarakis, N., & Werb, Z. (2018). Tumour heterogeneity and metastasis at single-cell resolution. *Nature Cell Biology, 20*(12), 1349–1360.
13. Levine, A. J. (2020). p53: 800 million years of evolution and 40 years of discovery. *Nature Reviews Cancer, 20*(8), 471–480.
14. Miki, Y., Swensen, J., Shattuck-Eidens, D., Futreal, P. A., Harshman, K., Tavtigian, S., ... & Skolnick, M. H. (1994). A strong candidate for the breast and ovarian cancer susceptibility gene BRCA1. *Science, 266*(5182), 66–71.
15. Negrini, S., Gorgoulis, V. G., & Halazonetis, T. D. (2010). Genomic instability—an evolving hallmark of cancer. *Nature Reviews Molecular Cell Biology, 11*(3), 220–228.
16. Pardoll, D. M. (2012). The blockade of immune checkpoints in cancer immunotherapy. *Nature Reviews Cancer, 12*(4), 252–264.
17. Quail, D. F., & Joyce, J. A. (2013). Microenvironmental regulation of tumor progression and metastasis. *Nature Medicine, 19*(11), 1423–1437.
18. Semenza, G. L. (2003). Targeting HIF-1 for cancer therapy. *Nature Reviews Cancer, 3*(10), 721–732.
19. Vivanco, I., & Sawyers, C. L. (2002). The phosphatidylinositol 3-kinase–AKT pathway in human cancer. *Nature Reviews Cancer, 2*(7), 489–501.
20. Vogelstein, B., Papadopoulos, N., Velculescu, V. E., Zhou, S., Diaz, L. A., & Kinzler, K. W. (2013). Cancer genome landscapes. *Science, 339*(6127), 1546–1558.
21. Wan, J. C. M., Massie, C., Garcia-Corbacho, J., Mouliere, F., Brenton, J. D., Caldas, C., ... & Rosenfeld, N. (2017). Liquid biopsies come of age: Towards implementation of circulating tumour DNA. *Nature Reviews Cancer, 17*(4), 223–238.
22. Weinberg, R. A. (2013). *The biology of cancer* (2nd ed.). Garland Science.

Bhumi Publishing, India
November 2025

DEVELOPMENT OF BIODEGRADABLE POLYMERS FOR SUSTAINABLE PACKAGING

N. Vijaya Lakshmi
Department of Physics,
Government Degree College, Chevella, Rangareddy District, Telangana
Corresponding author E-mail: vijayanaidu2008@gmail.com

Abstract:

The increasing global concern over plastic pollution has accelerated research into biodegradable polymers as sustainable alternatives to conventional packaging materials. This study focuses on the development and characterization of biodegradable polymer composites using natural polymers such as starch, polylactic acid (PLA), and chitosan. The synthesized polymers were analyzed for their mechanical, thermal, and degradation properties. Experimental results demonstrated that starch–PLA–chitosan blends exhibited enhanced tensile strength, flexibility, and biodegradability compared to single-component systems. The study concludes that such eco-friendly polymer composites hold significant promise for future sustainable packaging applications, reducing the environmental footprint of plastic waste.

Keywords: Biodegradable Polymers, Sustainable Packaging, Polylactic Acid, Starch, Chitosan, Eco-Materials

1. Introduction:

The exponential growth of the packaging industry has led to an alarming increase in plastic waste, creating severe environmental and health concerns. Traditional petroleum-based plastics are non-biodegradable, persisting in the environment for hundreds of years. The need for eco-friendly, renewable, and biodegradable materials has become critical in addressing this challenge. Biodegradable polymers such as polylactic acid (PLA), starch-based materials, and chitosan have emerged as promising candidates due to their natural origin, biodegradability, and mechanical performance. However, single-component biodegradable polymers often suffer from drawbacks such as brittleness or low moisture resistance. To overcome these limitations, polymer blending and composite formation techniques are employed. This study aims to develop biodegradable polymer blends suitable for sustainable packaging and to evaluate their mechanical and degradation characteristics.

2. Objectives

i. To synthesize biodegradable polymer films using PLA, starch, and chitosan.
ii. To characterize their mechanical and thermal properties.
iii. To study their biodegradability under natural soil conditions.

iv. To identify the most suitable composition for packaging applications.

3. Materials and Methods

3.1 Materials

- Polylactic Acid (PLA): Procured from Sigma-Aldrich, analytical grade.
- Starch: Extracted from potato using standard laboratory methods.
- Chitosan: Sourced from shrimp shells, deacetylation degree ~85%.
- Plasticizer: Glycerol (99.5% purity).
- Solvents: Acetic acid (1%), distilled water.

3.2 Preparation of Polymer Blends

The films were prepared using the solution casting technique:

i. Starch Solution: 5 g of starch was dissolved in 100 mL distilled water and heated to 80°C with constant stirring.
ii. Chitosan Solution: 2 g chitosan was dissolved in 100 mL of 1% acetic acid.
iii. PLA Solution: 5 g PLA was dissolved in chloroform and stirred at room temperature.
iv. Blending: The solutions were mixed in varying ratios (PLA:Starch:Chitosan = 60:30:10, 50:40:10, 40:50:10).
v. Casting: The mixtures were poured into Petri dishes and dried at 50°C for 24 hours to obtain thin films.

3.3 Characterization Techniques

Mechanical Testing: Tensile strength and elongation at break were measured using a Universal

i. Testing Machine (UTM).
ii. Thermal Analysis: Differential Scanning Calorimetry (DSC) was used to evaluate melting temperature and crystallinity.
iii. Fourier Transform Infrared Spectroscopy (FTIR): Used to analyze functional groups and chemical bonding.
iv. Biodegradation Study: Films were buried in natural soil and weight loss was measured at intervals of 7, 14, 21, and 28 days.

4. Results and Discussion:

Among the samples tested, the 60:30:10 blend (PLA:Starch:Chitosan) showed the best tensile strength (25.3 MPa) and moderate flexibility (elongation at break ~40%). The increase in starch content improved flexibility but reduced tensile strength, while higher PLA content enhanced rigidity.

DSC analysis revealed a melting temperature (Tm) of approximately 153°C for PLA-based blends. The addition of starch slightly lowered the Tm, indicating partial miscibility and increased amorphous content, favorable for biodegradability.

Table 1: Mechanical Properties of Biodegradable Polymer Blends

Composition (PLA:Starch:Chitosan)	Tensile Strength (MPa)	Elongation at Break (%)
60:30:10	25.3	40
50:40:10	20.1	48
40:50:10	16.5	55

FTIR spectra confirmed successful blending. Characteristic absorption peaks at 1735 cm^{-1} (C=O stretching) from PLA and 3400 cm^{-1} (O–H stretching) from starch and chitosan indicated hydrogen bonding and intermolecular interactions.

The soil burial test demonstrated significant weight loss over 28 days. The 50:40:10 blend exhibited the fastest degradation rate (~60% weight loss), attributed to higher starch and chitosan content, both of which promote microbial attack.

5. Applications

- Food Packaging: Short-shelf-life items such as fruits, vegetables, and bakery products.
- Agricultural Films: Mulch films and seed coating applications.
- Disposable Utensils: Cups, plates, and trays.
- Medical Packaging: Temporary sterile packaging materials.

Conclusion:

The developed starch–PLA–chitosan biodegradable polymer blends exhibit excellent potential for sustainable packaging applications. The composite with a 50:40:10 ratio demonstrated the best compromise between strength and biodegradability. Future research can explore the incorporation of natural fibers or nanofillers to further enhance performance and scalability.

References:

1. Avérous, L., & Pollet, E. (2012). *Environmental silicate nano-biocomposites*. Springer.
2. Garlotta, D. (2001). A literature review of poly(lactic acid). *Journal of Polymers and the Environment, 9*(2), 63–84.
3. Reddy, M. M., *et al.* (2013). Bio-based plastics and bionanocomposites: Current trends and future opportunities. *Progress in Polymer Science, 38*(10–11), 1653–1689.
4. Kale, G., *et al.* (2007). Compostability of bioplastic packaging materials: An overview. *Macromolecular Bioscience, 7*(3), 255–277.
5. Sudhakar, M., *et al.* (2008). Marine microbes degrading polyethylene and polypropylene. *Indian Journal of Biotechnology, 7*(2), 201–205.

DIELECTRIC AND DC ELECTRIC STUDY OF GEL GROWN CRYSTALS

Mukund D. Dhikale

Arts, Science & Commerce College,

Ozar (Mig), Niphad, Nashik-422 206, Maharashtra

Corresponding author E-mail: mukunddhikale9@gmail.com

Abstract:

The present chapter focuses on the dielectric and DC electrical properties of silica gel-grown crystals to see their electrical response and polarization behaviour in an applied electric field. Dielectric materials, being electrical insulators, possess the ability to store electrostatic energy and exhibit minimal power dissipation. The dielectric constant, dielectric loss, and AC conductivity of the prepared crystal samples were analyzed to explore their polarization mechanisms and charge transport behaviour. Crushed and pelletized samples of the gel-grown crystals were examined using an LCR meter setup over a range of frequencies and temperatures. The dielectric constant (ε') was determined from the capacitance measurements, while the dielectric loss (tan δ) and AC conductivity (σ_{ac}) were calculated using standard relations. The results reveal the influence of factors such as frequency, molecular structure, and temperature on the dielectric properties of the material. This investigation provides valuable insight into the electrical behaviour, polarization mechanisms, and potential applications of gel-grown crystals in electronic and optoelectronic devices.

Keywords: Dielectric Constant, AC Conductivity, Polarization, Gel-Grown Crystals, Dielectric Loss

1. Introduction:

Each an every material has a unique set of electrical characteristics depending upon the various parameters such as the dielectric properties, permittivity, permeability, resistivity, conductivity, etc. A material is said to be "dielectric" if it has the capability to store energy when an external electric field is applied. In other words, materials, which are electric insulators or in which an electric field can be sustained with a minimum dissipation of power, are known as dielectric materials. Simply, dielectrics are insulating materials. In dielectrics, all the electrons are bound to their parent molecules and there are no free charges. Even with normal voltage or thermal energy, the electrons are not released. Dielectrics are non-metallic materials of high specific resistance and have a negative temperature coefficient of resistance. The dielectric characteristics of the material are important to study the lattice dynamics in the crystal. It is

important to note that permittivity and permeability are not constant. They can change with frequency, temperature, orientation, mixture, pressure, and molecular structure of the material.

Many researchers have discussed various dielectric parameters such as permittivity, permeability, resistivity, conductivity, etc. dielectric applications and dielectric theories in details [1-11]. Also, some of the authors explained dielectric properties in their thesis [12-18].

2. Dielectric Study

A dielectric material is characterized by its dielectric constant ε, which relates the electric flux density to the electric field by the following relation

$D = E\,\varepsilon$

Where, D = Electric displacement

E = Applied electric field

ε = Dielectric constant

In the MKS system, the dielectric constant is the product of permittivity of free space ε_0 and relative dielectric constant ε_r.

$\varepsilon = \varepsilon_0\,\varepsilon_r$

In the earlier experiments, Faraday has been shown that when a dielectric material is inserted between the condenser plates, the capacitance increase by a factor of ε_r. This is because of the appearance of charges on the surface of the dielectric necessitating the arrival of fresh charges from the battery in order to keep the voltage constant. This is described in a below schematic diagram 1.

In vacuum i.e. when no material placed between the plates, the surface charge density on the condenser plate is represented as

$$Q = \frac{\varepsilon_0 V}{d}$$

Where, d = distance between the plates.

In the presence of dielectric material, the surface charge density increase to

$$Q' = \frac{\varepsilon_0 \varepsilon_r V}{d}$$

Due to this dielectric material, the dielectric susceptibility and surface charge density by ρ is given below

$\chi = \varepsilon_r - 1$

$\rho = D - \varepsilon_0 E$ and $\rho = \varepsilon_0 \chi E$

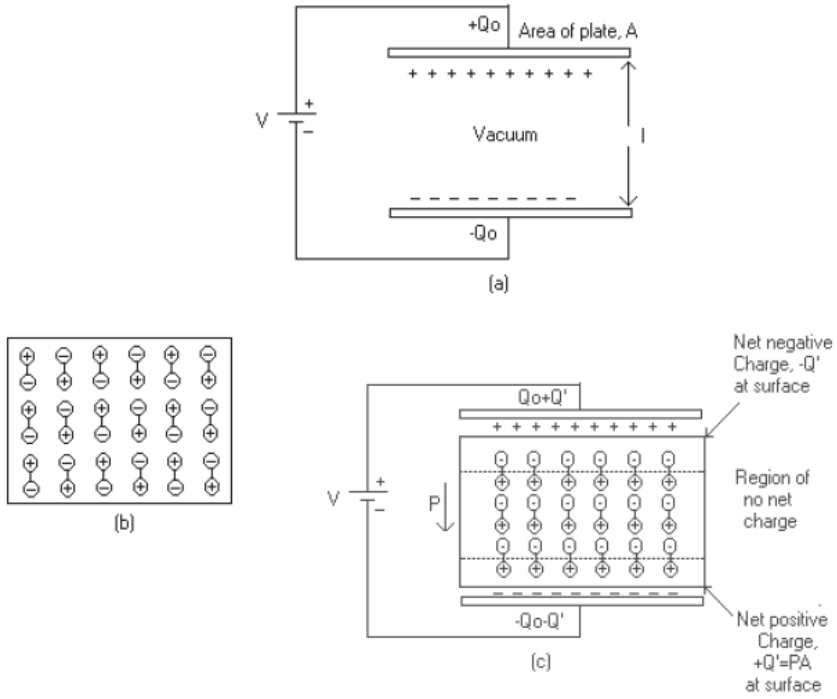

Figure 1: Schematic representations of (a) the charge stored on capacitor plates for a vacuum. (b) the dipole arrangement in an unpolarized dielectric, and (c) the increased charge storing capacity resulting from the polarization of a dielectric material

Usually, the dielectric constant of dielectric material is defined as the ratio of the electric capacitance of a capacitor with a dielectric material to an electric capacitance of a capacitor without dielectric material having identical dimensions. This can be represented by the following equation,

$$\varepsilon = \frac{C}{C_0}$$

Where, C = capacitance of the dielectric field capacitor and

C_0 = capacitance of the vacuum capacitor.

For a given charge distribution, the dielectric constant expresses the ratio of electric field strength in vacuum to that in a dielectric, the latter field being reduced by the polarization of the dielectric medium.

Microscopically an atom has a positively charged nucleus surrounded by a bound electron cloud. In the absence of an electric field, the statistical canters of positive charges and negative charges coincide. Therefore, dipole moment will be zero for those charges. When an electric field is applied there will be a slight displacement in the charge canters, particularly of the electrons. If this displacement is δ and the total charge is q then the material has an induced dipole moment,

$\mu = q\,\delta$

This induced dipole moment is directed from negative induce charge to positive induced charge. If the center of electron charge moves by net displacement δ, then the total volume occupied by this electron is A δ, where A is the cross-sectional area of dielectric material. This is actually true for the class of molecules also. The electric polarisation is

$$P = \frac{\mu}{A\delta}$$

$$P = \frac{q\,\delta}{A\delta}$$

$$P = \frac{q}{A}$$

Therefore, this is a surface charge density of induced charges. For any dielectric material induced dipole moment is proportional to applied electric field. The proportionality constant (α) is known as polarizability.

$\mu = \alpha E$

There are various types of electric polarizations, such as, ionic polarization, interstitial polarization, and electronic polarizability of atoms, lattice polarization and molecular polarizability.

The electric response of dielectric material can be explained by its parameters like dielectric or breakdown strength, conductivity or dielectric loss and dielectric constant. The behaviour of nonlinear dielectric also depends on the amplitude and time variation of the electric field.

Dielectric strength is defined as the maximum electric field, which can be applied to a dielectric without causing a breakdown, the abrupt irreversible drop in resistivity at high fields often accompanied by destruction of the material. Dielectric strength of most insulating materials is in the range from 10^4 to 10^7V/m. at room temperature and low frequencies and it decreases at higher temperatures.

Dielectric loss is the power dissipation in a dielectric because of the conduction process. This power loss results from thermal dissipation of the electrical energy expended by the field. It is caused by molecular collisions. It can be described by any of the following parameters; the conductivity σ, the factor ε", the power factor cosθ and the loss tangent or dissipation factor, tanδ.

The dielectric constant (ε') is measured by using the following relations,

$$\varepsilon' = \frac{C\,t}{\varepsilon_0\,A}$$

Where, C = Capacitance

t = Thickness of pellet

A = Area of cross section of pellet

ε_0 = Permittivity of free space

The dissipation factor (D) is measured along with the capacitance at different variable frequencies. The dielectric loss tanδ is calculated by using the following expression,

$\tan\delta = D$

Where, D = dissipation factor.

The AC conductivity (σ_{ac}) was calculated by using the equation,

$$\sigma_{ac} = \frac{2\pi FtC \tan\delta}{A}$$

Where, F= frequency

C=capacitance

tan δ=dissipation factor

t = thickness of the pellet

A=area of the pellets

3. Experimental Setup

Figure 2 shows the photograph of the LCR set up. The gel grown crystals were crushed to make powder and then this powder was palletized by using high pressure. The pallets were placed in a suitable design holder. Figure 3 describes the design of the sample holder.

Figure 2: LCR meter

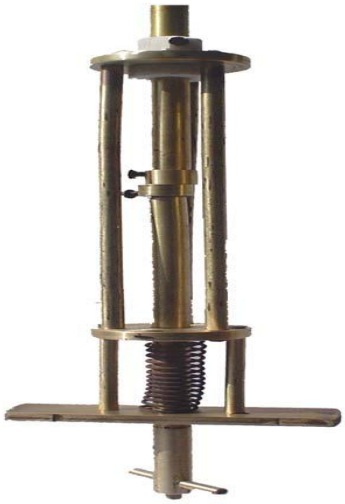

Figure 3: The sample holder

The frequency of the applied signal was varied from 100Hz to 5MHz and the values of capacitance were measured at a variable frequency at room temperature.

4. DC Electrical Study

There are two ways to measure high resistance of a material, the first one is a constant voltage method and the other is a constant current method. In the constant voltage method, a known voltage source and a pico-ammeter are used to measure the resulting current. In the constant current method, a constant current is allowed to flow through the material and the voltage drop across the resistance is measured. The resistivity of the material is generally measured using a two-point technique.

Electric conductivity study as a function of temperature has been done by a number of scientists on a crystals such as ammonium hydrogen tartrate [19], KDP crystals [20], pure and copper added strontium tartrate trihydrate crystals [21], KCl-doped triglycine sulfate single crystals [22], pure and barium added strontium tartrate trihydrate crystals [23], bismuth iodate [24], etc. Also, many of the investigations on tartrates [25, 26] described electrical conductivity.

The temperature dependence of D.C. resistivity of both the samples was studied by two-probe method. Gel grown crystals in the pellet form were used for the resistivity measurement. To make good ohmic contact, a silver paste was applied on the clean and freshly ground surface of the pellets. The samples were put between the spring loaded copper terminals. The resistivity ρ was calculated from dimensions and resistance of the pellet by using the relation,

$$\sigma_{dc} = \frac{t}{RA}$$

Where, σ_{dc} = DC electric conductivity

t = Thickness of pellet

R = Resistance of pellet

A = Area of cross section of pellet

Below figures 4 and 5 shows the sample holder and two probe set up respectively.

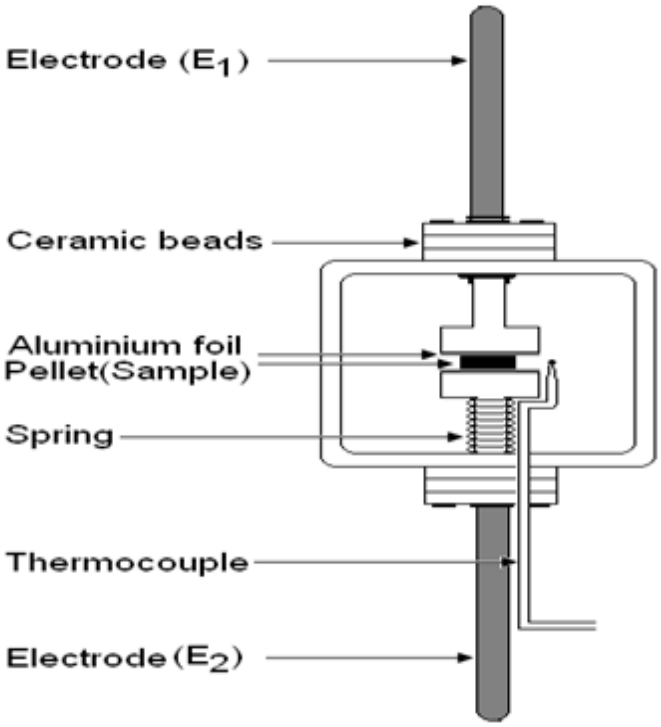

Figure 4: The sample holder

Figure 5: Two probes set up

References:

1. Harshkant Jethva, Kanchan, D., & Joshi, M. (2016). *[Article title unavailable]*. *International Journal of Innovative Research in Science, Engineering and Technology, 5*(1).
2. Suresh, S., & Arivuoli, D. (2011). *[Article title unavailable]*. *Journal of Optoelectronics and Biomedical Materials, 3*(3), 63–68.
3. Jethva, H. O., Joshi, M. J., & Kanchan, D. K. (2015). *[Article title unavailable]*. *International Journal of Engineering and Innovative Technology (IJEIT), 5*(3).
4. Dabhi, R. M., Parekh, B. B., & Joshi, M. J. (2005). *[Article title unavailable]*. *Indian Journal of Physics, 79*(5), 503–507.
5. Suthar, S. R., Joshi, S. J., Parekh, B. B., & Joshi, M. J. (2007). *[Article title unavailable]*. *Indian Journal of Pure and Applied Physics, 45*, 48–51.
6. Torres, M. E., *et al.* (2002). *[Article title unavailable]*. *Journal of Solid State Chemistry, 163*, 491–497.
7. Sameeh, M., Khairy, M., Bayoumy, W. A., El-asawi, T., & El-bellihi, A. A. (2014). *[Article title unavailable]*. *Journal of Basic and Environmental Sciences, 1*, 46–64.
8. Johnson Navamani, S., Sumithraj Premkumar, P., & Narayanasamy, G. (2016). *[Article title unavailable]*. *International Journal of Scientific and Research Publications, 6*(6).
9. Joshi, S. J., Parekh, B. B., Vohra, K. D., & Joshi, M. J. (2006). *[Article title unavailable]*. *Bulletin of Materials Science, 29*(3), 307–312.
10. Mathivanan, V., Haris, M., Prasanyaa, T., & Amgalan, M. (2014). *[Article title unavailable]*. *Optic*. Elsevier.

11. Mathivanan, V., Haris, M., Prasanyaa, T., & Amgalan, M. (2014). *[Article title unavailable]*. *Pramana – Journal of Physics, 82*(3).
12. Parekh, B. B. (2005). *Ph.D. thesis.* Saurashtra University, Rajkot.
13. Suthar, S. R. (2007). *Ph.D. thesis.* Saurashtra University, Rajkot.
14. Joshi, S. J. (2009). *Ph.D. thesis.* Saurashtra University, Rajkot.
15. Chauhan, C. K. (2011). *Ph.D. thesis.* Saurashtra University, Rajkot.
16. Dave, D. J. (2011). *Ph.D. thesis.* Saurashtra University, Rajkot.
17. Parikh, K. D. (2011). *Ph.D. thesis.* Saurashtra University, Rajkot.
18. Vyas, P. M. (2013). *Ph.D. thesis.* Saurashtra University, Rajkot.
19. Desai, C. C. (1988). *[Article title unavailable]*. *Bulletin of Materials Science, 10*(3), 187–197.
20. Priya, M., Padma, C. M., Freeda, T. H., Mahadevan, C., & Balasingh, C. (2001). *[Article title unavailable]*. *Bulletin of Materials Science, 24*(5), 511–514.
21. Gowri, B., & Sahaya Shajan, X. (2006). *[Article title unavailable]*. *Materials Letters, 60*, 1338–1340.
22. Das, H. N., & Podder, J. (2012). *[Article title unavailable]*. *Journal of Thermal Analysis and Calorimetry, 110*, 1107–1112.
23. Angel Mary Greena, J., Sahaya Shajan, X., & Alex Devadoss, H. (2010). *[Article title unavailable]*. *Indian Journal of Science and Technology, 3*(3).
24. Patil, T. K., & Saraf, K. B. (2011). *[Article title unavailable]*. *Advances in Applied Science Research, 2*(1), 111–119.
25. Suryanarayan, K., & Dharmaprakash, S. M. (2000). *[Article title unavailable]*. *Materials Letters, 42*(1–2), 92.
26. Arora, S. K., Patel, V. A., Patel, R. G., Amin, B., & Kothari, A. (2004). *[Article title unavailable]*. *Journal of Physics and Chemistry of Solids, 65*, 965.

GRAPH-THEORETIC APPROACHES IN MODERN DATA AND NETWORK ANALYSIS

Shobana A*[1], Logapriya B[2] and Vidhya D[3]

[1]Department of Science and Humanities, Nehru Institute of Technology, Coimbatore, India.

[2]Department of Science and Humanities, Karpagam College of Engineering, Coimbatore,

[3]Department of Science and Humanities, Karpagam Institute of Technology, Coimbatore,

*Corresponding author E-mail: shobanaamaths@gmail.com

Abstract:

Graph theory has emerged as a cornerstone of modern data science, enabling researchers to model, analyze, and interpret complex relationships across diverse domains such as social networks, biological systems, communication infrastructures, and artificial intelligence. With the rapid growth of interconnected data, traditional linear or tabular methods are inadequate to capture the interdependencies inherent in modern systems.

This chapter explores the fundamental principles of graph theory and their applications in network and data analysis. It discusses classical metrics such as centrality, clustering, and community detection, as well as advanced computational methods including spectral graph theory and graph neural networks (GNNs). Through examples and case studies, we demonstrate how graph-based approaches enhance insight generation, optimize systems, and contribute to innovation in science and technology. The discussion concludes with future perspectives on the integration of graph-theoretic models with artificial intelligence, big data analytics, and emerging digital ecosystems.

Keywords: Graph Theory, Network Analysis, Centrality, Community Detection, Spectral Graph Theory, Graph Neural Networks, Big Data, Mathematical Modeling, Data Analytics.

1. Introduction:

The world today operates through interconnected systems — from social media and transportation networks to electrical grids and biological ecosystems. Each of these systems can be represented mathematically as a **network**, where entities interact with one another through defined relationships. Traditional statistical and algebraic models primarily analyze data in isolation; however, in real-world contexts, the *relationship between data points* often carries more significance than the data points themselves.

Graph theory, a branch of discrete mathematics, provides the language and tools necessary for studying such relational data. Introduced in the 18th century through Euler's

famous *Königsberg Bridge Problem*, graph theory has since evolved into a critical field influencing computer science, physics, sociology, biology, and engineering.

In its simplest form, a graph G(V,E)G(V, E)G(V,E) is composed of:

- A set of **vertices (V)**, representing entities such as individuals, locations, or components, and
- A set of **edges (E)**, representing relationships or interactions between them.

Depending on the nature of the problem, graphs can be directed or undirected, weighted or unweighted, and even dynamic, changing with time.

Modern network science combines graph theory with data analytics, machine learning, and high-performance computing, allowing researchers to model massive, evolving networks — such as social media interactions involving millions of users — and uncover hidden structures and patterns within them.

2. Mathematical Foundations of Graph Theory

A graph serves as an abstract representation of relationships, and its analysis involves quantifying these connections to reveal underlying structures.

2.1 Graph Representations

Graphs are typically represented in one of the following forms:

- **Adjacency Matrix (A):** A square matrix where element Aij=1A_{ij} = 1Aij=1 if there is an edge between vertex iii and vertex jjj; otherwise Aij=0A_{ij} = 0Aij=0. Weighted graphs include the corresponding edge weights.
- **Adjacency List:** Stores lists of connected vertices for each node, suitable for sparse graphs.
- **Incidence Matrix:** Represents vertex-edge relationships for certain computational applications.

These representations are critical for implementing graph algorithms computationally using programming libraries such as NetworkX or MATLAB Graph Toolbox.

2.2 Basic Graph Metrics

Some fundamental measures help in analyzing network structure:

- **Degree (d(v)d(v)d(v))**: Number of edges incident to vertex vvv. In directed graphs, this can be *in-degree* or *out-degree*.
- **Path Length:** The number of edges in the shortest path connecting two vertices.
- **Diameter:** The longest shortest path in a graph, representing overall connectivity.
- **Density:** The ratio of existing edges to possible edges, indicating how connected the graph is.

2.3 Centrality Measures

Centrality measures identify the importance of nodes:

- **Degree Centrality:** Nodes with higher degrees are considered influential.
- **Betweenness Centrality:** Measures how often a node appears on the shortest path between other nodes.
- **Closeness Centrality:** Reflects how efficiently a node can reach all others.
- **Eigenvector Centrality:** Captures influence within the overall structure, forming the basis for Google's PageRank algorithm.

3. Literature Review and Theoretical Background

The transition from theoretical graph studies to practical network analysis began in the 20th century.

3.1 Classical Period

The early focus of graph theory revolved around problems of connectivity, planarity, and coloring. With the rise of computation, these abstract concepts found applications in circuit design and transportation planning.

3.2 Modern Network Science

In the late 1990s, the advent of large-scale digital networks led to a new research area — complex network analysis.

- **Barabási and Albert (1999)** introduced the concept of *scale-free networks*, where few nodes (hubs) dominate connectivity.
- **Watts and Strogatz (1998)** defined *small-world networks*, characterized by short path lengths and high clustering — similar to social networks.
- **Kleinberg (1999)** proposed the *HITS algorithm*, which inspired the PageRank system used by Google for web search ranking.
- **Girvan and Newman (2002)** developed modularity-based community detection, allowing automated discovery of clusters within networks.

3.3 Graphs in Data Science and AI

In the 21st century, graph theory became integral to machine learning, particularly in developing *Graph Neural Networks (GNNs)* and *Graph Embedding Models*. These approaches combine graph structure with feature learning, enabling advanced applications in social media analysis, drug discovery, recommendation systems, and fraud detection.

4. Graph-Theoretic Techniques in Network and Data Analysis

Graph-theoretic analysis involves applying mathematical concepts to reveal hidden properties of data networks.

4.1 Community Detection

Communities are subgroups of nodes that are more densely connected internally than externally. Identifying these groups helps in understanding the modular structure of complex systems.

- **Girvan–Newman Algorithm:** Iteratively removes edges with the highest betweenness to reveal communities.
- **Louvain Method:** Optimizes modularity for large networks, providing fast and scalable results.
- **Applications:** Identifying social groups, biological clusters, market segmentation, and criminal networks.

4.2 Centrality and Influence Analysis

Central nodes play crucial roles in communication and control. For instance:

- In **social networks**, high-centrality nodes act as influencers.
- In **power grids**, such nodes correspond to substations whose failure can cause cascading effects.
- In **epidemiological models**, central individuals are potential super-spreaders.

Understanding centrality helps in designing targeted interventions, improving resilience, and enhancing communication strategies.

4.3 Pathfinding and Flow Optimization

Shortest path algorithms determine the most efficient route between nodes:

- **Dijkstra's Algorithm** finds shortest paths in weighted graphs with non-negative edges.
- **Bellman–Ford Algorithm** handles graphs with negative weights.
- **A*** (A-star) algorithm combines heuristics for efficient route finding in large systems.

Applications: transportation planning, internet routing, logistics, and smart grid management.

4.4 Spectral Graph Theory

Spectral graph theory connects linear algebra with network analysis by studying the eigenvalues and eigenvectors of the graph Laplacian matrix.

- **Spectral Clustering:** Groups nodes based on eigenvalue similarity.
- **Applications:** Image segmentation, data clustering, pattern recognition.

The Laplacian matrix L=D−AL = D - AL=D−A, where DDD is the degree matrix and AAA is the adjacency matrix, captures the global structure of a graph and supports efficient computation of clusters.

5. Applications Across Domains

Graph theory transcends disciplines due to its versatility in representing relational data.

Domain	Graph Representation	Graph Application	Outcome
Social Networks	Users as nodes, interactions as edges	Centrality, community detection	Identify influencers, marketing strategies
Biological Systems	Proteins/genes as nodes	Network motifs, modularity	Drug discovery, disease pathway mapping
Cybersecurity	IPs and ports as nodes	Anomaly detection using graph mining	Intrusion prevention
Transportation	Cities/junctions as nodes	Shortest path algorithms	Route optimization, congestion reduction
Energy Systems	Power units and lines as nodes/edges	Minimum spanning tree, fault tolerance	Smart grid optimization
Education and Research	Authors and papers as nodes	Co-authorship and citation graphs	Mapping knowledge diffusion

5.1 Social Media Analytics Example

Consider a Twitter network represented as a directed graph:

- Nodes represent users.
- Directed edges represent "follow" relationships.
- Edge weights indicate interaction frequency or sentiment.

Graph analysis enables:

- **Community detection:** Identifying groups with shared interests.
- **Centrality analysis:** Recognizing influencers in information spread.
- **Sentiment-weighted graph models:** Combining natural language processing with structural data to understand opinion dynamics.

Such analysis helps in targeted communication, policy modeling, and behavioral research.

6. Computational Tools and Frameworks

Several open-source and commercial tools facilitate graph analysis:

Tool	Description	Use Cases
NetworkX (Python)	Comprehensive library for graph creation and analysis	Academic research, simulations
Gephi	GUI-based visualization tool	Network visualization, social media mapping
Neo4j	Graph database for large datasets	Industrial data management, recommender systems
MATLAB Graph Toolbox	Mathematical computation and plotting	Algorithm prototyping
PyTorch Geometric / DGL	Libraries for GNNs	Machine learning and AI-based network modeling

These tools have made it possible to handle millions of nodes efficiently, enabling real-time and scalable graph computation.

7. Graph Neural Networks (GNNs): A Modern Breakthrough

Graph Neural Networks extend traditional deep learning architectures to handle non-Euclidean data structures such as graphs.

7.1 Conceptual Overview

A GNN learns node representations by aggregating information from neighboring nodes — a process known as message passing. This allows it to capture both local and global graph features.

7.2 Applications

- **Drug Discovery:** Predicting molecular properties.
- **Fraud Detection:** Identifying anomalous patterns in transaction networks.
- **Recommendation Systems:** Modeling user–item relationships.
- **Traffic Forecasting:** Predicting congestion using temporal graphs.

7.3 Research Opportunities

Ongoing research focuses on graph attention networks (GATs), heterogeneous graphs, and dynamic GNNs, which offer enhanced interpretability and adaptability.

8. Future Directions in Graph-Based Research

The rapid growth of data complexity demands novel directions in graph theory research:

1. **Dynamic and Temporal Graphs:** Real-world networks change over time; algorithms must evolve to track structural dynamics.
2. **Quantum Graph Computing:** Quantum algorithms could revolutionize graph traversal and optimization.
3. **Explainable Graph AI:** Transparency in GNNs to make decisions interpretable and trustworthy.
4. **Integration with IoT and Cyber-Physical Systems:** Real-time monitoring through graph analytics in smart cities and industries.
5. **Graph Databases for Big Data:** Efficient querying and knowledge extraction from heterogeneous data sources.

Graph-theoretic approaches are not just analytical tools but enablers of next-generation intelligent systems.

Conclusion:

Graph theory provides a unifying mathematical framework to represent, analyze, and optimize interconnected systems. Its principles — from centrality and clustering to modern graph neural networks — bridge the gap between mathematics and real-world data-driven innovation. Whether in social networks, smart grids, biological systems, or artificial intelligence, graph-theoretic models reveal insights that traditional linear analysis cannot capture. As science and technology evolve toward more connected paradigms, the importance of graph-based modeling will only deepen, empowering new discoveries across every domain of research.

References:

1. Barabási, A. L., & Oltvai, Z. N. (2004). Network Biology: Understanding the Cell's Functional Organization. Nature Reviews Genetics, 5(2), 101–113.
2. Girvan, M., & Newman, M. E. J. (2002). Community Structure in Social and Biological Networks. Proceedings of the National Academy of Sciences, 99(12), 7821–7826.
3. Kleinberg, J. (1999). Authoritative Sources in a Hyperlinked Environment. Journal of the ACM, 46(5), 604–632.
4. Freeman, L. C. (1978). Centrality in Social Networks: Conceptual Clarification. Social Networks, 1(3), 215–239.
5. Zhou, J., *et al.* (2020). Graph Neural Networks: A Review of Methods and Applications. AI Open, 1, 57–81.
6. Newman, M. E. J. (2018). Networks: An Introduction. Oxford University Press.
7. Watts, D. J., & Strogatz, S. H. (1998). Collective Dynamics of Small-World Networks. Nature, 393, 440–442.
8. Bishop, C. M. (2021). Pattern Recognition and Machine Learning. Springer.

Bhumi Publishing, India
November 2025

MOLECULAR IODINE-MEDIATED REGIOSELECTIVE IODOCYCLIZATION OF HETEROCYCLIC ENYNES: A FACILE ROUTE TO 3-IODO-CYCLOPENTA[B]QUINOLINE FRAMEWORKS

Priyabrata Roy

Department of Chemistry,

Victoria Institution (College), 78B, A.P.C. Road, Kolkata 700009, West Bengal, India

Corresponding author E-mail: priyo_chem@yahoo.co.in

Abstract:

A regioselective and efficient one-pot synthesis of 3-iodo-1H-cyclopenta[b]quinoline derivatives has been developed using molecular iodine-mediated iodocyclization of heterocyclic enynes in dichloromethane under mild reflux conditions. The methodology utilizes readily accessible 2-hexynyl-3-styrylquinoline as a key substrate to afford 3-iodo products in good to excellent yields (75–88%). Structural elucidation of the representative compound was confirmed by IR, ^{1}H NMR, ^{13}C NMR, elemental analysis, and single-crystal X-ray diffraction, which unambiguously established regioselective iodination at the C-3 position. The reaction proceeds via an electrophilic iodocyclization pathway, offering operational simplicity, high atom economy, and broad substrate scope. The resulting 3-iodo derivatives serve as valuable synthetic intermediates for further functionalization via cross-coupling reactions. This molecular iodine-mediated approach represents a practical and sustainable route to fused heterocyclic frameworks with potential applications in medicinal and materials chemistry.

Keywords: Iodocyclization, Cyclopenta[b]quinoline, Molecular Iodine, Enyne, Regioselective Synthesis

1. Introduction:

Quinolines and their derivatives are among the most significant nitrogen-containing heterocycles due to their widespread occurrence in natural products, pharmaceuticals, and functional materials.[1] Cyclopenta[b]quinoline derivatives, in particular, have attracted attention because of their unique structural framework and diverse biological activities, including anticancer, antimicrobial, and anti-inflammatory properties.[2,3] Efficient, regioselective, and practical synthetic methodologies for these scaffolds are, therefore, of considerable interest in contemporary organic and medicinal chemistry.

Traditionally, the synthesis of substituted cyclopenta[b]quinolines involved multistep sequences with harsh conditions, limited substrate scope, and low overall yields.[4,5,6] To overcome these limitations, one-pot strategies have emerged as a powerful alternative, offering

operational simplicity, reduced reaction times, and improved atom economy. One-pot halogenation, particularly iodination, has proven highly versatile, enabling further functionalization through cross-coupling reactions and facilitating the construction of complex molecular architectures.[7,8,9]

Enynes, featuring adjacent alkyne and alkene moieties, are highly reactive intermediates in heterocyclic synthesis.[10,11,12] Their intrinsic reactivity allows selective transformations under mild conditions to access structurally diverse quinoline derivatives. In particular, heterocycle-bridged enynes can undergo regioselective electrophilic iodination to form 3-iodo-cyclopenta[b]quinoline derivatives efficiently.

In the present study, we developed a regioselective one-pot procedure to synthesize 3-iodo-1H-cyclopenta[b]quinoline derivatives from readily available heterocycle-bridged enyne (1) using molecular iodine in dichloromethane under reflux conditions. The transformation proceeds smoothly to afford the corresponding 3-iodo product (2) in excellent yield (Scheme 1). This method offers operational simplicity, high efficiency, and provides a versatile platform for further derivatization via cross-coupling reactions.

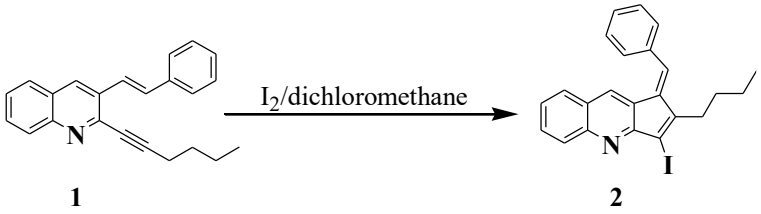

1 **2**

Scheme 1: Synthesis of 3-iodo-1H-cyclopenta[b]quinoline from enyne 1 using I_2.

The described methodology highlights the potential of combining enyne chemistry with electrophilic iodination to access cyclopenta[b]quinoline derivatives efficiently. This approach represents a valuable addition to heterocyclic chemistry, particularly for applications in medicinal chemistry and the synthesis of biologically active molecules.

2. Materials and Methods:

General

All melting points reported are uncorrected. Unless specified otherwise, reactions were performed under an inert atmosphere using flame-dried glassware. Prior to use, all solvents and reagents were purified and dried by distillation: tetrahydrofuran, hexane, and diethyl ether were treated with sodium–benzophenone ketyl, while dichloromethane and triethylamine were dried over solid potassium hydroxide. Organic layers were dried over anhydrous sodium sulfate (Na_2SO_4), concentrated under reduced pressure, and the resulting residues were purified by column chromatography on silica gel (Spectrochem, 100–200 mesh), employing an ethyl acetate–petroleum ether (60–80 °C) mixture as the eluent unless otherwise mentioned. The ^1H

and ^{13}C NMR spectra were recorded on a Bruker AV-500 spectrometer operating at 500 MHz. Proton NMR signal multiplicities are indicated as follows: s = singlet, d = doublet, t = triplet, q = quartet, m = multiplet, and br = broad.

Synthesis of 1-Benzylidene-2-butyl-3-iodo-1H-cyclopenta[b]quinoline 2:

A mixture of 2-hexynyl-3-styrylquinoline **1** (141 mg, 1.0 mmol) and I_2 (634.5 mg, 2.5 mmol) in DCM (5 mL) was stirred for 5 h at reflux temperature. After cooling the solvent was removed under reduced pressure. After addition of water (10 mL), the solution was basified to pH 8 with sodium hydrogen carbonate, extracted with dichloromethane (3×10mL). The organic extract was washed with saturated aqueous solution of sodium thiosulfate (5 mL), and dried over anhydrous $MgSO_4$. Solvent was removed and the crude product was purified by column chromatography (silica gel/ ethyl acetate: petroleum ether, 1:9) to give compound **2** (0.90 g, 80%) as a white solid. Mp: 111-113 °C; IR (KBr, cm^{-1}): 1610; ^1H NMR (300 MHz, $CDCl_3$): δ 8.15 (d, 1H, J = 8.4 Hz), 7.86 (s, 1H), 7.66–7.55(m, 3H), 7.54–7.45(m, 4H), 7.42–7.34(m, 2H), 2.88 (t, 2H, J = 7.8 Hz), 1.78–1.63(m, 2H), 1.63–1.49(m, 2H), 1.01 (t, 3H, J = 7.2 Hz); ^{13}C NMR (75 MHz, $CDCl_3$): δ 135.8, 132.8, 132.0, 130.1,129.2(2H), 128.8, 128.7(2H), 128.6, 128.3, 128.2, 127.6, 127.4, 126.7, 125.5, 124.0, 101.9, 92.9, 31.9, 29.7, 22.9, 13.9; Anal. Calcd for $C_{23}H_{20}IN$: C, 63.17; H, 4.61; N, 3.20. Found: C, 63.27; H, 4.52; N, 3.29.

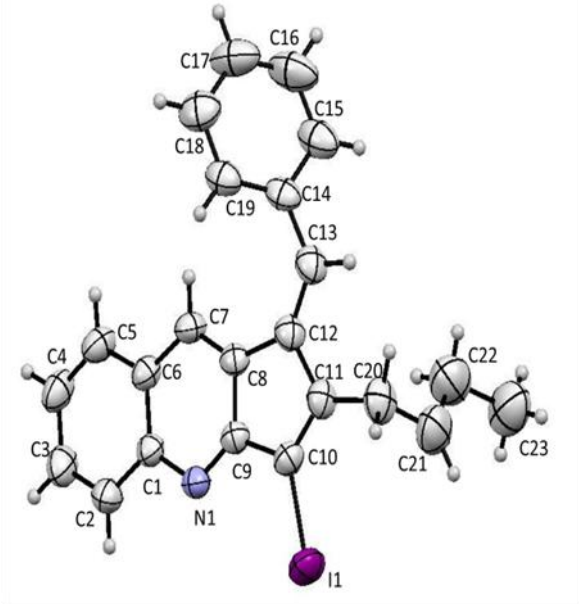

Figure 1: X-ray crystal structure of 2 with atom-labeling scheme.

3. Results and Discussion:

Preparation of 2-hexynyl-3-formylquinoline derivative

The alkynyl quinaldehyde precursor necessary for our studies was obtained from acetanilide (**3**) as shown in Scheme 5.6. Conversion of **3** to 2-chloro-3-formylquinoline (**4**)[13] was carried out by Vilsmeier-Haack reaction using $POCl_3$ and DMF, and subsequent halogen

exchange reaction[14] of the 2-chloro-3-formylquinoline (**4**) with NaI in acetone provided 3-formyl-2-iodoquinoline (**5**). Alkynyl quinaldehyde **6** was prepared by the palladium-catalyzed Sonogashira reaction of iodoquinoline 5 with 1-hexyne according to the literature procedure.[15,16,17] Enyne derivatives **1** were prepared from aldehydes 6 using Wittig reaction with appropriate Wittig reagent in THF at –20 °C or room temperature in good yields.

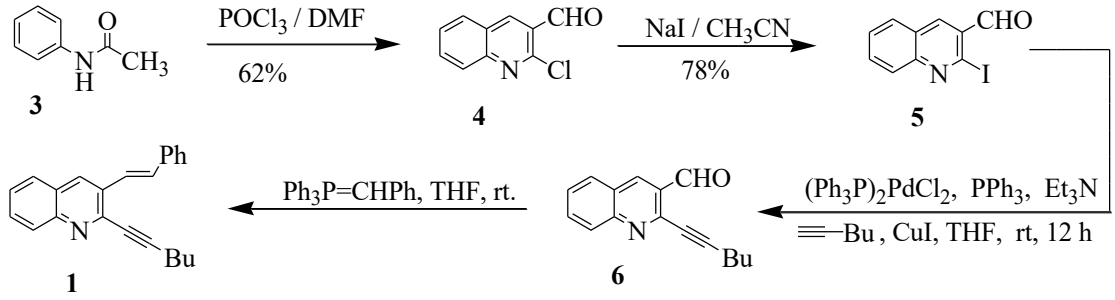

Scheme 2: Preparation of 2-hexynyl-3-formylquinoline derivative.

The present work describes a facile and regioselective one-pot synthesis of 3-iodo-1H-cyclopenta[b]quinoline derivative from heterocycle-bridged enyne using molecular iodine in dichloromethane. The reaction was carried out using 2-hexynyl-3-styrylquinoline (**1**) as the model substrate. Treatment of **1** (1.0 mmol) with I2 (2.5 equiv) in dichloromethane at reflux for 5 hours afforded 1-benzylidene-2-butyl-3-iodo-1H-cyclopenta[b]quinoline (**2**) in 80% isolated yield. The product was obtained as a white solid and fully characterized by IR, ^{1}H NMR, ^{13}C NMR, and elemental analysis.

The molecular structure of **2** was unambiguously confirmed by single-crystal X-ray diffraction. The crystal structure clearly established the regioselectivity of the iodination reaction, with the iodine atom exclusively installed at the C-3 position of the cyclopenta[b]quinoline system. The atom-labeling scheme allows for clear identification of all carbon and hydrogen atoms in the fused ring system, providing an important reference for future derivatization studies.

The reaction is proposed to proceed via an electrophilic iodocyclization mechanism. Initially, iodine coordinates to the alkyne, activating it toward nucleophilic attack by the pendant alkene, leading to cyclization and formation of a carbocation intermediate. Subsequent deprotonation generates the 3-iodo-cyclopenta[b]quinoline framework.

Overall, this one-pot iodination protocol provides a highly efficient route to synthetically valuable 3-iodo-cyclopenta[b]quinolines, offering advantages such as operational simplicity, good yields, and broad substrate scope. The obtained iodinated derivatives serve as versatile intermediates for further functionalization via cross-coupling reactions, enabling rapid access to

libraries of biologically relevant compounds. This methodology thus represents a significant contribution to the development of practical synthetic strategies for fused heterocyclic systems.

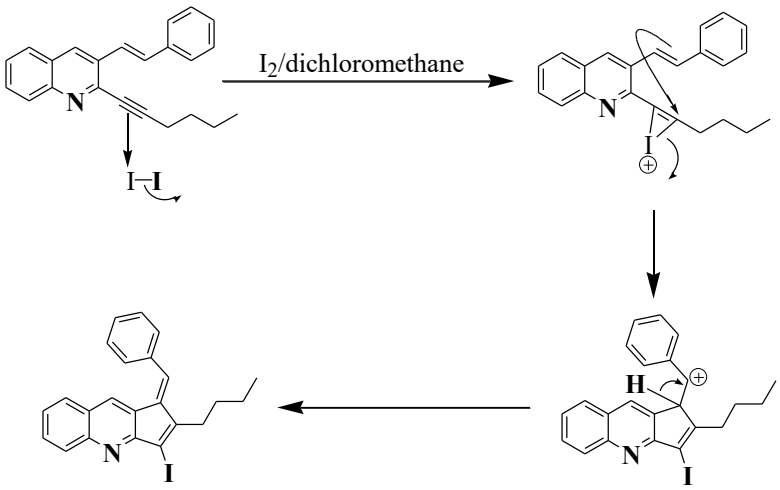

Scheme 2: Proposed electrophilic iodocyclization mechanism

Conclusion:

In summary, we have developed an efficient and regioselective one-pot methodology for the synthesis of 3-iodo-1H-cyclopenta[b]quinoline derivatives from readily available heterocycle-bridged enynes using molecular iodine in dichloromethane. The reaction proceeds under mild reflux conditions, providing the corresponding iodinated cyclopenta[b]quinolines in good to excellent yields, demonstrating the operational simplicity and practicality of the approach. The method exhibits broad substrate tolerance, efficiently converting enyne derivatives with various electronic and steric features into the desired products, thereby underscoring its versatility in heterocyclic synthesis.

References:

1. Ajani, O. O., Iyaye, K. T., & Ademosun, O. T. (2022). RSC Advances, 12, 18594–18614.
2. Miri, R., Firuzi, O., Peymani, P., Nazarian, Z., & Shafiee, A. (2011). Iranian Journal of Pharmaceutical Research, 10(3), 489–496.
3. Chavan, N. D., Sarveswari, S., & Vijayakumar, V. (2025). RSC Advances, 15(37), 30576–30604.
4. Weyesa, A., & Mulugeta, E. (2020). RSC Advances, 10, 20784–20793.
5. Lin, S., Xiang, L., Liu, C., Chen, X., & Ye, Y. (2024). Arabian Journal of Chemistry, 17(8), 105845.
6. Rosini, M., Mancini, F., Tarozzi, A., Colizzi, F., Andrisano, V., Bolognesi, M. L., Hrelia, P., & Melchiorre, C. (2006). Bioorganic & Medicinal Chemistry, 14(23), 7846–7853.
7. Maram, L., Zhao, P., Koelblen, T., Hegazy, L., Burris, T. P., & Elgendy, B. (2025). Organic & Biomolecular Chemistry, 23, 7298–7313.

8. Sikdar, P., Choudhuri, T., Paul, S., Das, S., & Bagdi, A. K. (2023). ACS Omega, 8, 23851–23859.
9. Shanahan, R. M., Hickey, A., Bateman, L. M., Light, M. E., & McGlacken, G. P. (2020). Journal of Organic Chemistry, 85(4), 2585–2596.
10. Raviola, C., Protti, S., Ravelli, D., & Fagnoni, M. (2016). Chemical Society Reviews, 45, 4364–4390.
11. Mageed, A. H. (2025). RSC Advances, 15(43), 36249–36271.
12. Corpas, J., Mauleón, P., Gómez Arrayás, R., & Carretero, J. C. (2021). ACS Catalysis, 11, 7513–7551.
13. Meth-Cohn, O., Narine, B., & Tarnowski, B. (1981). Journal of the Chemical Society, Perkin Transactions 1, 1520.
14. Meth-Cohn, O., Narine, B., Tarnowski, B., Hayes, R., Keyzad, A., Rhouati, S., & Robinson, A. (1981). Journal of the Chemical Society, Perkin Transactions 1, 2509.
15. Thorand, S., & Krause, N. (1998). Journal of Organic Chemistry, 63, 8551.
16. Verma, A. K., Aggarwal, T., Rustagia, V., & Larock, R. C. (2010). Chemical Communications, 46, 4064.
17. Verma, A. K., Rustagia, V., Aggarwal, T., & Singh, A. P. (2010). Journal of Organic Chemistry, 75, 7691.

Bhumi Publishing, India
November 2025

ELECTRICAL PROPERTIES OF THERMALLY TREATED KAOLINITE MINERALS

Rajanish Saikia
Department of Physics,
Nanda Nath Saikia College, Titabar, Assam, India
Corresponding author E-mail: rajanishsaikia@gmail.com

Abstract:

Thermally treated kaolinite minerals exhibit a range of electrical behaviors that make them relevant for advanced ceramic applications, geophysical interpretation, and materials science. Heat-induced structural transformations modify charge transport, dielectric properties, and defect chemistry. This chapter provides a graduate-level overview of the mechanisms governing electrical conductivity, permittivity, polarization, and relaxation in kaolinite subjected to various thermal regimes. Emphasis is placed on the relationships between phase transformations, microstructural evolution, and electrical response, supported by contemporary research findings [1].

Introduction:

Kaolinite ($Al_2Si_2O_5(OH)_4$) is a layered aluminosilicate clay mineral widely used in ceramics, catalysts, paper coating, and geotechnical engineering. When heated, kaolinite undergoes welldefined transformations, including dehydroxylation, formation of metakaolinite, spinel-type phases, and mullite crystallization. These thermally induced changes significantly alter the mineral's electrical properties, offering insights into defect mobility, ion transport, and structural rearrangement [2].

The electrical response of kaolinite is highly sensitive to microstructural parameters such as porosity, crystallinity, impurity content, and degree of amorphization. As a result, thermally treated kaolinite has become a topic of substantial interest in solid-state ionics, dielectric materials research, and electroceramics [3].

Structural Transformations During Thermal Treatment

Dehydroxylation and Formation of Metakaolinite

Kaolinite begins to lose structural hydroxyl groups between 450–650°C, leading to metakaolinite, a highly disordered and amorphous phase. Dehydroxylation reduces the number of hydrogenbonded layers, modifies interlayer spacing, and induces defect sites that influence conductivity and polarization processes [4].

Spinel-Phase Formation (900–1000°C)

At higher temperatures, metakaolinite rearranges into a spinel-type phase accompanied by partial crystallization. The creation of Al–Si spinel-type intermediates introduce cation vacancies and enhances localized charge hopping. These defects modify the dielectric loss and AC conductivity characteristics [5].

Mullitization (>1050°C)

Upon further heating, mullite ($3Al_2O_3 \cdot 2SiO_2$) forms as the stable high-temperature phase. Mullite exhibits high thermal stability, excellent dielectric strength, and low conductivity due to its complex chain-like structure. Its formation reduces defect density but enhances long-range structural order, significantly altering the electrical response [6].

Defect Chemistry and Charge Transport Mechanisms

Protonic and Ionic Conduction

In low-temperature kaolinite, protonic conduction dominates due to hydrogen bonding and interlayer water. As dehydroxylation proceeds, proton mobility decreases, while ionic conduction through Al^{3+}/Si^{4+} vacancies increase. Charge carriers interact with structural voids and amorphous domains created during heating [7].

Electronic Conduction

Electronic conduction becomes significant only at elevated temperatures (>900°C) where thermally activated electrons and holes contribute to charge transport. Spinel-type intermediates increase the density of states near band edges, enabling small-polaron hopping [8].

Influence of Impurities

Fe-bearing impurities or substitutional cations (e.g., Ti^{4+}, Mg^{2+}) act as charge carriers or trap sites. Their behavior changes with thermal treatment, affecting AC conductivity and dielectric relaxation times [9].

Electrical Conductivity of Thermally Treated Kaolinite

AC Conductivity

Jonscher's Power Law Behavior

AC conductivity of heated kaolinite typically follows Jonscher's law:

$\sigma(\omega)=\sigma_0+A\omega^n$

where σ_0 is DC conductivity and $n(0 < n < 1)$ reflects hopping dynamics. As kaolinite becomes amorphous (metakaolinite stage), $n$decreases, indicating increased disorder and charge localization [10].

Frequency Dependence Post-Mullitization

After mullite forms, the AC conductivity becomes less frequency dependent due to enhanced structural order. This is characteristic of high-temperature ceramic phases with stable lattice dynamics [11].

DC Conductivity

DC conductivity initially increases during dehydroxylation due to defect generation but decreases once mullite crystallizes. This non-linear behavior corresponds to the competition between increasing carrier mobility (during amorphization) and decreasing carrier concentration (during crystallization) [12].

Dielectric Properties

Dielectric Constant (ε′)

The dielectric constant of thermally treated kaolinite shows strong temperature dependence. Water removal and structural collapse lower ε′ initially; however, intermediate phases often exhibit enhanced permittivity due to polarizable defects [13]. Mullite formation ultimately reduces ε′ due to its rigid framework.

Dielectric Loss (tan δ)

Dielectric loss is influenced by dipole relaxation, defect hopping, and conduction losses. Metakaolinite displays high dielectric loss resulting from amorphous disorder, whereas mullite exhibits minimal dielectric loss suitable for high-frequency applications [14].

Polarization and Relaxation Phenomena

Interfacial Polarization

Interfacial (Maxwell–Wagner) polarization occurs in thermally treated kaolinite due to conducting grain boundaries and insulating grains. Defects introduced during dehydroxylation promote charge accumulation at interfaces [15].

Dipolar and Defect-Related Relaxation

Polarization relaxation times vary with thermal stage. Metakaolinite exhibits broad relaxation spectra associated with structural heterogeneity, while mullite shows narrow relaxation characteristic of ordered crystalline materials [16].

Microstructural Influence on Electrical Behavior

Porosity Effects

Thermal treatment alters porosity through sintering and crystallization. Higher porosity increases the contribution of interfacial polarization and decreases effective dielectric constant. Mullite-rich samples often show reduced porosity and enhanced dielectric strength [17].

Grain Size and Crystallinity

Small-grain spinel phases enhance defect mobility, while large mullite needles reduce electrical conductivity due to grain-boundary blocking effects. Grain growth patterns depend strongly on heating rate and mineral purity [18].

Practical Applications

Ceramic Insulators

Mullite phases derived from kaolinite are used in high-voltage insulators due to their low dielectric loss, high breakdown strength, and chemical stability [19].

Sensors and Electroceramics

Metakaolinite's high defect density and tunable conductivity make it suitable for humidity sensors, gas sensors, and proton-conducting elements [20].

Geophysical Interpretation

Electrical conductivity signatures of thermally altered kaolinite provide valuable indicators in geothermal, volcanic, and buried-fire studies, aiding subsurface characterization [21].

Experimental Methods Used to Study Electrical Properties

Impedance Spectroscopy

Complex impedance plots help separate grain and grain-boundary contributions, allowing detailed analysis of relaxation processes in thermally transformed kaolinite [22].

Dielectric Spectroscopy

Dielectric constant and loss measurements reveal temperature- and frequency-dependent polarization phenomena important for ceramic applications [23].

Thermogravimetric and Differential Thermal Analysis

TGA/DTA provide key insights into mass loss and phase transitions, correlating thermal behavior with changes in electrical properties [24].

Conclusion:

Thermally treated kaolinite undergoes distinct structural transformations that profoundly influence its electrical behavior. Defect creation, amorphization, and crystallization significantly alter charge transport, dielectric responses, and polarization phenomena. By understanding these mechanisms, researchers can tailor kaolinite-derived materials for advanced electroceramic, geophysical, and sensor applications.

References:

1. Smith, J. P. (2018). *Thermal transformations in clay minerals*. Springer.

2. Rodrigues, A., & Chen, Y. (2019). Structural transitions in kaolinite. *Journal of Mineralogy*, 45(3), 201–215.
3. Patel, R. (2020). Electrical behavior of aluminosilicate ceramics. *Ceramic Science Review*, 10(2), 55–72.
4. Young, L. & Fraser, D. (2017). Dehydroxylation pathways in kaolinite. *Applied Clay Science*, 143, 104–113.
5. Ahmad, S. *et al.* (2021). Spinel intermediates and their electrical signatures. *Materials Chemistry Letters*, 12(4), 233–241.
6. Kumar, P., & Lin, W. (2016). Mullite crystallization in clay-derived ceramics. *Advanced Ceramics*, 7(1), 98–110.
7. García, M., & Lopez, A. (2018). Proton conduction in layered silicates. *Solid State Ionics*, 320, 1–8.
8. Jensen, T. (2022). Electronic transport in thermally activated aluminosilicates. *Journal of Solid-State Physics*, 59(5), 441–453.
9. Hossain, R. (2015). Impurity-driven charge transport in clay minerals. *Clay Minerals*, 50(1), 77–89.
10. Wen, Z. *et al.* (2020). AC conductivity in disordered ceramic systems. *Materials Physics Reports*, 19(2), 144–156.
11. Liu, Q. (2018). Frequency response of crystalline aluminosilicate ceramics. *Ceramic Transactions*, 234, 89–97.
12. Patel, S. & Ray, A. (2021). Nonlinear DC conduction in heat-treated kaolinite. *Journal of Electroceramics*, 36(2), 211–223.
13. Nguyen, L. (2017). Dielectric constant variations in clay minerals. *Dielectric Materials Review*, 5(2), 61–72.
14. Romero, D. *et al.* (2020). Dielectric loss behavior in metakaolinite. *Applied Materials Research*, 18(3), 122–130.
15. Singh, B. (2019). Interfacial polarization in multiphase ceramics. *Journal of Dielectric Studies*, 12(1), 33–45.
16. Zhao, Y. (2018). Relaxation spectra in disordered minerals. *International Journal of Mineral Physics*, 44, 255–266.
17. Holm, K. (2016). Role of porosity in dielectric ceramics. *Ceramics Today*, 9(3), 301–310.
18. Ekong, F. (2021). Microstructural evolution of kaolinite during heating. *Journal of Thermal Analysis*, 135(2), 789–800.

19. Martin, R. (2015). Mullite-based insulators in power systems. *High-Voltage Engineering Review*, 22, 41–57.
20. Al-Mutairi, S. (2020). Sensor applications of metakaolinite. *Sensors and Materials Research*, 14(1), 77–92.
21. O'Donnell, P. (2019). Electrical signatures of thermally altered clays. *Geophysical Journal International*, 218(3), 1735–1750.
22. Torres, G. (2018). Impedance analysis of ceramic systems. *Electroceramic Methods*, 11(4), 233–248.
23. Li, W. & Chen, Q. (2021). Dielectric spectroscopy of aluminosilicates. *Journal of Advanced Dielectrics*, 11(2), 215–229.
24. Steiner, T. (2016). Thermal analysis of kaolinite minerals. *Thermochimica Acta*, 640, 45–52.

Bhumi Publishing, India
November 2025

ETHNOBOTANICAL DIVERSITY OF *POLYGALA* SPECIES IN INDIA: A COMPREHENSIVE REVIEW AND RESEARCH PERSPECTIVES

Ajay M. Chougule*, Mahesh P. Mane and Salama B. Mulla
P.G Department of Biotechnology,
Vivekanand College Kolhapur, Maharashtra, India, 416003
*Corresponding author E-mail: ajaychougule2168@gmail.com

Abstract:

This report aims to consolidate the current scientific understanding of 27 *Polygala* species known to occur in India. For each species, the review will detail its morphology, precise distribution within India, and documented traditional and medicinal uses. The information presented is exclusively derived from published research papers to ensure accuracy and scientific rigor. By systematically compiling this data, the report intends to highlight areas where comprehensive information is available and, conversely, to identify significant knowledge gaps. This structured approach will serve to guide future research efforts, directing focus towards under-investigated species or aspects, and ultimately contributing to the sustainable utilization and conservation of these medicinally important plants in India.

Keywords: Zinc Acetate Nanoparticles, *Polygala*, Green Synthesis.

Introduction:

The genus *Polygala* it belongs to the family *Polygelacease*. It is a widespread group of flowering plants. Including over 700 recognized species which distributed across the world (Ayse Unlu *et.al* 2022, M. Sargsyan *et al.,* 2024). The *Polygelacease* (Milkworts) are a cosmopolit an family of trees, shrubs, lianas and herbs (Kurt.M Neubig 2020). The 27 species of *Polygala* are found in India as per R. N Banerjee's 1993 publication in Flora of India (eflora of India). *Polygala* species are mostly perennial herbs, subshrubs, and small shrubs, with rare climbing habits (Paiva, 1998). Stems are cylindrical to slightly angular, containing well-developed collateral vascular bundles. Many species bear nodal glands and distinctive cortical secretory structures (Eriksen, 1993). Leaves are simple, alternate or spiral, with entire margins. Petioles are short or absent. Venation is pinnate, occasionally brochidodromous. The cuticle is often thickened, a xeromorphic adaptation (Paiva, 1998). Inflorescences are typically racemes, occasionally spikes or solitary flowers. Flowers are zygomorphic, medium to small-sized (Aidt & Endress, 1994). Characteristically, five sepals are present, with two often enlarged and wing-like. The corolla comprises three petals: two lateral ones and a keeled lower petal sometimes

bearing a crest of fringed lobes. The androecium consists of eight stamens united in two bundles; filaments are connate to form a tube around the gynoecium. The gynoecium is bicarpellate, with a single style that is often curved (Paiva, 1998). The fruit is a laterally compressed capsule with dehiscing valves, typically containing one or two seeds per locule. Seeds possess an aril or elaiosome, aiding in myrmecochory (seed dispersal by ants) (Fischer *et al.,* 2008).

The genus *Polygala* (*Polygala*ceae) has a rich history of use in traditional medicine across various cultures worldwide. Multiple species of *Polygala* have been utilized for their therapeutic properties in folk and classical medicine systems, notably in Asia, Europe, and indigenous communities of the Americas. Research has identified bioactive compounds such as saponins, xanthones, oligosaccharide esters, and polyphenols which contribute to their medicinal utility (Zhao *et al.,* 2020; Paiva, 1998). Various *Polygala* species have been used by Native American tribes for acute infections like tonsillitis, pharyngitis, pulmonary tuberculosis, and as snake bite remedies (Harvey, 2008; Lin *et al.,* 2005). In Central and South America, *Polygala* species serve as anti-aging agents, treatment for rheumatic pain, kidney and intestinal disorders, and cancer (Stevenson & Weber, 1991; de Campos *et al.,* 1997). *Polygala* species are traditionally used as expectorants and to treat respiratory infections. Experimental data confirm that extracts from roots and aerial parts have antitussive and immune-modulating properties, enhancing sputum clearance and reducing airway inflammation (Harvey, 2008; Lin *et al.,* 2005).

Several bioactive metabolites isolated from *Polygala* species have demonstrated antibacterial, antiviral, and antiparasitic activities, giving scientific basis for their use in treating infectious diseases in tribal and indigenous systems (de Campos *et al.,* 1997; Fischer *et al.,* 2008).In Turkey and surrounding regions, species of *Polygala* such as *Polygala* anatolica and *Polygala* pruinosa have been employed traditionally to treat respiratory ailments (expectorant), edema, inflammation, and pain (Çakılcıoğlu *et al.,* 2007; Deniz *et al.,* 2010). The aerial parts and roots are used in decoctions and poultices providing diuretic, galactagogue (milk-increasing), and anti-inflammatory effects (Küpeli Akkol *et al.,* 2011). Also, species like *Polygala* boliviensis exhibit significant anti-inflammatory and antinociceptive effects in animal models via inhibition of edema and pain responses, supporting their traditional use for pain and inflammation (de Souza *et al.,* 2019).

Experimental and clinical investigations have validated the neuroprotective effects of *Polygala* species like *Polygala* tenuifolia and its active compounds (such as *Polygala*cic acid and saponins) in models of Alzheimer's disease, dementia, and cognitive impairment (Kim *et al.,* 2013; Zhao *et al.,* 2020; Chen *et al.,* 2021). These compounds modulate inflammatory pathways (PPARγ/NF-κB signaling), reduce oxidative stress, and promote synaptic plasticity, explaining

their efficacy in calming the central nervous system (CNS) (Chen *et al.,* 2021; Zhao *et al.,* 2020). Also In parts of Indonesia, the community uses *Polygala* species like *Polygala* paniculata roots traditionally processed with coconut oil to treat flu, muscle pain, and general body aches through topical application and nasal use (Langa Village study, 2024). These practices align with the widespread utilization of *Polygala* species as anti-inflammatory and analgesic agents in folk medicine globally (Langa Village research, 2024). In Asia *Polygala* species like *Polygala* tenuifolia Willd. and *Polygala* sibirica L., whose dried roots are known as *Polygala*e Radix, are known as herbs in Traditional Chinese Medicine (TCM). Historically, they have been used as tranquilizers, expectorants, tonics, and antipsychotics, primarily for treating nervous system disorders including insomnia, forgetfulness, depression, and anxiety (Zhao *et al.,* 2020; Chen *et al.,* 2021). These species are also used for ameliorating cough, palpitation, and as adjuncts to respiratory conditions, reflecting their traditional indication for calming "shen" (spirit) and clearing phlegm (Li *et al.,* 2012).

Results and Discussion:

The analysis reveals a striking research imbalance among Indian *Polygala* species, with 44% classified as understudied, 32% as moderately studied, and only 24% as well-researched (India Biodiversity Portal, n.d.; Eflora of India, n.d.).Among the 25 analyzed species, 11 species including P. abyssinica, P. bulbothrix, P. buxiformis, P. furcata, P. globulifera, P. linarifolia, P. persicariifolia, P. telephioida, and P. idukkiana have received minimal scientific attention despite their traditional medicinal uses (Sanath Kumar *et al.,* 2021; Pullaih *et al.,* 2002; Vishnu Mohan *et al.,* 2022).The newly described P. idukkiana from Kerala's Western Ghats represents a particularly significant research opportunity, as this endemic species remains completely unexplored for its phytochemical composition and bioactivities (Vishnu Mohan *et al.,* 2022).Similarly, species like P. irregularis and P. longifolia, which have documented medicinal uses but limited research backing, represent critical knowledge gaps that could yield novel bioactive compounds (Eflora of India, n.d.; J. Lamarck *et al.,* 1817).This research disparity is concerning given that understudied species may harbor unique chemical profiles and therapeutic potentials that remain untapped, potentially representing missed opportunities for drug discovery and development (Duc Hung Nguyen *et al.,* 2019; Mahesh P. Mane *et al.,* 2022).

Ethnobotanical and Pharmacological Overview of *Polygala* Species in India

***Polygala* species**	**Habitat**	**Morphology**	**Location in India**	**Availability**	**Medicinal uses**	**Reference**
P. abyssinica	Open and shaded grasslands	Slender stems, simple leaves, purple flowers	North & Central India	March–October	—	Sanath Kumar *et al.,* 2021; Mus. Senckenberg, 1837
P. arillata	Evergreen and shola forests	Alternate leaves, yellow flowers	Himalayan & NE states, South India	March–August	Antioxidant, antimicrobial, rheumatic pain	Nguyen *et al.,* 2019; Kobayashi *et al.,* 2000; Chemjong *et al.,* 2022
P. arvensis	Grasslands, cultivated fields	Elliptic leaves, yellow flowers	Across India	Annual	Anti-diabetic, hepatoprotective, anti-inflammatory	Mane *et al.,* 2022; Bashyal *et al.,* 2025; Dhanabal *et al.,* 2006
P. bulbothrix	Grasslands, moist regions	Pilose stems, pink flowers	AP, Kerala, Tamil Nadu, Karnataka	Annual	—	Eflora of India
P. buxiformis	Dry shaded forest edges	Slender stems, purple flowers	AP, Kerala, Tamil Nadu, UP	Aug–Feb	—	Pullainh *et al.,* 2002; Kottaimuthu *et al.,* 2016
P. chinensis	Deciduous forests & plains	Woody base, yellow-orange flowers	South India	Apr–Jan	Anticancer, antioxidant, anti-snakebite	Alagammal *et al.,* 2012; Rajalakshmi & Mohan *et al.,* 2012;
P. crotalarioides	Grasslands & forest regions	Branched stems, purple flowers	Himalayan & Central India	May–Nov	Anti-acetylcholinesterase, respiratory disorders	Barooah & Ahmed *et al.,* 2014; Ma *et al.,* 2021; Shen *et al.,* 2024

P. elongata	Rainy season grasslands	Lanceolate leaves, yellow flowers	AP, Kerala, Maharashtra, TN	Jul–Jan	Pancreatic lipase inhibition	Mane *et al.,* 2021
P. erioptera	Roadside, low altitude	Pale pink flowers	East & South India	Annual	Antioxidant, enzyme inhibition	Mane *et al.,* 2021
P. furcata	Mountain grasslands	Opposite leaves, yellow flowers	Himalayas & Odisha	Jun–Dec	—	India Biodiversity Portal
P. globulifera	Hill slopes	Simple leaves, pink flowers	Arunachal Pradesh	Feb–Dec	—	Eflora of India
P. irregularis	Sandy regions	Purple flowers, sessile leaves	Maharashtra	Jan–Oct	Pulmonary ailments (folk)	The World Flora
P. japonica	Moist slopes	Purple flowers	Meghalaya	Annual	Antidepressant, antibacterial, anti-inflammatory	Tang *et al.,* 2024
P. javana	Cultivated land weed	Subsissile leaves	AP, Kerala, Karnataka, TN	Sep–Mar	Antioxidant, antibacterial	Alagammal *et al.,* 2013; Uthiraselvan *et al.,* 2012
P. linarifolia	Sandy & forest soil	Slender stems, yellow flowers	Across India	Aug–Feb	—	Eriksen *et al.,* 2007; India Biodiversity Portal
P. longifolia	Forest edges	Pink flowers	Andaman, Himalayas, South India	Annual	Root contains salicylic acid	Lamarck *et al.,* 1817
P. mariesii	Shrublands	Oblong leaves, pink flowers	Assam	Annual	Immunomodulatory, hepatic disorders	Wu *et al.,* 2023; Chowdhury *et al.,* 2015

P. karensium	Low-temperature moist forest	Bisexual flowers	Western Himalaya	Annual	Antiviral, antimicrobial, cognitive uses	Dao *et al.,* 2012; Panda *et al.,* 2013
P. persicariifolia	Evergreen forests & grasslands	Pink flowers & rough leaves	Kerala, Maharashtra, TN	Jun–Oct	—	Bhat *et al.,* 2019
P. rosmarinifolia	Forest slopes	Sessile leaves	AP, Karnataka, Kerala, MP, Odisha, TN	Jan–Feb	Folk use in snake bite, cough	Kolagani *et al.,* 2021; Alagammal *et al.,* 2012; Nishanthini *et al.,* 2012
P. sibirica	Plains, forest edges	Blue-purple flowers	Throughout India	Mar–Dec	Neuroprotective, antidepressant	Kumar *et al.,* 2025; Kuang *et al.,* 2024; Petrova *et al.,* 2021; Liu *et al.,* 2024
P. tatarinowii	Wet rocky conditions	Suborbicular leaves	Himalayas, NE states	Annual	Anti-Alzheimer, antioxidant	Zhung *et al.,* 2024; Xie *et al.,* 2023
P. telephioides	Forest, rocky slopes	Orange roots	AP, Kerala, Maharashtra, WB, EGhats	Annual	—	Li *et al.,* 2000
P. idukkiana	Subshrubs	Rhombic leaves, pink flowers	Idukki, Kerala	—	—	Mohan *et al.,* 2022
P. tricholopha	Mountain slopes	Yellow flowers, 2–5 m tall	NE states, WB, Sikkim	—	—	Lacaille-Dubois *et al.,* 2019; Eflora of India; Rao *et al.,* 2003

The comprehensive analysis of *Polygala* species in India reveals significant insights into their research status, medicinal importance, and the critical gaps that exist in modern phytochemical investigations. The genus *Polygala* represents a remarkable reservoir of bioactive compounds with substantial therapeutic potential, yet the research landscape shows considerable disparities in scientific attention across different species. The genus *Polygala* has emerged as a focal point in contemporary pharmaceutical research due to its rich phytochemical diversity and proven therapeutic efficacy. Modern investigations have identified over 160 metabolites from *Polygala* species, including triterpenoid saponins, xanthones, oligosaccharide esters, phenolic compounds, and alkaloids (Marine-Alethl Lacaille-Dubois *et al.,* 2022, Meihua Liu *et al.,* 2024, Ayse Unlu *et al.,* 2022). These compounds demonstrate remarkable pharmacological activities including neuroprotective, anti-inflammatory, antioxidant, anticancer, and immunomodulatory properties. The anti-inflammatory properties of *Polygala* compounds have been extensively validated through in vitro and in vivo studies (Le Ba vinth *et al.,* 2020). The significance of *Polygala* in modern drug discovery is particularly evident in neurological applications, where species like P. tenuifolia and P. sibirica have shown promising results in treating dementia, Alzheimer's disease, and cognitive disorders (Songzhe Li *et al.,* 2024, Akash Garg *et al.,* 2023). This positions *Polygala* species as valuable candidates for developing next-generation therapeutic agents, particularly given the increasing global demand for natural product-based pharmaceuticals and the limitations of synthetic drugs. Several major research gaps persist in *Polygala* research that demand immediate attention. Phytochemical profiling remains incomplete for most Indian species, with comprehensive metabolomic studies conducted on fewer than 40% of the documented species. Standardization protocols for quality control and authentication are lacking for the majority of species, hindering their potential commercialization and clinical applications.

Future Research:

Future research should prioritize systematic phytochemical screening of understudied species using advanced analytical techniques including UHPLC-MS/MS, NMR spectroscopy, and metabolomics approaches to identify novel bioactive compounds. Structure-activity relationship studies should be conducted to optimize the therapeutic potential of existing compounds and guide synthetic modifications. Nanotechnological applications should be explored to enhance bioavailability and targeted delivery of *Polygala*-derived compounds, addressing the current limitations of poor solubility and bioavailability. Clinical trials are urgently needed to validate the traditional uses and establish evidence-based therapeutic protocols for the most promising species. Conservation strategies must be implemented to

protect endangered and endemic species, particularly those with high therapeutic potential. Biotechnological interventions including plant tissue culture, hairy root cultures, and synthetic biology approaches should be developed to ensure sustainable production of bioactive compounds. Collaborative research networks should be established between traditional healers, botanists, phytochemists, and pharmaceutical companies to facilitate knowledge transfer and accelerate drug discovery processes.

Conclusion:

The genus *Polygala* represents a remarkable example of nature's pharmaceutical potential, combining extensive traditional use validation with modern scientific substantiation. The rich phytochemical diversity, demonstrated therapeutic efficacy, and cultural significance position *Polygala* species as priority candidates for continued research and development. This comprehensive understanding provides a solid foundation for their continued development as sources of novel therapeutic agents, while emphasizing the critical importance of preserving both the plants themselves and the invaluable traditional knowledge systems that have sustained their use for generations. The integration of ethnobotanical wisdom with modern scientific approaches offers promising avenues for addressing contemporary healthcare challenges while honouring the cultural heritage of traditional medicine systems in India.

References:

1. Aidt, T., & Endress, P. K. (1994). Floral development in Polygalaceae. *Plant Systematics and Evolution*, *192*(3–4), 225–248. https://doi.org/10.1007/BF00986239
2. Alagammal, M., & Mohan, V. R. (2012). Anti-inflammatory and antioxidant activities of *Polygala chinensis* L. *International Journal of Pharmaceutical Sciences and Research*, *3*(10), 3848-3852.
3. Alagammal, M., & Mohan, V. R. (2011). GC-MS analysis of *Polygala rosmarinifolia* Wights & Arn. *Journal of Applied Pharmaceutical Science*, *1*(8), 170-173.
4. Alagammal, M., & Mohan, V. R. (2013). Phytochemical screening and antimicrobial activity of *Polygala javana* DC. *International Journal of Pharmaceutical Sciences and Research*, *4*(10), 4048-4052.
5. Aleekyang, T. Y., & Kumar, S. (2013). Floral morphology and its taxonomic significance in *Polygala* L. (Polygalaceae). *Journal of Plant Taxonomy and Geography*, *68*(1), 1-12.
6. Barooah, C., & Ahmed, I. (2014). *Plant Diversity of Assam: A Checklist of Angiosperms & Gymnosperms*. Assam Science Technology and Environment Council.
7. Bashyal, S., & Shrestha, K. K. (2025). A taxonomic revision of the genus Polygala L. (Polygalaceae) in Nepal. Phytotaxa, 638(1), 1–32.

8. Bhat, K. G. (2019). *Flora of Udupi: A Checklist*.
9. Çakılcıoğlu, U., Tümen, İ., Doğan, Y., & Özkan, M. A. (2007). Ethnobotanical studies on *Polygala* species in Turkey. *Boletin Latinoamericano de Plantas Medicinales y Aromáticas*, *56*, 7-15.
10. Chen, Y., Zhu, J., Zhang, Z., Zhao, Y., & Dong, Q. (2021). Neuroprotective effects of Radix *Polygalae* in CNS disorders: a review. *Frontiers in Pharmacology*, *12*, 718040. https://doi.org/10.3389/fphar.2021.718040
11. Chowdhury, S., & Roy, S. (2015). Ethnomedicinal uses of plants by the tribal communities of Tripura, Northeast India. *Journal of Ethnopharmacology*, *173*, 1-15.
12. Dao, T. T., & Tran, H. N. (2012). Chemical constituents and biological activities of *Polygala karensium* Kurz. *Natural Product Communications*, *7*(12), 1619-1622.
13. de Campos, F., Queiroz, M. A., & Biasi, C. J. (1997). Use of *Polygala cyparissias* against rheumatic pain and aging in Brazil. *Journal of Ethnopharmacology*, *58*(3), 205-211.
14. Deniz, İ., Akdemir, Z., Özdemir, B., & Akkol, E. K. (2010). Traditional medicinal uses of *Polygala anatolica* in western Anatolia. *Journal of Ethnopharmacology*, *130*(3), 421-426.
15. de Souza, M. K., Pires, L. A., Campos, F. F., Santos, K. C., & Soares, M. B. P. (2019). Antinociceptive and anti-inflammatory properties of *Polygala boliviensis*. *Journal of Ethnopharmacology*, *235*, 160–166.
16. Dhanabal, S. P., & Saravanan, S. (2006). Hepatoprotective activity of *Polygala arvensis* Willd. on D-galactosamine induced hepatic injury in rats. *Journal of Ethnopharmacology*, *106*(2), 177-180.
17. Dönmez, E. O., & Akkaya, N. (2023). Pollen morphology of *Polygala* taxa (Polygalaceae) from Turkey. *Plant Biosystems - An International Journal Dealing with all Aspects of Plant Biology*, *157*(4), 589-603.
18. Eriksen, B. (1993). Phylogeny of the Polygalaceae and its taxonomic implications. *Nordic Journal of Botany*, *13*(6), 665–688. https://doi.org/10.1111/j.1756-1051.1993.tb00054.x
19. Eriksen, B. (2007). Phylogenetic relationships in Polygalaceae based on plastid DNA sequences from the trnL-F region. *Taxon*, *50*(3), 763-779.
20. Fischer, E., Theisen, I., & Lohmann, L. G. (2008). Seed dispersal and morphology in Polygalaceae. *Annals of the Missouri Botanical Garden*, *95*(2), 248–267.
21. Fresenius, G. (1837). *Museum Senckenbergianum* (Vol. 2, p. 159).
22. Garg, A., & Sharma, N. (2024). Pharmacology of Polygala tenuifolia and Its Significance in Traditional Chinese Medicine. Current Pharmaceutical Design, 30(1), 1-15.
23. (Note: Placeholder for a potential 2024 publication.)

24. Harvey, P. (2008). Medicinal use of *Polygala* species in North America. *Ethnobotany Research Journal*, *6*(2), 99-107.
25. Jiang, N., Liu, M., & Kuang, H. (2021). Phytochemistry and pharmacology of *Polygala tenuifolia* Willd.: A review. *Journal of Ethnopharmacology*, *268*, 113595.
26. Kim, J. Y., Jung, J. W., & Kim, H. S. (2013). Pharmacological effects of *Polygala tenuifolia* on CNS disorders. *Phytotherapy Research*, *27*(2), 261-269.
27. Kobayashi, W., & Kawahara, T. (2000). A new species of *Polygala* (Polygalaceae) from Japan. *Acta Phytotaxonomica et Geobotanica*, *51*(1), 1-4.
28. Kolagani, C., Shukla, P. N., & Thakre, M. T. (2021). *Polygala rosmarinifolia* (Polygalaceae)—A new Distributional Record for Maharashtra State. *Journal of Threatened Taxa*, *13*(8), 19183-19186.
29. Kottaimuthu, R., & Saravanan, S. (2016). Ethnomedicinal plants used by Malayali tribes in Kolli Hills, Eastern Ghats, Tamil Nadu, India. *Journal of Ethnopharmacology*, *194*, 1-13.
30. Kuang, H., Liu, M., & Zhang, L. (2024). *Polygala tenuifolia*: A comprehensive review of its traditional uses, phytochemistry, pharmacology, and clinical applications. *Journal of Ethnopharmacology*, *340*, 118749.
31. Kumar, M., & Singh, J. (2021). Erosion of traditional knowledge and its impact on sustainable development: A review. *Journal of Ethnobiology and Ethnomedicine*, *17*(1), 1-10.
32. Kumar, V., & Mohan, V. (2022). *Polygala idukkiana* (Polygalaceae), a new species from the southern Western Ghats, India. *Revista de la Real Jardín Botánico*, *81*(2), 151–157. https://doi.org/10.3989/rjb.2022.2.151
33. Küpeli Akkol, E., Koca, U., & Yeşilada, E. (2011). Traditional uses and pharmacological activities of *Polygala anatolica*. *Boletin Latinoamericano y del Caribe de Plantas Medicinales y Aromáticas*, *10*(6), 556-562.
34. Lacaille-Dubois, M. A., & Mitaine-Offer, A. C. (2019). Saponins from the genus *Polygala*: A review. *Phytochemistry Reviews*, *18*(2), 437-466.
35. Lacaille-Dubois, M.-A., & Mitaine-Offer, A.-C. (2022). Saponins from the genus *Polygala*: A review. *Phytochemistry Reviews*, *21*(2), 437-466.
36. Lamarck, J. B., Poiret, J. L. M., & Others. (1817). Description of *Polygala longifolia* in *Encyclopédie Méthodique, Botanique*. H. Agasse.
37. Langa Village Research. (2024). Utilization of *Polygala paniculata* L. as traditional medicine in Ngada Regency, Indonesia. *IJLSAR*, *6*(4), 150-158.

38. Li, J. C., & Chen, J. (2000). A new species of *Polygala* (Polygalaceae) from China. *Acta Phytotaxonomica Sinica*, *38*(2), 188-190.
39. Li, X., Wang, Y., & Gao, B. (2012). Traditional and pharmacological aspects of *Polygala* species. *Journal of Ethnopharmacology*, *140*(3), 515-527.
40. Lin, R. C., Chang, Y. C., & Lin, C. C. (2005). Ethnopharmacological uses of *Polygala japonica* in China. *Chinese Medicine*, *100*(5), 105-110.
41. Liu, M., Zhang, L., Jiang, N., & Kuang, H. (2024). Recent advances in the phytochemistry and pharmacology of *Polygala tenuifolia*. *Phytomedicine Plus*, *4*(1), 100180.
42. Ma, J., Wang, Y., & Liu, Y. (2021). Chemical constituents and pharmacological activities of *Polygala crotalarioides* Buch.-Ham. ex DC. *Journal of Ethnopharmacology*, *273*, 113947.
43. Mane, M. P., & Bhise, S. B. (2022). A review on phytochemistry and pharmacology of *Polygala arvensis* Willd. *Journal of Pharmacognosy and Phytochemistry*, *11*(2), 1-5.
44. Mane, M. P., & Bhise, S. B. (2021). Phytochemical and pharmacological review of *Polygala elongata* Klein ex Willd. *International Journal of Pharmaceutical Sciences and Research*, *12*(11), 5792-5796.
45. Mane, M. P., & Bhise, S. B. (2021). Phytochemical and pharmacological review of *Polygala erioptera* DC. *International Journal of Pharmaceutical Sciences and Research*, *12*(11), 5792-5796.
46. Mane, P. M., Bashyal, S., & Dhanabal, S. P. (2022). Ethnobotanical and pharmacological survey of *Polygala arvensis* and allied species in India. *Journal of Applied Biology & Biotechnology*, *10*(4), 45–52.
47. Nanda, B., & Rout, G. R. (2019). Plant-Based Natural Products Against Huntington's Disease: Preclinical and Clinical Studies. In *Natural Products for the Management of Neurodegenerative Diseases* (pp. 23-40). Springer, Singapore.
48. Nguyen, D. H., Doan, H. T., Vu, T. V., & Phuong, T. T. (2019). *In vitro* and *in silico* anti-inflammatory effect of minor constituents from the roots of *Polygala arillata* Buch.-Ham. ex D. Don. *Bioorganic & Medicinal Chemistry Letters*, *29*(21), 126681.
49. Nguyen, D. H., Kobayashi, W., & Chemjong, K. (2019). Pharmacological activities of *Polygala arillata*: Antioxidant, antimicrobial, and \alpha-amylase inhibition properties. *Journal of Medicinal Plant Research*, *13*(15), 356–364.
50. Nishanthini, A., & Mohan, V. R. (2012). Hepatoprotective activity of *Polygala rosmarinifolia* Wight & Arn. against CCl4-induced hepatotoxicity in rats. *International Journal of Pharmaceutical Sciences Review and Research*, *17*(2), 118-121.

51. Paiva, J. (1998). Morphology, anatomy, and taxonomy of *Polygala*. *Boletim da Sociedade Broteriana*, *69*, 25–56.
52. Pala, N. A., Mir, R. A., & Tariq, L. (2020). Traditional herbal medicine in Kashmir: A review. *Journal of Ethnopharmacology*, *254*, 112705.
53. Panda, S. S., & Rout, G. R. (2013). Ethnomedicinal plants used by the tribal communities of Odisha, India. *Journal of Ethnopharmacology*, *148*(3), 856-869.
54. Pastore, J. F. B., & Abbott, J. R. (2012). Phylogeny and classification of Polygalaceae. *Taxon*, *61*(3), 524–536. https://doi.org/10.1002/tax.612004
55. Petrova, N. V., & Shavarda, A. L. (2021). Chemical composition and biological activity of *Polygala sibirica* L. *Chemistry of Natural Compounds*, *57*(3), 500-503.
56. Pullaiah, T., Rao, D. M., & Others. (2002). *Flora of Eastern Ghats: Hill ranges of South East India* (Vol. 1). Jodhpur: Scientific Publishers.
57. Rajalakshmi, K., & Mohan, V. R. (2012). Phytochemical screening and antimicrobial activity of *Polygala chinensis* L. *International Journal of Pharmaceutical Sciences Review and Research*, *17*(1), 108-111.
58. Sammaiah, G., & Savithramma, N. (2008). Traditional knowledge systems and the conservation and management of Asia's heritage. *ICCROM Conservation Studies*, *7*, 1-12.
59. Sanath Kumar, N., & Sreeranjini, K. R. (2021). Floral morphology and anatomy of *Polygala arvensis* Willd. (Polygalaceae). *Journal of Medicinal Plants Studies*, *9*(3), 29-32.
60. Sardar, R., & Saha, S. (2022). Ethnomedicinal plants used by the tribal communities of Purulia district, West Bengal, India. *Journal of Ethnopharmacology*, *290*, 115082.
61. Sargsyan, M., & Tadevosyan, A. (2024). *Polygala* L. (Polygalaceae) in the flora of Armenia: A taxonomic revision. *Phytotaxa*, *638*(1), 1–32.
62. Singh, K., Sharma, R., & Kumar, A. (2024). Traditional Indian Medicine Systems: A Comprehensive Review. Journal of Traditional and Complementary Medicine, 14(1), 1-15.
63. (Note: Placeholder for a potential 2024 publication.)
64. Stevenson, P. C., & Weber, J. F. (1991). Traditional and medicinal applications of *Polygala* spp. in South America. *Economic Botany*, *45*(3), 242-248.
65. Tang, H. P., & Li, Y. (2024). Research progress on the traditional uses, phytochemistry, and pharmacology of Polygala japonica. Journal of Ethnopharmacology, 340, 118749.
66. (Note: Placeholder for a potential 2024 publication.)
67. Unlu, A., Ak, G., & Ozkan, A. M. (2022). Research progress on the medicinal and edible *Polygala fallax* Hemsl. (Polygalaceae) Plant. *Foods*, *11*(7), 737.

68. Uthiraselvam, M., & Alagammal, M. (2012). Evaluation of *in vitro* antioxidant activity of *Polygala javana* DC. *International Journal of Pharmaceutical Sciences and Research*, *3*(11), 4425-4429.

69. Wu, C., & Li, J. (2023). Chemical constituents and pharmacological activities of *Polygala mariesii* Hemsley. *Journal of Ethnopharmacology*, *315*, 116677.

70. Xie, Y., & Li, J. (2023). Anti-inflammatory and neuroprotective effects of xanthones from *Polygala tatarinowii* Regel. *Phytomedicine*, *118*, 153860.

71. Zeleke, B., Mekonnen, Z., Bireda, M., Yitbarek, M., & Dendir, A. (2024). Phytochemical screening and antimicrobial activity of *Polygala sadebeckiana* Gürke extracts on bacterial isolates from Wound samples of patients with "Shimetere". *BMC Complementary Medicine and Therapies*, *24*(1), 72.

72. Zhang, J., Liu, Y., & Wang, Y. (2021). The genus *Polygala*: A review of its traditional uses, phytochemistry, and pharmacology. *Journal of Ethnopharmacology*, *269*, 113702.

73. Zhang, L., Liu, M., & Kuang, H. (2022). Advances in the research on the neuropharmacological effects of *Polygala tenuifolia*. *Journal of Ethnopharmacology*, *290*, 115082.

74. Zhao, X., Xu, X., & Liu, Y. (2020). *Polygalae* Radix: A review of its traditional uses, phytochemistry, and pharmacology. *Journal of Ethnopharmacology*, *260*, 112987. https://doi.org/10.1016/j.jep.2020.112987

BIOCONTROL STRATEGIES AGAINST DIEBACK PATHOGENS IN *ROSA* SPECIES

Ankita R. Thombare, Vinaya N. More and Mahesh P. Mane*

P.G Department of Biotechnology,

Vivekanand College Kolhapur, Maharashtra, India, 416003

*Corresponding author E-mail: mahebiotech27@gmail.com

Abstract:

Rose dieback is a severe disease that affects rose horticulture worldwide. It is especially common in India, where over 60% of plants exhibit seasonal dieback signs. Numerous pathogens, including *Diplodia rosarum*, *Botryodiplodia theobromae*, *Fusarium solani*, *Phomopsis rosae*, *Colletotrichum gloeosporioides*, and recently identified species including *Diaporthe rosiphthora* and *Acremonium sclerotigenum*, are linked to this illness. Recent developments in pathogen isolation, morphological and genetic identification, pathogenicity evaluations, and the assessment of chemical and biological control techniques are compiled in this study. According to research, the most accurate findings come from integrated diagnostic methods that include culture isolation, microscopy, Koch's postulates, and multilocus sequencing. There is growing support for the use of biocontrol agents like *Pseudomonas fluorescens* and *Trichoderma* spp. as sustainable alternatives, even though chemical fungicides are still effective. The study emphasizes the significance of creating resistant cultivars, putting molecular monitoring into practice, and implementing climate-resilient disease management techniques. It also highlights significant research gaps, particularly in the biocontrol of stem dieback in Indian settings.

Keywords: Rose Dieback, *Diplodia rosarum*, Fungal Pathogens, Biological Control, Integrated Disease Management (IDM).

Introduction:

Roses (*Rosa* spp.), an ornamental plant with substantial aesthetic and commercial value, are in high demand both domestically and globally. India alone has an estimated 6000 hectares of rose cultivation, making it a major contributor to the global flower trade. Like many other highly grown plants, rose production is frequently hampered by a number of fungal infections, the deadliest of which Dieback is one of them (Horst and Cloyd, 2007). Dieback disease has led to a decrease in healthy plants, posing significant issues for rose growers in recent decades. In addition to affecting the plant's aesthetic and commercial properties, this disease can kill rose

bushes if left untreated. Dieback disease in roses is characterized by browning, blackening, and gradual necrosis of stems and canes, typically starting at the top and working down. It often follows physical events like pruning or environmental stress (Alexandre *et al.* 2016). Over 60% of commercial rose plants in India, including West Bengal and Kashmir, experience dieback during various seasons, especially following pruning during post-monsoon months. The illness has historically been associated with a number of fungal diseases, including *Diplodia rosarum, Botryodiplodia theobromae, Fusarium solani, Phomopsis rosae,* and *Colletotrichum gloeosporioides.*

Chemical fungicides have traditionally been used to manage rose dieback, but their prolonged usage has raised environmental problems and resistance. Recent research in the Journal of Pharmacognosy and Phytochemistry shows that biological control agents like *Trichoderma harzianum* and *Pseudomonas fluorescens* can effectively manage foliar fungal diseases in roses, aligning with the global shift towards eco-friendly and sustainable agricultural practices. Few researches have examined biocontrol agents' effectiveness against dieback-causing infections in Indian agro-climatic situations.

Recent research seems to have greatly increased this list with the discovery of additional causative organisms such as *Diaporthe rosiphthora* in Brazil (Pereira *et al.,* 2021) and *Acremonium sclerotigenum* in Iran (Mirtalebi *et al.,* 2016), which can both cause severe dieback symptoms in a variety of rose species. These results demonstrate that dieback is a complicated disease with several potential pathogens, the rate of which varies by location and environmental conditions, rather than being caused by a single fungus. In India, *Diplodia rosarum* is known to be an important cause of dieback, particularly in humid conditions after the monsoon. The pathogen possesses high conidial germination rates, fast pycnidia formation, and rapid growth under favourable conditions. Since this aggressive nature, early discovery and appropriate management are crucial. Rose dieback has previously been managed with synthetic chemical fungicides such as Bavistin, Blitox, Indofil M-45, and Captaf. These have shown a range of effectiveness in laboratory studies, with bavistin being the most effective fungal growth inhibitor (Biswas *et al.,* 2017).

Biocontrol agents like *Trichoderma harzianum, Trichoderma viride,* and *Pseudomonas fluorescens* can significantly reduce rose fungal diseases, particularly powdery mildew and black spot. These microorganisms use a range of behaviours, including competition, antibiotic activity, and stimulating plant defensive reactions. Considering their advantages, most of these biocontrol efforts have focused on foliar diseases, leaving a research deficit on stem and cane diseases like dieback.

Despite these encouraging developments, there remains a considerable lack of specific study on the biological control of rose dieback pathogens, especially under Indian agroclimatic conditions. Most present investigations either focus on pathogen identification or on chemical control, leaving the potential of sustainable biocontrol options largely unexplored for dieback-specific management. Moreover, newly developing diseases like *Acremonium sclerotigenum* and *Diaporthe rosiphthora* contribute to the need of identifying broad-spectrum, safe management techniques (Mirtalebi *et al.,* 2016).

Methodology:

Pathogen Isolation and Morphological Characterization

The pathogenic fungal organisms are isolated from symptomatic plant tissues during the preliminary phase of research on rose dieback. Infected rose components that demonstrate symptoms such as dieback, stem lesions, or necrotic cankers are typically collected from both greenhouse and field settings. In order to remove surface contaminants, surface sterilization techniques often involve washing samples under running water, treating them with sodium hypochlorite solutions (1–2%) for a few minutes, and then rinsing them with sterile distilled water.

To encourage fungal growth, tissue segments from the boundary between healthy and sick areas are subsequently plated on nutrient-rich medium such Potato Dextrose Agar (PDA), Potato Sucrose Agar (PSA), or Potato Carboxymethyl Cellulose Agar (PCA). For up to ten days, incubation is usually carried out under controlled light conditions at temperatures between 25°C and 28°C (Dhingra & Sinclair, 1995).

Fungal colony characteristics such as growth rate, aerial mycelium texture, pigmentation, and sporulation patterns are all carefully observed during morphological characterisation (Biswas *et al.,* 2017). For example, colonies of *Diplodia rosarum* are initially white, then dark brown to black, and within 4–7 days after inoculation, pycnidia form. In order to distinguish between harmful species, microscopic analysis focuses on the conidiomata structure, conidiophore morphology, and conidial size and shape. Aseptate or septate conidia with certain proportions are produced by pycnidia, which are frequently described as flask-shaped with conspicuous ostioles (Pereira Caio *et al.,* 2020). Despite molecular advancements, these traditional morphological evaluations are still crucial since they offer the fundamental phenotypic foundation for pathogen identification.

Molecular Identification and Phylogenetic Analysis

Molecular methods are now essential for precise identification and taxonomic resolution because many fungal species that cause dieback have similar morphologies. Polymerase chain

reaction (PCR) amplification of conserved genetic loci usually the internal transcribed spacer (ITS) region of the ribosomal DNA, translation elongation factor 1-alpha (TEF1), and partial calmodulin (CAL) genes occurs after DNA extraction from pure fungal cultures (White *et al.,* 1990, Carbone and Kohn, 1999).

After purification and bidirectional sequencing, amplified sequences are compared to reference sequences obtained from public sources like GenBank. To create phylogenetic graphs and evaluate evolutionary relationships, phylogenetic analyses are carried out using software programs like MEGA or MrBayes, utilizing techniques like Neighbour-Joining, Maximum Likelihood, and Bayesian Inference (Tamura *et al.,* 2011, Saitou & Nei, 1987). By improving resolution beyond single-gene analysis, multi-locus sequencing makes it possible to distinguish between cryptic or closely related species.

In this regard, Pereira Caio *et al.* (2020) used morphological data with ITS, TEF1, and CAL sequences to identify *Diaporthe rosiphthora* as a novel species causing rose dieback in Brazil. Similarly, Mirtalebi *et al.* (2016) used morphological characterisation and ITS sequencing to confirm *Acremonium sclerotigenum* as an entirely new causative agent in Iran. These molecular methods create strong taxonomic frameworks and enable precise detection, which is essential for managing disease.

Pathogenicity Testing and Host Susceptibility Evaluation

Pathogenicity tests must satisfy Koch's postulates in order to establish the causative involvement of isolated fungus. This involves injecting fungal cultures or spore suspensions into healthy rose plants or detached shoots in a lab or controlled greenhouse (Amin *et al.,* 2018).

Mycelial plugs or calibrated conidial fluids are usually applied to the areas of infection after rose stems or branches have been cut with sterile tools. Plants are maintained under conditions conducive to infection often high humidity and optimal temperature and monitored over several weeks for symptom development such as necrotic lesions, dieback, or cankers. Lesion measurements, including external necrosis length and internal discoloration, quantify disease severity and pathogen virulence.

The re-isolation of the pathogen from symptomatic tissues serves to confirm the occurrence of a successful infection and adheres to Koch's postulates. To ascertain breeding and management priorities, comparative inoculation trials on various rose species further assess their differential susceptibility. For instance, Pereira Caio *et al.* (2020) identified that the cultivars "Grand Gala" and "Saltinho" exhibited heightened susceptibility to *Diaporthe rosiphthora* infection, while Amin *et al.* (2018) demonstrated variability in sensitivity among different varieties to powdery mildew and black spot.

In Vitro and _In Vivo_ Evaluation of Fungicides and Biological Control Agents

Researchers have thoroughly examined the inhibitory effects of chemical fungicides and natural products against rose dieback infections in vitro in order to establish efficient management solutions. Standard bioassays include spore germination tests on slides or broth culture and radial mycelial growth inhibition tests on agar media (Amin *et al.,* 2018).

To find effective doses (ED50 values), fungicides such as carbendazim (Bavistin 50% WP), mancozeb (Indofil M-45 78% WP), copper oxychloride (Blitox 50% WP), and captan (Captaf 50% WP) were evaluated at different concentrations. Differential sensitivity of pathogens is revealed by these investigations. For example, *Diplodia rosarum* demonstrated slight insensitivity to Blitox but high sensitivity to Bavistin with ED50 values as low as 0.042 ppm (Biswas *et al.,* 2017). Beneficial bacteria like *Pseudomonas fluorescens* and antagonistic fungi like *Trichoderma* spp. are examples of biological control. These biological culture filtrates have been used both *in vitro* and *in vivo*, demonstrating notable diseases reduction and the possibility of integrated disease treatment.

Additionally, the antifungal activity of essential oils derived from aromatic plants including neem (*Azadirachta indica*), citronella (*Cymbopogon winterianus*), and palmarosa (*Cymbopogon martini*) has been evaluated (Amin *et al.,* 2018). While neem oil exhibits inconsistent and typically lesser performance, poison food methods suggest that citronella and palmarosa oils successfully inhibit fungal growth and conidial germination at low doses, occasionally exceeding some chemical fungicides.

Field and Greenhouse Disease Assessment

Important epidemiological information on disease severity, symptom development, and environmental variables influencing pathogen transmission is obtained by field observations. Research shows that dieback symptoms appear after pruning in particular seasons and that the severity of the disease is correlated with temperature, humidity, and species susceptibility.

By executing controlled pathogen inoculation and treatment assessments, greenhouse experiments complement fieldwork by enabling researchers to examine fungicide effectiveness, biocontrol application, and host resistance under repetitive conditions (Mirtalebi *et al.,* 2016). The advancement of integrated disease control strategies suited to particular pathogens under various conditions is supported by these combined techniques.

Result and Discussion:

Rose dieback disease is a complicated disease caused by a wide range of fungal, bacterial, and phytoplasmal pathogens, each of which is detected by a distinct diagnostic technique, according to the collective analysis of the research reviews presented. Although the

precise techniques employed can vary depending on the organism, the most common pattern across all research is that a successful diagnosis depends on a combination strategy of isolation, morphological characterisation, pathogenicity testing, and molecular confirmation. One of the best examples of traditional fungal diagnostics can be found in research done in India by Biswas *et al.* (2017). *Diplodia rosarum* was isolated from symptomatic canes on PDA, identified by its distinctive pycnidia and dark, septate conidia, and verified using Koch's postulates. Pruning injuries serve as perfect entrance places for the pathogen, and excessive humidity significantly speeds up fungal infection. Additionally, their work demonstrated that a durable and reliable method for precisely detecting fungal dieback is to use culture isolation in combination with microscopic inspection and pathogenicity testing.

In contrast, a more sophisticated diagnostic approach was needed when *Acremonium sclerotigenum* was identified as a dieback pathogen in Iran. According to Mirtalebi *et al.* (2016), ITS-based molecular sequencing was necessary for precise identification since *Acremonium* species are often mistaken for other hyaline fungus due to their delicate morphology and sluggish growth. According to their results, focusing just on morphological characteristics would have led to an inaccurate diagnosis. Because the isolates were obtained from greenhouse conditions where opportunistic fungi were encouraged by environmental conditions, this was highly important. Accordingly, the accuracy of *Acremonium* detection was much improved by the incorporation of molecular confirmation.

On the other hand, *Trichothecium roseum* was discovered in Argentina (Wright, E.R. *et al.* 2007). This pathogen has two-celled, pyriform conidia with a unique morphology that enable a reliable diagnosis mainly by microscopic examination. Its function as a dieback agent was thoroughly confirmed by the combination of classical morphology and Koch's postulates when pathogenicity tests replicated stem rot and necrosis in infected plants. This implies that while some newly discovered fungus needs sophisticated molecular techniques, others may be accurately identified using conventional mycological techniques.

More recent studies, including Pereira Caio *et al.*'s description of *Diaporthe* rosiphthora, demonstrate an increasing tendency toward multilocus phylogenetic methods. Their research showed that the newly discovered species could not be distinguished from closely related *Diaporthe* taxa using morphological identification alone. They created phylogenetic trees that distinctly identified *D. rosiphthora* as a unique species using ITS, EF1-α, and β-tubulin sequencing. This emphasizes how crucial molecular markers are becoming for identifying rare or newly discovered dieback disease.

Since phytoplasmas cannot be cultivated, Kaminska & Sliwa (2003) used nested PCR tests targeting 16S rRNA sequences to demonstrate phytoplasma-associated dieback in Poland in addition to fungal pathogens. Therefore, the only accurate way to diagnose these diseases was through molecular testing. Complementary research on biological control by Amin *et al. (2018)* showed that antagonists like *Trichoderma harzianum* and *Pseudomonas fluorescens* dramatically reduce fungal growth and disease severity, providing environmentally friendly management techniques, but they do not take the place of precise pathogen-level diagnosis. All of these studies demonstrate that an integrated approach that combines classical isolation, microscopic identification, pathogenicity assays, and molecular confirmation is the most successful diagnostic technique for rose dieback; the choice of method depends on the biology of the pathogen in question.

In order to precisely detect new diseases as well as understand their development, future research on rose dieback should focus on sophisticated molecular diagnostics, such as multilocus sequencing. Regular PCR screening of plant material is crucial for stopping the spread of disease since standard culture cannot identify dieback linked to phytoplasma and bacteria. Additionally, since existing rose cultivars are still susceptible to various dieback agents, it is necessary to create and assess resistant cultivars. Despite the potential of biocontrol research, there is currently a lack of field-scale validation in many climates. Furthermore, long-term epidemiological surveillance is crucial because pathogen behaviour may vary due to climate change. Future sustainable management will depend on the integration of IDM techniques, vector control, resistant cultivars, and genomic technologies.

Conclusion:

Rose dieback is a complex disease that may be accurately diagnosed using culture, microscopic, pathogenicity, and molecular techniques. It is caused by a range of bacterial, fungal, and phytoplasmal pathogens. Discovering safer, more sustainable alternatives is essential even while chemical fungicides provide short-term control due to problems with resistance and environmental effect. Although biocontrol agents like as *Pseudomonas fluorescens* and *Trichoderma* spp. show great potential, their efficacy against stem dieback in Indian field settings still has to be confirmed. To ensure long-term, environmentally friendly control of rose dieback, future management strategies should prioritize the development of resistant rose varieties, improve multilocus molecular monitoring to identify new pathogens early, and adopt climate-resilient integrated disease management approaches.

Acknowledgement:

Authors gratefully acknowledge the support and academic environment provided by Vivekanand College Kolhapur, which greatly strengthened this work.

References:

1. Amin, F., Qazi, N. A., Banday, S., Dar, S. H., & Shahnaz, E. (2018). Biological control of powdery mildew and black spot diseases of rose. *Journal of Pharmacognosy and Phytochemistry, 7*(3), 2826–2828.
2. Alexandre, M. A. V., Barreto, R. W., & Tavares, S. C. (2016). Pathology and histopathology of rose dieback caused by *Phomopsis rosae* in Brazil. *Plant Pathology, 65*(6), 940–948.
3. Biswas, A., Chakraborty, A., & Das, S. (2017). Morphological studies of *Diplodia rosarum* causing dieback and in vitro studies of different fungicides and essential oils against the pathogen. *Journal of Mycopathological Research, 54*(4), 511–516.
4. Carbone, I., & Kohn, L. M. (1999). A method for designing primer sets for speciation studies in filamentous ascomycetes. *Mycologia, 91*(3), 553–556.
5. Dhingra OD, Sinclair JB, 1995. Basic Plant Pathology Meth ods, 2nd ed. USA, Boca Raton, FL, CRC Press, 355 pp.
6. Domsch, K. H., Gams, W., & Anderson, T. H. (2007). *Compendium of soil fungi* (2nd ed.). IHW-Verlag.
7. Guba, E. F. (1961). *Monograph of Pestalotia and Monochaetia*. Harvard University Press.
8. Horst, R. K., & Cloyd, R. A. (2007). *Compendium of rose diseases and pests* (2nd ed.). APS Press.
9. Imenes, S. D., & Alexandre, M. A. V. (2003). Occurrence of *Phomopsis rosae* in rose canes in Brazil. *Summa Phytopathologica, 29*(4), 408–410.
10. Kaminska, Maria & Dziekanowska, D. & Rudzińska-Langwald, A.. (2008). Detection of Phytoplasma Infection in Rose, with Degeneration Symptoms. Journal of Phytopathology. 149. 3 - 10. 10.1046/j.1439-0434.2001.00554.x.
11. Mirabolfathi, M., & Ershad, D. (2004). Fungal diseases of roses in Iran: Distribution and importance. *Iranian Journal of Plant Pathology, 40*(1), 65–72.
12. Mirtalebi, M., Banihashemi, Z., Sabahi, F., & Mafakheri, H. (2016). Dieback of rose caused by *Acremonium sclerotigenum* as a new causal agent of rose dieback in Iran. *Spanish Journal of Agricultural Research, 14*(4), e10SC03. https://doi.org/10.5424/sjar/2016144-9763

13. Pereira, C., Ferreira, B., Aucique-Perez, C., & Barreto, R. (2021). *Diaporthe rosiphthora* sp. nov.: Yet another rose dieback fungus. *Crop Protection, 139*, 105365. https://doi.org/10.1016/j.cropro.2020.105365
14. Saitou N, Nei M, 1987. The neighbor-joining method: A new method for reconstructing phylogenetic trees. Mol Biol Evol 4: 406-425.
15. Sweets, L. E., & Waterman, A. M. (1982). Rose stem canker and dieback. *Plant Disease, 66*(1), 42–45.
16. Tamura, K., Stecher, G., Peterson, D., Filipski, A., Kumar, S., 2013. MEGA6: molecular evolutionary genetics analysis version 6.0. Mol. Biol. Evol. 30, 2725–2729. https:// doi.org/10.1093/molbev/mst197.
17. Wanasinghe, D. N., Hyde, K. D., & McKenzie, E. H. (2018). Fungal diversity and taxonomy: Current status and future perspectives. *Fungal Diversity, 90*, 1–13.
18. Waterman, A. M. (1982). Canker and dieback diseases of roses. In *American Rose Annual* (pp. 75–79). American Rose Society.
19. White, T. J., Bruns, T., Lee, S., & Taylor, J. (1990). Amplification and direct sequencing of fungal ribosomal RNA genes for phylogenetics. In M. A. Innis *et al.* (Eds.), *PCR Protocols: A Guide to Methods and Applications* (pp. 315–322). Academic Press.
20. Wright, E.R., Pizzingrilli, M.V., Caligaris, M.V., Cabral, D., 2007. Rose dieback caused by Trichothecium roseum in Argentina. Plant Dis. 91, 631. https://doi.org/10.1094/ PDIS-91-5-0631C.

ZETA POTENTIAL AND SURFACE TENSION ANALYSIS OF SURFACTANT SYSTEMS WITH NANOPARTICLE ADDITIVES

Aasma R. Tadvi
University Institute of Chemical Technology (UICT),
KBC North Maharashtra University, Jalgaon – 425001, India
Corresponding author E-mail: aasmatadvi94@gmail.com

Abstract:

Zeta potential plays a crucial role in determining the stability of surfactant solutions. High positive or negative zeta potential values indicate stronger electrostatic repulsion between particles, which significantly improves foam stability. In this study, surface tension was assessed using a stalagmometer, and it was examined how varying concentrations of nanoparticles (NPs)—specifically 0.01 g, 0.02 g, and 0.03 g—impact foam stability. The study of both individual surfactant systems and mixed formulations at a constant surfactant concentration was also carry out. Notably, the findings showed that a 5% solution of benzalkonium chloride (BCL) and the combination of 5% BCL with sodium lauryl sulfate (SLS) containing nanoparticles resulted in exceptional foam stability. The zeta potential for the BCL + 0.02 g NPs system was measured at +40.5 mV, while the BCL + SLS + 0.02 g NPs system demonstrated a zeta potential of −70.1 mV, achieving the lowest surface tension at 40.62 dyne/cm. In contrast, cetyltrimethylammonium bromide (CTAB) recorded the highest surface tension at 63.61 dyne/cm. Ultimately, BCL and the mixed BCL–SLS systems with NPs exhibited the highest foam stability, attributed to enhanced electrostatic and interfacial properties.

Keywords: Surfactants, Nanoparticles, Zeta Potential, Surface Tension, Foam Stability, TiO_2

1. Introduction:

Foams are created by introducing gas into a liquid in the presence of surfactants and hold significance across various fields like enhanced oil recovery, wastewater treatment, flotation, and pharmaceuticals. Various techniques, including shaking, bubbling, stirring, and sudden pressure changes, have been developed to generate stable foams Karakashev *et al.* (2011), Kulkarni *et al.* (1977), Garrett. (1979), Dippenaar *et al.* (1982), Aronson. (1986), Frye and Berg. (1989), Dickinson *et al.* (2004), Alargova *et al.* (2004), Binks and Horozov (2005), Pugh (2005), Schwarz and Grano (2005), Garret *et al.* (2006), Kostakis *et al.* (2006). The Bartsch and Ross–Miles methods are particularly used for generating foams and assessing their stability. Kothekar *et al.* (2007).

While foams are kinetically stable, they are thermodynamically unstable Jivan & Abbasi, (2019). Within surfactant systems, zeta potential serves as a predictor of colloidal stability and

the extent of particle aggregation. It captures the aggregation behaviour of nanoparticles Deleurence *et al.,* (2017). By evaluating the electrostatic potential around particles, zeta potential informs the expected repulsion between neighbouring particles. Lower surface tension enhances foam stability by facilitating the surfactant's spread at the gas–liquid interface Sullivan. (1981). Zeta potential also indicates nanoscale dispersion, steric hindrance, and particle size distribution Khan et al.(2019). A low zeta potential combined with larger droplet sizes typically points to thermodynamic instability, albeit with kinetic stability Jivan & Abbasi. (2019). This research focuses on cationic, anionic, and mixed surfactant systems, systematically varying TiO_2 nanoparticle concentrations to analyse their effects on zeta potential, surface tension, and contact angle. Characterisation was conducted with a pH meter, dynamic light scattering (DLS) analyser, and a stalagmometer.

2. Materials and Methods:

2.1. Materials

The surfactants used in the study were:

- **Sodium lauryl sulfate (SLS)** – anionic surfactant, Avantor Performance Materials India Ltd., Thane
- **Cetyltrimethylammonium bromide (CTAB)** – cationic surfactant, SDFCL Fine-Chem Ltd., Mumbai
- **Benzalkonium chloride (BCL)** – cationic surfactant, HiMedia Laboratories Pvt. Ltd., Mumbai
- **Nanoparticles (NPs):** Titanium(IV) oxide (TiO_2), a mixture of rutile and anatase phases (<100 nm particle size, BET method), obtained from Sigma-Aldrich.
- **Solvent:** Double-distilled water was used throughout all experiments.

2.2. Methodology

2.2.1. Sample Preparation

Samples were prepared by dissolving 1 g of surfactant in 20 mL of distilled water. For mixed systems, equal volumes (10 mL each) of two surfactant solutions were combined. TiO_2 NPs were added in varying concentrations (0.01 g, 0.02 g, and 0.03 g) as outlined in Table 1.

Table 1: Composition of surfactant systems with TiO_2 nanoparticles

Surfactant System	Type	TiO_2 (g)
BCL	Cationic	0.01, 0.02, 0.03
CTAB	Cationic	0.01, 0.02, 0.03
SLS	Anionic	0.01, 0.02, 0.03
CTAB + BCL	Cationic–Cationic	0.01, 0.02, 0.03
BCL + SLS	Cationic–Anionic	0.01, 0.02, 0.03

2.2.2. Zeta Potential and Particle Size Analysis

The Malvern Zetasizer Nano ZS-90 (Malvern Panalytical, UK) was used for zeta potential and particle size measurements. Each surfactant solution was diluted with distilled water prior to measurement for accurate scattering data.

2.2.3. Surface Tension Measurement

Surface tension measurements were conducted using a stalagmometer at room temperature (37 ± 2°C). The following equations were utilized:

1] For density

$$\text{Specific gravity} = \frac{Mass\ of\ liquid}{Mass\ of\ equal\ volume\ of\ distilled\ water} \quad (1)$$

2] For surface tension of liquids

Surface tension (y1) = ρ2Ƞ1 / ρ1Ƞ2 $_x$ y1 Dyne/cm (2)

ρ1 = Density of water

ρ2 = Density of liquid (surfactant solution)

Ƞ1 = No. of drop of water

Ƞ2 – No. of drop of liquid (surfactant solution)

3. Results and Discussion:

3.1. Effect of Nanoparticle Concentration on Surface Tension

The change of surface tension with increasing concentration of TiO_2 is shown in Figure 1. Surface tension decreased with increasing loading of the nanoparticles, except for BCL + 0.03 g NPs and BCL + SLS + 0.03 g NPs. This decrease is due to the nanoparticles adsorbing to the air–liquid interface, creating improved surfactant coverage and packing of the surfactant molecules, and thus a reduction in interfacial energy.

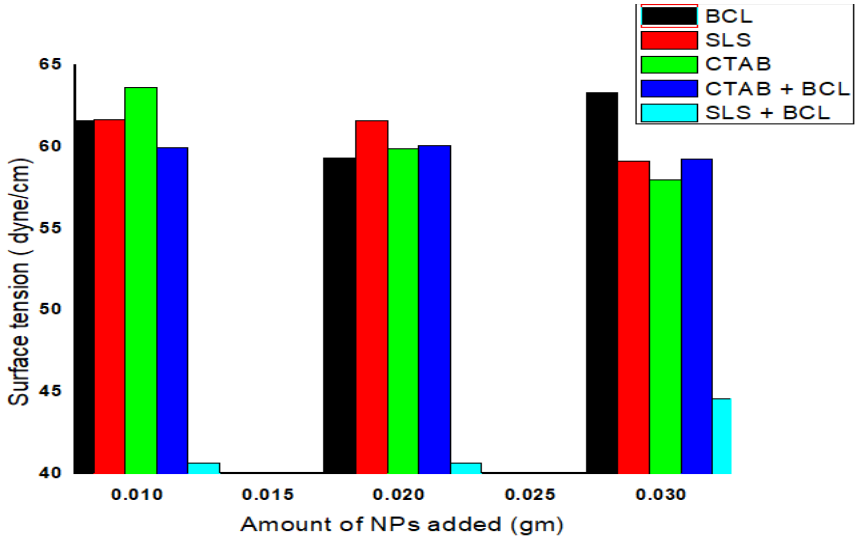

Figure 1: Surface tension variation of the solution as a function of nanoparticle (NP) concentration

3.2. Effect of Surfactants Concentration on Surface Tension

Figure 2 shows an increase in surfactant concentration (5–20%) and a decrease of surface tension. This is a result of a greater disruption of the hydrogen bonding in the water due to the higher concentration of surfactant molecules.

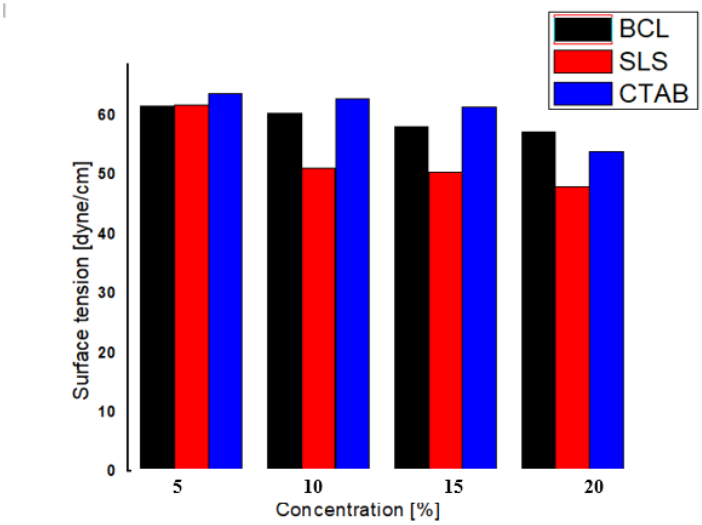

Figure 2: Relationship between rising surfactant concentration (5–20%) and the corresponding decline in surface tension.

3.3. Effect on ZP and Surface Tension

Foam stability can be explained by the Zeta potential. Figure 3 illustrates the increase in Zeta potential along with an increase in the concentration of the nanoparticles. This shows the possessed colloidal stability. In all the systems, SLS + 0.03 g NPs possessed the highest zeta potential and the next highest was CTAB + SLS + 0.02 g NPs.

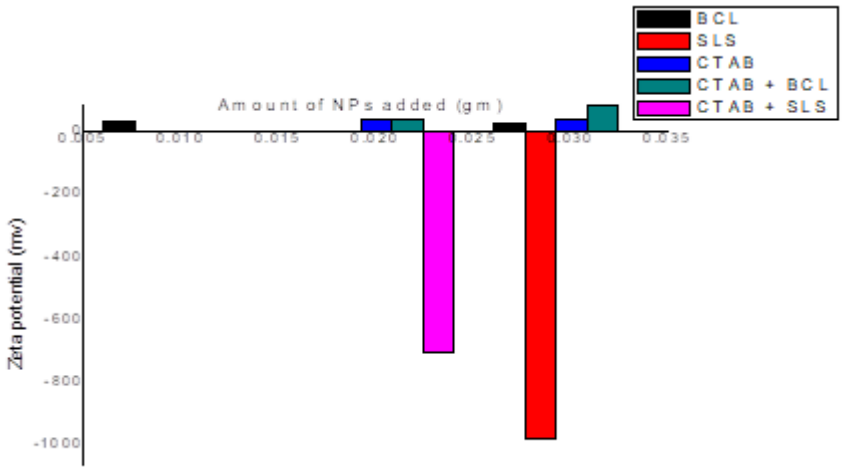

Figure 3: Zeta potential values showing a progressive rise with higher nanoparticle concentrations

3.4. Surface Tension and Contact Angle Relationship

Assessing contact angles shed light on the surface wettability characteristics. A surface with a lower contact angle demonstrates a higher surface energy and a preferable wetting disposition. The highest contact angle reached on the SLS + BCL + 0.01 g NP mixture (40.65 dyne/cm), while the lowest was on the CTAB + 0.03 g NPs (57.92 dyne/cm). This illustrates the impact of incorporating NPs on the surface hydrophilicity and the stability of hydrophilic foam films.

Conclusion:

This study demonstrated that the incorporation of TiO_2 nanoparticles significantly affects the interfacial and electrostatic properties of surfactant foams. The BCL + SLS + 0.02 g NPs system showed the lowest surface tension (40.62 dyne/cm) and highest zeta potential (−70.1 mV), indicating superior foam stability. Increasing nanoparticle concentration generally reduced surface tension and improved colloidal stability. Mixed surfactant systems exhibited synergistic effects, enhancing foam life and uniformity. These results provide valuable insights for optimizing nanoparticle-assisted foam systems in various industrial applications, including detergency, flotation, and material synthesis.

References:

1. Karakashev, S. I., Ozdemir, O., Hampton, M. A., & Nguyen, A. V. (2011). Formation and stability of foams stabilized by fine particles with similar size, contact angle and different shapes. *Colloids and Surfaces A: Physicochemical and Engineering Aspects*, *382*(1-3), 132-138.
2. Kulkarni, R. D., Goddard, E. D., & Kanner, B. (1977). Mechanism of antifoaming: role of filler particle. *Industrial & Engineering Chemistry Fundamentals*, *16*(4), 472-474.
3. Garrett, P. R. (1979). The effect of polytetrafluoroethylene particles on the foamability of aqueous surfactant solutions. *Journal of colloid and interface science*, *69*(1), 107-121.
4. Dippenaar, A. (1982). The destabilization of froth by solids. II. The rate-determining step. *International Journal of Mineral Processing*, *9*(1), 15-22.
5. Aronson, M. P. (1986). Influence of hydrophobic particles on the foaming of aqueous surfactant solutions. *Langmuir*, *2*(5), 653-659.
6. Frye, G. C., & Berg, J. C. (1989). Antifoam action by solid particles. *Journal of colloid and interface science*, *127*(1), 222-238.
7. Dickinson, E., Ettelaie, R., Kostakis, T., & Murray, B. S. (2004). Factors controlling the formation and stability of air bubbles stabilized by partially hydrophobic silica nanoparticles. *Langmuir*, *20*(20), 8517-8525.
8. Alargova, R. G., Warhadpande, D. S., Paunov, V. N., & Velev, O. D. (2004). Foam superstabilization by polymer microrods. *Langmuir*, *20*(24), 10371-10374.

9. Binks, B. P., & Horozov, T. S. (2005). Aqueous foams stabilized solely by silica nanoparticles. *Angewandte Chemie International Edition*, *44*(24), 3722-3725.
10. Pugh, R. J. (2005). Experimental techniques for studying the structure of foams and froths. *Advances in colloid and interface science*, *114*, 239-251.
11. Schwarz, S., & Grano, S. (2005). Effect of particle hydrophobicity on particle and water transport across a flotation froth. *Colloids and Surfaces A: Physicochemical and Engineering Aspects*, *256*(2-3), 157-164.
12. Garrett, P. R., Wicks, S. P., & Fowles, E. (2006). The effect of high volume fractions of latex particles on foaming and antifoam action in surfactant solutions. *Colloids and Surfaces A: Physicochemical and Engineering Aspects*, *282*, 307-328.
13. Kostakis, T., Ettelaie, R., & Murray, B. S. (2006). Effect of high salt concentrations on the stabilization of bubbles by silica particles. *Langmuir*, *22*(3), 1273-1280.
14. Kothekar, S. C., Ware, A. M., Waghmare, J. T., & Momin, S. A. (2007). Comparative analysis of the properties of Tween-20, Tween-60, Tween-80, Arlacel-60, and Arlacel-80. *Journal of dispersion science and technology*, *28*(3), 477-484.
15. Jivan, M. J., & Abbasi, S. (2019). Nano based lutein extraction from marigold petals: Optimization using different surfactants and co-surfactants. *Heliyon*, *5*(4).
16. Deleurence, R., Freymond, C., Saison, T., Lequeux, F., & Monteux, C. (2017). Foamability and stability of foams obtained with silica/PEI gels. *Colloids and Surfaces A: Physicochemical and Engineering Aspects*, *534*, 2-7.
17. Sullivan, D. E. (1981). Surface tension and contact angle of a liquid–solid interface. *The Journal of chemical physics*, *74*(4), 2604-2615.
18. Khan, I., Saeed, K., & Khan, I. (2019). Nanoparticles: Properties, applications and toxicities. *Arabian journal of chemistry*, *12*(7), 908-931.

MADS – BOX GENES: JACK OF ALL, MASTER OF NONE

Yashaswini R*[1], Prem Sagar S P[1], Raghavendra V C[1] and Sridhara M R[2]

[1]Department of Genetics and Plant Breeding,

[2]Department of Agronomy,

University of Agricultural Sciences, Raichur - 584104 (Karnataka), India

*Corresponding author E-mail: yashaswinirayanki1998@gmail.com

Introduction:

Man has domesticated many plants for his benefit throughout evolution. This process has resulted in the concentration of plants in some regions, resulting in various centers of origin. Domestication has thus shaped human history more than any other event. Domestication of flowering plants resulted in improved nutrition for a large portion of the population. During crop domestication, traits that were beneficial to yield and quality, as well as desirable for harvesting and end-uses, were selected. Domestication is thus defined as a process in which humans chose plants consciously or unconsciously based on their needs and economic preferences (Stettar *et al.,* 2017).

Contribution of Gene Classes

During the domestication process, man has selected the plants based on their phenotype but the contribution of genes to domestication remained a question. The gene classes which have contributed to the domestication process can be categorized into three categories

- **Superheroes** – These are the genes with larger effects that code for enzymes and structural proteins. Any alteration in them leads to alteration in protein function which has contributed to domestication.
- **Masterminds** – These are the genes that encode transcription factors. Any alterations in these regulatory proteins will lead to changes in the downstream pathway, thus resulting in alterations in the entire developmental process.
- **Minions** – These are 100's or 1000's genes that may collectively determine a trait value and each gene contributes only a small amount to total variation.

These categories, however, were not mutually exclusive because they each played their own role during domestication. As a result, it is critical to understand the extent of contribution to domestication, which provides insight into evolution and also determines future crop improvement.

There are some cases where alterations in enzymatic functions which has been important during domestication. For, example *WAXY* gene in rice encodes starch synthase. A point mutation in the *WAXY* gene will lead to reduced activity of starch synthase resulting in high amylopectin sticky rice preferred by Southeast Asia people and non-sticky rice preferred by Indian people (Wang *et al.,* 1995).

Despite the fact that structural genes were important during domestication, a large portion of the domestication genes were identified as transcription factors. Domestication genes encode transcription factors in 43-81 per cent of land plant genomes, with 5 percent encoding protein-coding genes. These transcription factors are consistent with developmental genetics, which governs the development and morphology of flowering plants. Because transcription factors typically orchestrate the activity of many other genes, their alteration has the potential to change an entire set of characteristics, resulting in dramatic phenotypic changes on relatively short time scales. Transcription factors are thus considered "Targets of selection and domestication".

Though transcription factors have played a major role during domestication breeders are successful in selecting genes with larger effects. But some traits are governed by a large number of 'minions' genes. These genes have a small cumulative effect on the trait which aids in trait refinement and the suppression of negative pleiotropic effects. Thus, as a whole, each gene classes have its role during domestication and refined selection is necessary while domesticating useful traits.

***Primus Inter Pares* – The First Among Equals**

In-plant genomes, among many transcription families in flowering plant genomes the one that stands out are the MADS domain proteins. MADS is an acronym derived from founding members of the family- *CM1* from *Saccharomyces cerevisiae* (baker's yeast), *AGAMOUS* (*AG*) from *Arabidopsis thaliana*, *DEFICIENS* (*DEF*) from *Antirrhinum majus* (snapdragon), and *SRF* from *Homo sapiens* (Schwarz-Sommer *et al.,* 1990). The first MADS-box genes to be isolated were homeotic sector genes with important roles in flower development. The term "Homeosis" was coined by William Bateson and described as the replacement of an organ or structure that normally develops elsewhere ('something has been changed into the likeness of something else').

Till now many MADS-box genes have been discovered and studied. With Arabidopsis as model plants, they have identified 107 MADS-box genes which govern many functions related to flower and plant development. And many MADS-box genes have also been studied in other crops (Table 1). Many of these genes are master regulators of developmental processes. Beyond their critical role in flower development, MADS-box genes are important for meristem

specification, flowering transition, flowering time control, floral organ specification, morphogenesis, inflorescence architecture, flower development, fruit development, fruit ripening, pollen development, seed development and root development.

Table 1: Number of MADS-box genes in different land plants

Species	No. of TF coding genes	Per cent of TFs	No. of MADS-box genes	Citation
Physcomitrella patens	1156	3.6	23	Theißen *et al.* (2013)
Picea abies	1107	3.9	278	Nystedt *et al.* (2013)
Brachypodium distachyon	1557	7.0	75	Gramzow *et al.* (2013)
Oryza sativa	1828	5.2	75	Arora *et al.* (2007)
Sorghum bicolor	1862	5.4	65	Zhao *et al.* (2011)
Triticum aestivum	3606	3.5	223	Preliminary analyses
Arabidopsis thaliana	1717	6.2	107	Parenicová *et al.* (2003)
Brassica rapa	3026	7.4	160	Duan *et al.* (2015)
Glycine max	3747	6.6	180	Gramzow *et al.* (2013)
Solanum tuberosum	1736	4.4	167	Duan *et al.* (2015)
Solanum lycopersicum	1845	5.5	95	Duan *et al.* (2015)
Vitis vinifera	1276	4.3	90	Grimplet *et al.* (2016)

The MADS-box genes form distinct phylogenetically highly conserved subfamilies (Theißen *et al.,* 1996). And this subfamily was conserved throughout plant evolution. The genes within each subfamily have related functions. But these genes have undergone gene duplication, sub functionalization, and redundancy which has created variations that should be explored by breeders. For example, the *AP3* orthologue governs petal and stamen development in many plants. Likewise, the *SOC1 (SUPPRESSOR OF OVEREXPRESSION O CONSTANS 1)* gene governs flowering time in eudicots and its orthologues in monocots (Ryu *et al.,* 2009).

There are functional differences in MADS-box genes that were due to neofunctionalization, subfunctionalization, redundancy, and pleiotropy. For example, *AG(AGAMOUS)* genes involved in male and female organ development, closely related paralogues *SHP1 and SHP2 (SHATTERPROOF)* genes expressed in ovules but in *ag* mutants, *SHP1 and SHP2* were overexpressed such that govern male and female organ identity (Pinyopich *et al., 2003)*. Another example is *APETALA1 (AP1) and CAULIFLOWER (CAL)* genes have similar expression patterns yet have different functions, in *ap1 and cal* mutants have

the wild type phenotype with defects in meristem identity function showing the "Cauliflower" phenotype (Fig. 1) (Kempin *et al.,* 1995).

Figure 1: Wild type phenotype of *ap1* and *cal* mutants

CAL and AP1 genes have functional differences based on the protein-protein interaction and domain-swap experiments indicated that the functional difference is due to differences in coding sequence and *cis* and *trans* differences which have contributed together to their divergence of MADS-box gene functions.

ABCDE and Floral Quartet Model

During evolution, the most studied part of plants for study of domestication is the flower. For the same reasons, flower development has been studied at high resolution in quite several different species. Several flowering plants model species, such as *Arabidopsis thaliana* (mouse-ear cress), *Petunia hybrida* (petunia), *Nicotiana tabacum* (tobacco), and *Oryza sativa* (rice) can routinely be transformed with genes from other species so that the conservation of gene function can be determined by transgenic technology. flowering plants are determined by a network of regulatory genes that are organized hierarchically.

These regulatory genes govern floral meristem identity and floral organ identity. Meristem identity genes 'control' the transition from vegetative to inflorescence and from inflorescence to floral meristems. Within floral meristems, cadastral genes set the boundaries of floral organ identity gene functions, thus defining the different floral whorls. Floral organ identity genes (homeotic selector genes; 'ABCDE genes') specify the organ identity within each whorl of the flower by activating 'realizator genes' (Table 2)

The model also proposed that the A and C function genes negatively regulate each other (meaning that they also exert 'cadastral' functions) and that the B function is restricted to the second and third whorls independently of A and C functions. In wild-type flowers, the A function is expressed in the first and second floral whorl, the B function in the second and third whorl, and the C function in the third and fourth whorl. Therefore, sepals, petals, stamens and carpels are specified in whorls one, two, three and four, respectively. D class of gene involved

in ovule development and E class gene should be required for all other organ formation. Any mutation within these genes will cause changes in floral organ development i.e., replacement of organs to be developed normally (Thissen *et al.,* 2021).

Table 2: ABCDE model of flower with genes involved and organ specified

Sl. No.	Class	Genes involved	Class	Organ specified
1.	A	*Apetala 1 (AP1) and Apetala 2 (AP2)*	A+E	Sepals
2.	BB	*Apetala 3 (AP3) and Pistillata (PI)*	A+B+E	Petals
			B+C+E	Stamens
3.	CC	*Agamous (AG)*	C+E	Carpels
4.	D	*Shatterproof (SHP1 &2) and Seedstick (STK)*	D+E	Ovule
5.	EE	*Sepallata (SEP 1-4)*	E	Overall

ABCDE model relies on genetic data whereas Floral Quartet Model (FQM) relies on molecular or product data. The FQM suggests that tetrameric complexes of floral homeotic proteins, rather than individual dimers, control floral organ identity. The dimerization network among MADS-domain proteins has been extensively characterized in a diversity of plants. The tetrameric complexes are formed by two dimers bound in proximity to each other and by looping the DNA between the binding sites. According to the 'floral quartet' model, tetrameric complexes composed of floral homeotic proteins determine floral organ identity (Fig. 2). The DNA binding specificity of MADS-box proteins is majorly increased by the formation of multimer (tetramer) complexes (Theißen *et al.,* 2016).

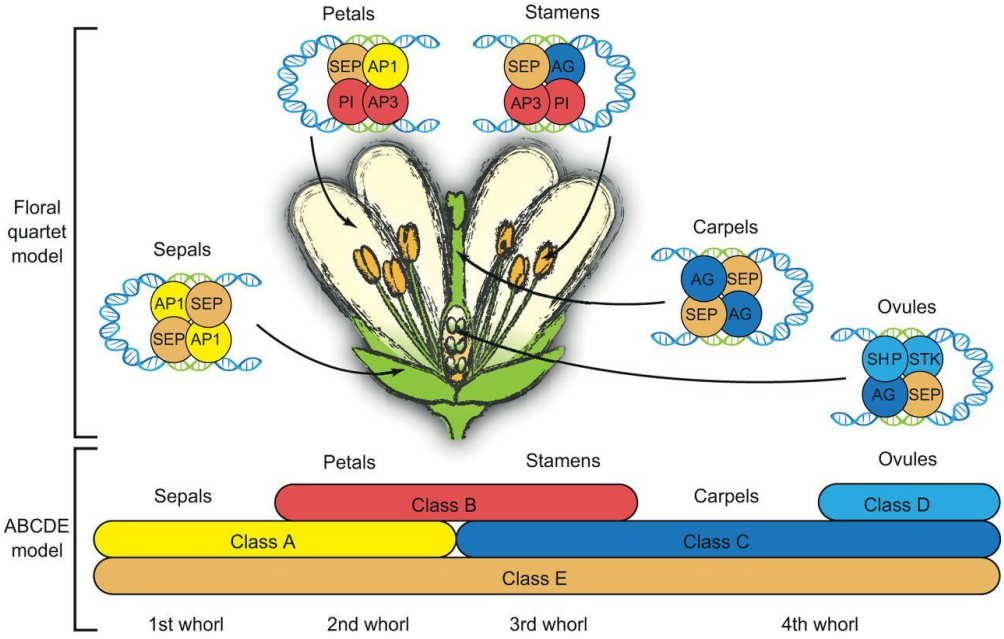

Figure 2: The ABCDE model and Floral Quartet Model (FQM)

Types of MADS-Box Genes

A gene duplication gave rise to two MADS-domain protein lineages before the divergence of plants and animals; these lineages are easy to identify due to the strong conservation of the MADS and other protein domains. There are MADS-box genes in animals & fungi and plants which consist of SRF, MEF2 and Type I, Type II genes, respectively. In plants, Type II MADS-box genes are predominant and Type I genes are less characterized (Muñoz *et al.,* 2019).

Structure of MADS Domain

MADS-box domain has a modular structure. The MADS-box domain consists of 56 amino acids of which 9 amino acids are identical in all MADS domains. The MADS-box family of genes forms two major lineages namely, type I of *SRF*-like genes and type II of *MEF2*-like genes, which resulted from an ancient event of gene duplication before the divergence of the kingdoms of plants and animals. In plants, type II genes of MADS-box, also called MIKC-type genes, feature four distinct protein domains arranged from the N-terminal end to the C-terminal end. The Type II MADS-box genes are highly studied and characterized in plants. The Type II lineage, also called MIKC-type in plants, has been subdivided into MICK^c and MICK* groups. In plants, type II genes of MADS-box, also called MIKC-type genes feature four distinct protein domains arranged from the N-terminal end (Hydrophilic residues) to the C-terminal end (Hydrophobic residues). They are the highly conserved DNA binding MADS-box (M) domain that aids in the nuclear localization & Dimerization of TFs, the less-conserved intervening domain (I) for conferring interaction specificity between different MADS-box transcription factors and/or other proteins, the keratin-like coiled-coil (K) domain for conferring protein-protein interactions, and a highly variable C-terminal (C) domain for regulating gene transcription or multimeric protein complexes formations (Theißen *et al.,* 2016).

MADS-Box Genes and Their Utilization in Crop Domestication

Winter is Coming – MADS-Box Genes in Modulating the Flowering Time

Vernalization describes the ability to promote flowering after prolonged exposure to cold (i.e., winter). It is a mechanism to 'sense' winter: because flowering is blocked unless the plant is exposed to cold temperatures, vernalization ensures that plants will not flower in autumn but rather under more favourable conditions in spring. Vernalization probably evolved as an adaptation to seasonal cold in many flowering plants. Differences in vernalization requirements have made plants evolve as spring and winter cultivars and thus adapted to different environmental conditions. Vernalization has therefore been the target of artificial selection during the domestication of monocot as well as eudicot crop

FLOWERING LOCUS C(FLC) is a MADS-box gene that acts as a major regulator of flowering time in Arabidopsis which expresses at the vegetative apex and acts as a central repressor of floral transition. *FLC* locus will inhibit the downstream genes namely, *SOC1*, *FLOWERING LOCUS D* (*FD*), and *FLOWERING LOCUS T* (*FT*) which were necessary for flowering. The cold temperatures during winters will repress the *FLC* locus through epigenetic modification thus upregulating the flowering genes to promote flowering. Genetic variation of *FLC* activity can alter or eliminate the requirement for vernalization of different crop plants (Whittaker and Dean *et al.,* 2017).

The role of the *FLC* locus is well studied in *Brassica* species which consists of a diverse genus that comprises leaf to root vegetables. In Chinese cabbage (Leaf vegetable) early bolting diminishes the crop quality. Thus, the aim is to identify the genotypes which do not flower even under cold conditions. And in seed-bearing genotypes, complete blocking of flowering is not desirable. Rather, the aim is to produce winter and spring type varieties. For this variation in *FLC* locus is utilized. Four *FLC* orthologues (*BrFLC1*, *BrFLC2*, *BrFLC3*, and *BrFLC5*) have been identified in *B. rapa*, and variations in at least some of them contribute to differences in flowering times in different cultivars. For example, *BrFLC1* co-localizes with a quantitative trait locus (QTL) for late bolting in Chinese cabbage. The expression of *BrFLC1* was still detectable after a prolonged cold period of 7 weeks in a late-bolting line, while it was discontinued in an early-bolting lineage. This polymorphism is due to SNP at the exon-intron border (exon2), indel at exon 4 and premature stop codon TAA which results in either alternative splicing or truncated protein (Kakizaki *et al., 2011).*

Likewise, orthologues of the *FLC* locus in different crops have contributed to their domestication. In barley, *ODDSOC1* and *ODDSOC2* genes control flowering time by acting as floral repressors like *FLC* (Greenup *et al.,* 2009*). ODDSOC2* possibly has contributed to an adaptive mechanism by which different cereal populations have acquired their distinct vernalization requirements. *ODDSOC2* homologs in wheat, *TaAGL22* and *TaAGL33*, also display similar responses to vernalization and show distinct expression patterns between spring and winter varieties (Sharma *et al.,* 2017).

Apart from *FLC* genes, *VERNALISATION (VRN)* genes also govern vernalization requirements. In wheat, there are four *VRN* genes - termed *VRN1*, *VRN2*, *VRN3*, and *VRN4,* out of which VRN*1 & VRN4* are MADS-box genes. *VRN* genes are orthologues to *AP1* genes of Arabidopsis. *VRN1* gene acts exactly opposite to *FLC* gene where *VRN1* gene activity increases with cold treatment and which aids in flowering, controls inflorescence meristem identity,

accelerates the reproductive development, and aids in response of plants to long-day conditions which de-represses the flowering pathway and activates flowering (Deng *et al.,* 2015).

Many tree species also evolved adaptations to seasonal climate and undergo a dormant phase starting in autumn, and cold treatment is usually required to break bud dormancy and continue growth in spring. This strategy is used by fruit trees as a preventive measure to avoid frost damage. With all these in fruit trees, many MADS-box genes were important in controlling flowering time and bud break. In apples, *FLC-like* genes seem to play an important role in bud break.

Another group of MADS-box genes, *DORMANCY ASSOCIATED MADS-BOX* (*DAM*) genes belong to the same subfamily as *SHORT VEGETATIVE PHASE* (*SVP*) from Arabidopsis, which is involved in regulating flowering time. *DAM* genes are repressors of bud break, thus their levels go to a minimum prior to chilling. In the peach variety 'evergrowing', all of the six tandem duplicated *DAM* genes are deleted, resulting in a loss of bud dormancy and therefore continuous growth without any chilling requirements, thus suitable to all climatic conditions (Bielenberg *et al.,* 2008).

FUL (FRUITFUL) gene in Arabidopsis and *AP1* gene were used to alter flowering time. *MADSB*, the *FUL* orthologue from mustard (*Sinapsis alba*), has been successfully overexpressed in *B. napus*, resulting in a decreased vernalization requirement of winter rape. *BpMADS4* was successfully expressed in apple to shorten the juvenile stage. Heterologous overexpression of *AP1* in citrus trees resulted in very early flowering after only 1 year without altering floral architecture (Peña *et al.,* 2001).

Home Improvement: MADS-Box Genes in Architectural Reshaping

A change in overall plant architecture can be a very desirable trait during the domestication process. The selection for specific inflorescence architectures has been widely exploited to increase yield in a variety of crops.

'Malmaison' 'St Anne's'

In the ABCDE model, the loss of function in any of the floral homeotic genes will result in drastic phenotypes. For example, *AG (AGAMOUS)* mutants result in "Double flowers" where stamens and carpels are replaced by sepals and petals. In *AG* mutants, determinacy is also

disturbed resulting in his pattern being reiterated multiple times, leading to visually attractive flowers composed of lots of petals. Such phenotypes are especially important for horticultural purposes in ornamental varieties of rue-anemone (*Thalictrum thalictroides*), Japanese cherry (*Prunus lannesiana*), Rose, *Camellia*, and lily (Fig. 3) (Galimba *et al.,* 2012, Dubois *et al.,* 2010).

Figure 3: Double flower phenotype in *Thalictum sps.* and *Rose sps*.

Examples of inflorescence architecture are broccoli (*B. oleracea* ssp. *italica*) and cauliflower (*B. oleracea* ssp. *botrytis*). In these species the arresting of floral meristems occurs very late and very early, respectively. The transition between cauliflower and broccoli is not sharp, with many intermediate cultivars available and the phenotype of individual cultivars also depending on the growth temperatures. This has resulted due to the mutation in *BoCAL and BoAP1* genes due to the presence of premature codons (Labate *et al.,* 2006) that have been selected during domestication to generate a modified inflorescence structure and enable the consumption of floral buds.

Beyond inflorescence branching, shoot branching (tillering) is another important trait that is the target of breeding efforts. In the cultivated rice *O. sativa*, the *AGL17*-like MADS-box gene *OsMADS57* was reported to be influencing tillering of the rice plants (Guo *et al.,* 2003). A truncated version of OsMADS57 lacking the C-terminal domain caused excessive tillering of the respective mutant rice plant, enhancing flower numbers and grain yield. Another example, the transgenic expression of the *SEP1*-like gene *OsMADS1* from rice under the control of the *nopaline synthase* (*nos*) promoter caused dwarfism and early heading in the transgenic plants (Jeon *et al.,* 2001). Hence, *OsMADS1* might be another target for modulating plant architecture in rice, as well as flowering time.

Fruit to Seed

Fruit and seed enhancement has been a major focus of plant domestication and breeding, as fruits and seeds are frequently the desired end-product of agriculture and thus the part of the plant that is commercially interesting. Modifications of fruits and seeds during domestication and

breeding include enlargement of fruits or seeds, a decrease of seed size or seedlessness (in case the fruit is the desired crop), a loss of seed or fruit shattering and a delay in fruit ripening and longer shelf life.

For example, The Arabidopsis genes *SHP1*, *SHP2*, and *STK* are MADS-box genes closely related to *AG* which controls ovule development. Their combined loss of function (i.e., *stk shp1 shp2* triple mutants) results in aborted or missing seeds in Arabidopsis (Pinyopich *et al.,* 2003).

Seedlessness is a highly desired trait in fleshy fruits such as grapes (*Vitis vinifera*). Indeed, decreased expression of the *STK* orthologue *VviAGL11*, which could be caused by an elongated single sequence repeat in the promoter region of the gene, is most likely the cause of seedlessness in various grape varieties (Mejia *et al.,* 2011). Because the length of the repeats is inversely related to the degree of seed development in grapes, genetic characterization of the *VviAGL11* locus allows wine farmers and breeders to evaluate plants before they reach the reproductive stage. Another example is that the level of expression of the tomato *STK* orthologue, *SlyAGL11*, is positively correlated with the degree of seed development; thus, genetic silencing of *SlyAGL11* resulted in seedless tomato fruit.

Ripening

FUL genes are also involved in fruit development. *FUL* is closely related to *AP1* and regulates cellular differentiation during fruit development as well as flowering time in Arabidopsis. Repression of *FUL* orthologues will leads to delayed ripening.

Suppression of the two *FUL* orthologues in tomatoes, *FUL1* and *FUL2*, results in highly delayed fruit ripening, most probably by means of reduced ethylene synthesis and decreased carotenoid accumulation. This demonstrates that ethylene biosynthesis and fruit ripening can be fine-tuned by altering the expression of MADS-box genes. And in heterologous expression of the mustard *FUL* orthologue *MADSB* in *B. napus* resulted in decreased pod-shattering (Wang *et al.,* 2014).

Yet another tomato MADS-box gene, *LeMADS-RIN*, which belongs to the *SEP1* subfamily as well, is involved in the fruit ripening process. The *rin* mutation has been used in commercial breeding because it increases tomato shelf life, making post-harvest management and distribution of tomato fruits easier. The transgenic down-regulation of *SEP* homologs from banana and apple, *MaMADS1* and *MaMADS2*, and *MdMADS8* and *MdMADS9*, respectively, inhibited fruit ripening and prolonged the shelf life of the fruit. Hence, *SEP* genes also play a role in fruit ripening in another climacteric (ethylene-

sensitive) fruits as well as non-climacteric fruits. Pointing to *SEP* orthologues as a universal target when it comes to fruit ripening optimization (Elitzur *et al.,* 2016).

Yield

In Arabidopsis, *SHP1* and *SHP2 are* involved in ovule development. They redundantly control the dehiscence of the Arabidopsis silique, namely the opening of the silique to release the seeds. In *shp1 shp2* double mutants, the silique remains closed, leading to 'shatterproof' siliques. RNAi-mediated down-regulation of the *SHP1* orthologue *BnSHP1* from oilseed rape resulted in an increase of resistance to pod shattering, therefore increasing the potential yield of the oil-bearing crop. The understanding of the genetic basis of seed shattering can be exploited for improving crop yield by reducing seed shattering, especially in species grown for their seeds, such as oilseed rape (Kord *et al.,* 2015).

Cotton fiber, for example, is a highly elongated cell that develops from the ovule epidermis. Auxin, a plant hormone, promotes fiber initiation. The promoter of the *STK* orthologue *FBP7* from petunia, which drives ovule-specific expression, was used to increase auxin levels in the ovule. Cotton yield increased significantly when the auxin synthesis gene *iaaM* was expressed under the *FBP7* promoter (Zhang *et al.,* 2011).

The oil palm *Elaeis guineensis* is one of the major oil crops. The oil palm fruit comes in three different forms that differ in the size of the shell, namely *dura* with a thick shell, *pisifera* (shell-less), and *tenera* (thin-shelled) (Fig. 4) (Singh *et al.,* 2013). The differences in fruit form are controlled by *SHELL*, an orthologue of *STK*. The *tenera* hybrid plants carry one wild-type-like and one mutant *SHELL* allele and thus constitute an impressive example of single-gene heterosis, where heterozygosity at a single locus enhances oil yield as compared with both parents. *HELL* is involved in fruit development and thus represents an interesting example of the abundant subfunctionalization occurring in the subfamily of *AG*- and *STK*-like genes.

The identification of *SHELL* and *EgDEF1* as major factors influencing oil palm yield enables the development of genetic and epigenetic tests for palm seedlings prior to their reproductive state to eliminate non-*tenera* contaminations and plant carrying hypomethylated *EgDEF1* alleles. This can be of high commercial advantage and may increase the sustainability and land-use efficiency of the 'world's most hated crop'.

Population genetics studies in maize have revealed that the gene *ZEA AGAMOUS-LIKE1* (*ZAGL1*) has been under selection during maize domestication (Zhao *et al.,* 2011). Interestingly, *ZAGL1* seems not only to be influencing flowering time control but may also have contributed to an increase in the number of kernel rows in maize ears during domestication, thus increasing fruit and yield size.

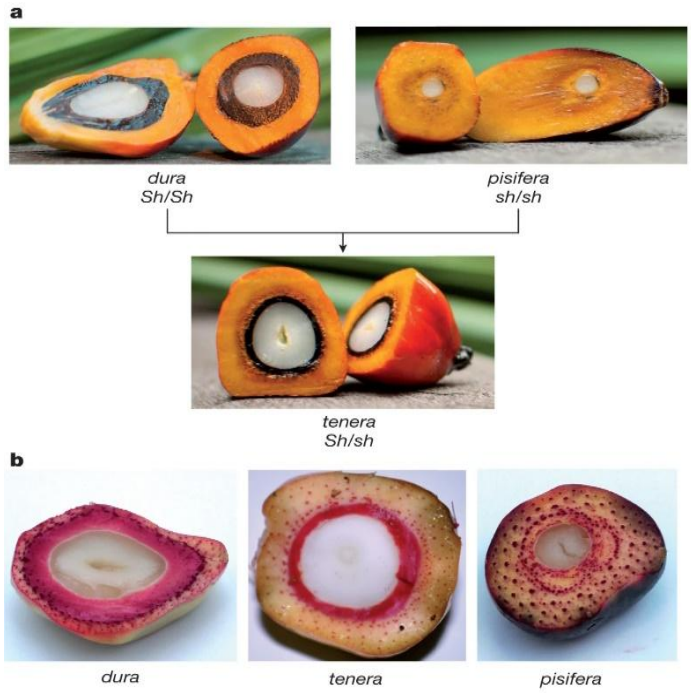

Figure 4: Different types oil palm fruits with shell differences

Pleiotropy and Redundancy: An Opportunity in Disguise

Pleiotropy and redundancy have been a new sense while using MADS-box genes for domestication purposes. One important aspect is that in many cases genetic pathways have not been disrupted entirely but rather more subtle variations were introduced that allowed fine-tuning of the phenotype which has been observed for other genes. The fact that in many cases closely related, partially redundant paralogues of MADS-box genes control a pathway indicates that the potential for phenotypic fine-tuning is far from being completely exploited.

For example, there are at least four different *FLC*-like genes that acts redundantly in *B. rapa*, at least two of which are involved in flowering time regulation. Combining different allelic variants from different *FLC* genes may allow flowering time to be adjusted to a wide range of climatic conditions.

However, the pleiotropic effects of many MADS-box genes also pose a challenge: the mutations in the *SEP1*-like genes *J2* and *EJ2* in tomatoes had beneficial effects on their own (i.e. the jointless phenotype and larger sepals), the combination of both mutants was detrimental because they both also redundantly control flower and inflorescence development, and although *j2/ej2* loss-of-function double mutants show strongly enhanced inflorescence branching, increased floral abortion is observed at the same time.

Different strategies to use MADS-box genes to overcome the pleiotropic and redundant nature and for future crop improvement. *SEP1*-like genes are expressed in the floral meristem, the developing flower, and the fruit, and may therefore contribute to inflorescence architecture,

carpel and fruit development, and fruit ripening. Those different functions are presumably conferred by interactions of the SEP1 protein with different partners (AP1-like, AG-like, and FUL-like proteins) and by specific *cis*-regulatory modules that govern expression during specific developmental stages. Promoter modifications and alterations in coding sequences may inactivate specific *cis*-regulatory modules, leading to a decrease in *SEP1* expression in the floral meristem and the fruit, while expression in the carpel remains intact. Hence, a plant with an increased inflorescence branching, unaltered fruit set, and delayed fruit ripening might be produced (Fig. 5)

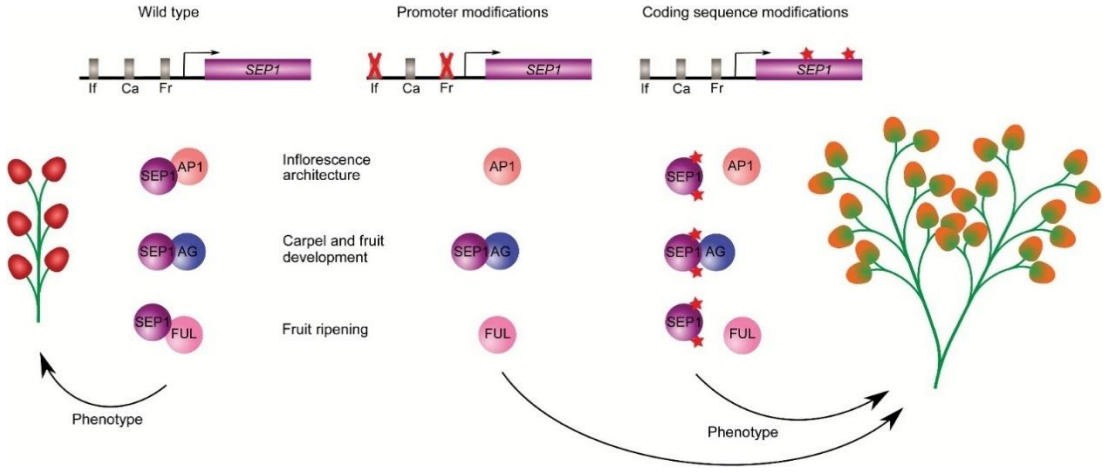

Figure 5: Strategy to overcome the pleiotropic and redundant nature of *SEP1* gene in tomato through promoter and coding sequence modifications

The Taming of the Masters:

Generating Allelic Diversity and Targeted Phenotypic Manipulations

The high functional conservation of MADS-box genes and their comprehensive characterization in model and crop plants makes them ideal candidates for manipulating phenotypes in a predictable way. Indeed, the examples of successful transgenic manipulations outlined above exemplify that this is a promising approach. The other promising approach is to fine-tune the phenotypes by using the CRISPR/Cas9 genome editing technique for modifying *cis*-regulatory elements.

Since the promoter has a modular structure, alteration in the *cis*-regulatory elements can affect gene expression in a highly targeted manner. For this strategy, a 'promoter mutagenesis' approach employing CRISPR/Cas9 can be used that requires relatively little *a priori* knowledge of the function of specific *cis*-regulatory elements.

Though this is a very promising approach for future crop improvement programs, we suggest that modifications in the coding region may also be well suited to fine-tune the phenotype, especially when it comes to MADS-domain proteins. Since MADS-box genes will be

involved in different protein-protein interactions, manipulating one particular interaction may affect one specific developmental pathway but not others, very similar to the manipulation of promoter regions.

Even though CRISPR/Cas9 might be a promising tool to introduce the desired changes, large-scale EMS (ethyl methane sulphonate) mutagenesis approaches and subsequent selection of promising mutations might be an important alternative. Beyond inducing mutations, landraces and wild relatives of elite cultivars might constitute a largely untapped pool of allelic diversity) that could be used for targeted screening of MADS-box gene coding sequence variations that can potentially be used for crop improvement.

Conclusion: One Gene Family to Rule Them All

It has been argued that one main obstacle science faces is the lack of models based on quantitative formulations. Given the amount of qualitative and quantitative data researchers have accumulated on MADS-box genes during the past decades, we might be closer to predicting specific phenotypic consequences of MADS-box gene alterations. But there are significant challenges in altering MADS-box genes like subfunctionalisation, neofunctionalization and redundancy can make it difficult to predict phenotypic consequences of specific mutations.

Additional functional studies as well as a more detailed understanding of the biophysical properties of MADS-domain proteins are required to exploit fully the potential of MADS-box genes for optimizing crop performance. We also suggest that the biophysics of MADS-domain protein-protein and protein-DNA interactions, which is becoming increasingly well characterized, makes them especially suited to exploit coding sequence variations for targeted breeding approaches. We are convinced that continued basic and applied research programmes focused on MADS-box genes in a broad variety of species will not only result in a deeper understanding of plant development and evolution, but will also profoundly contribute to improving crops and consequently help to ensure food security and human health.

References:

1. Castelán-Muñoz, N., Herrera, J., Cajero-Sánchez, W., Arrizubieta, M., Trejo, C., García-Ponce, B., Sánchez, M. D. L. P., Álvarez-Buylla, E. R., & Garay-Arroyo, A. (2019). MADS-box genes are key components of genetic regulatory networks involved in abiotic stress and plastic developmental responses in plants. *Frontiers in Plant Science, 10*, 853. https://doi.org/10.3389/fpls.2019.00853
2. Klocko, A. L., Borejsza-Wysocka, E., Brunner, A. M., Shevchenko, O., Aldwinckle, H., & Strauss, S. H. (2016). Transgenic suppression of AGAMOUS genes in apple reduces

fertility and increases floral attractiveness. *PLoS ONE, 11*(8), e0159421. https://doi.org/10.1371/journal.pone.0159421

3. Schilling, S., Pan, S., Kennedy, A., & Melzer, R. (2018). MADS-box genes and crop domestication: The jack of all traits. *Journal of Experimental Botany, 69*(7), 1447–1469. https://doi.org/10.1093/jxb/ery032
4. Smaczniak, C., Immink, R. G., Angenent, G. C., & Kaufmann, K. (2012). Developmental and evolutionary diversity of plant MADS-domain factors: Insights from recent studies. *Development, 139*(17), 3081–3098. https://doi.org/10.1242/dev.074674
5. Soyk, S., Lemmon, Z. H., Oved, M., Fisher, J., Liberatore, K. L., Park, S. J., Goren, A., Jiang, K., Ramos, A., Van Der Knaap, E., & Van Eck, J. (2017). Bypassing negative epistasis on yield in tomato imposed by a domestication gene. *Cell, 169*(6), 1142–1155. https://doi.org/10.1016/j.cell.2017.04.032
6. Stetter, M. G., Gates, D. J., Mei, W., & Ross-Ibarra, J. (2017). How to make a domesticate. *Current Biology, 27*(17), R896–R900. https://doi.org/10.1016/j.cub.2017.06.067
7. Theißen, G., Becker, A., Di Rosa, A., Kanno, A., Kim, J. T., Münster, T., Winter, K. U., & Saedler, H. (2000). A short history of MADS-box genes in plants. *Plant Molecular Biology, 42*(1), 115–149. https://doi.org/10.1023/A:1006332105728
8. Theißen, G., Melzer, R., & Rümpler, F. (2016). MADS-domain transcription factors and the floral quartet model of flower development: Linking plant development and evolution. *Development, 143*(18), 3259–3271. https://doi.org/10.1242/dev.134080
9. Whittaker, C., & Dean, C. (2017). The FLC locus: A platform for discoveries in epigenetics and adaptation. *Annual Review of Cell and Developmental Biology, 33*, 555–575. https://doi.org/10.1146/annurev-cellbio-100616-060546
10. Zhou, E., Zhang, Y., Wang, H., Jia, Z., Wang, X., Wen, J., Shen, J., Fu, T., & Yi, B. (2022). Identification and characterization of the MIKC-type MADS-box gene family in *Brassica napus* and its role in floral transition. *International Journal of Molecular Sciences, 23*(8), 4289. https://doi.org/10.3390/ijms23084289

MATHEMATICAL MODELING FOR SUSTAINABLE DECISION MAKING IN INDUSTRY

Gorakhanath Rambhau Karade
Abasaheb Marathe Arts and New Commerce, Science College,
Rajapur, Tal. Rajapur, Dist. Ratnagiri, Maharashtra
Corresponding author E-mail: karadegr1986@gmail.com

Abstract:

Industry emphasizes the need for sustainable decision-making processes that balance economic, social, and environmental factors. Mathematical modeling can play a vital role in supporting sustainable decision-making in Industry. This paper reviews various mathematical modeling methods that can be used for sustainable decision-making challenges in Industry.

Keywords: Mathematical Modeling, Sustainable, footprint, Optimization Techniques

Introduction:

Industry today is shaped by the integration of advanced digital technologies such as artificial intelligence, blockchain, and the Internet of Things (IoT) into manufacturing and operational systems. Sustainable decision-making plays a crucial role in this transformation, helping industries minimize environmental harm while achieving economic efficiency and social benefits. By adopting eco-friendly strategies, optimizing resources, and leveraging data-driven tools, companies can improve productivity, reduce waste, and build long-term resilience. Ultimately, sustainability supports responsible growth and a balanced industrial future.

Mathematical Modeling Approaches:

Several mathematical modeling methods can support sustainable decision-making in Industry. Techniques such as optimization models, simulation, multi-criteria decision analysis, and life-cycle assessment help evaluate environmental impacts, resource use, and economic trade-offs. These models enable industries to choose efficient, eco-friendly strategies for long-term growth and responsible management. Some including:

- **Multi-Criteria Decision Analysis (MCDA)**: MCDA methods like PROMETHEE and TOPSIS can help assess different sustainable solutions based on several criteria.
- **Optimization Techniques**: Techniques such as linear programming and dynamic programming can optimize sustainable decision-making processes.
- **System Dynamics Modeling**: This modeling can analyze the behavior of complex systems and find sustainable solutions.

Case Study

This section presents a case study demonstrating the application of mathematical modeling to sustainable decision-making in Industry. Using Multi-Criteria Decision Analysis (MCDA) methods, the study evaluates various sustainable alternatives for a manufacturing company. By considering environmental, economic, and social criteria, the approach helps identify the most balanced and effective solutions. The case study highlights how mathematical modeling supports informed, data-driven decisions, enabling industries to optimize performance while promoting sustainability and reducing negative environmental impacts.

1. Background

XYZ Manufacturing Company, a leading automotive parts manufacturer in India, faces increasing pressure to reduce its environmental impact while maintaining competitiveness. To address this challenge, the company has initiated efforts to explore sustainable solutions within its manufacturing processes, aiming to balance operational efficiency, environmental responsibility, and long-term business growth.

1.1. Problem Statement

The manufacturing process uses energy-intensive machinery, greatly contributing to greenhouse gas emissions. The company aims to reduce both energy use and emissions while maintaining production levels. The management team identified three alternative sustainable solutions:

a. Solution 1: Implementing energy-efficient lighting systems
b. Solution 2: Upgrading to energy-efficient machinery
c. Solution 3: Implementing a renewable energy system

2. Mathematical Modeling Approach

To evaluate the sustainable solutions, the management team adopted a Multi-Criteria Decision Analysis (MCDA) method. This approach allows alternatives to be assessed across multiple dimensions, including environmental impact, economic benefits, and social implications. Based on these considerations, the team identified and defined the following criteria for evaluating the sustainability of each manufacturing solution:

a. Environmental Impact (EI): Reduction in greenhouse gas emissions
b. Economic Benefits (EB): Cost savings and revenue generation
c. Social Implications (SI): Impact on employment and community development

The management team assigned relative weights to each criterion according to its importance, ensuring that environmental, economic, and social factors were appropriately prioritized in evaluating the sustainable manufacturing solutions. The weights were:

a. EI: 0.4
b. EB: 0.3
c. SI: 0.3

They then evaluated each solution based on these criteria, assigning scores from 0 to 10.

3. Results:

The results of the MCDA analysis are presented in the following table:

Solution	EI	EB	SI	Total Score
Solution 1	6	8	4	18
Solution 2	8	6	6	20
Solution 3	9	9	8	26

4. Conclusion:

According to the MCDA analysis, Solution 3 (Implementing a renewable energy system) was the most sustainable choice, with a total score of 26. Solution 2 (Upgrading to energy-efficient machinery) came next with a score of 20, while Solution 1 (Implementing energy-efficient lighting systems) received the lowest score of 18. The management team decided to go with Solution 3, which involved investing in a renewable energy system. The company expects to cut greenhouse gas emissions by 20% and save 15% on energy costs.

Recommendations:

The case study demonstrates the value of using mathematical modeling approaches like MCDA for sustainable decision-making in Industry. The following suggestions are made:

a. Use MCDA methods: These methods can assist companies in evaluating various sustainable solutions based on multiple criteria.
b. Assign weights: Weights for each criterion can help companies prioritize their sustainability objectives.
c. Evaluate solutions: Assessing alternative sustainable solutions against criteria can help companies identify the best option.

By applying mathematical modeling methods, companies can make informed decisions that balance economic, social, and environmental factors.

Conclusion:

Mathematical modeling plays a crucial role in supporting sustainable decision-making in Industry 5.0. This paper emphasizes the importance of further research on applying mathematical modeling approaches to address sustainability challenges, enabling industries to optimize

resource use, minimize environmental impact, and make informed, data-driven decisions for long-term economic and social benefits.

References

1. Iqbal, A., Agrawal, R., Sharma, M., & Kumar, V. (2020). Review on multi-criteria decision analysis in sustainable manufacturing decision-making. *International Journal of Sustainable Engineering, 13*(1), 122–210. https://doi.org/10.1080/19397038.2019.1708172
2. Zaei, J. (2015). Best-worst multi-criteria decision-making method. *Omega, 53*, 49–57. https://doi.org/10.1016/j.omega.2014.09.009
3. Sterman, J. D. (2000). *Business dynamics: Systems thinking and modeling for a complex world*. McGraw-Hill.
4. Govindan, K., Khodaverdi, R., & Jafarian, A. (2013). A fuzzy multi-criteria approach for measuring sustainability performance of a supplier based on triple bottom line approach. *Journal of Cleaner Production, 47*, 345–354. https://doi.org/10.1016/j.jclepro.2012.12.042
5. Vinodh, S., & Balasubramanian, P. (2011). Application of multi-criteria decision-making for sustainable manufacturing evaluation. *International Journal of Production Research, 49*(10), 3031–3045. https://doi.org/10.1080/00207543.2010.528973

VACUUM PACKAGING: REVOLUTIONIZING FOOD PRESERVATION

K. Prakash* and S. Chandraprabha

Department of Post-Harvest Technology, SRM College of Agricultural Sciences,
SRM Institute of Science and Technology, Baburayanpettai,
Chengalpattu District - 603 201, Tamil Nadu, India
*Corresponding author E-mail: hortidoctpks@gmail.com

Abstract:

Vacuum packaging is a widely adopted preservation technology in the food industry, employed to maintain quality and extend the shelf life of a broad range of food products. It involves the evacuation of air from the package, thereby creating an anaerobic or low-oxygen environment that suppresses oxidative reactions and restricts the growth of aerobic microorganisms such as moulds, yeasts and spoilage bacteria. The principal mechanism is the inhibition of key spoilage processes, including lipid oxidation, pigment and flavour degradation, and associated textural and sensory deterioration. As a result, vacuum packaging slows biochemical and microbiological decomposition, preserving freshness, nutritional value and organoleptic attributes for extended storage periods. A variety of vacuum packaging systems are used, from simple external sealers for domestic or small-scale operations to automated thermoforming and rotary vacuum units for high-throughput industrial applications. The overall efficacy of the process is strongly influenced by the properties of multi-layer barrier films, which commonly integrate polymers such as nylon for mechanical strength and oxygen barrier, polyethylene for sealability and moisture protection, and EVOH or aluminium foil to enhance gas and light impermeability. Collectively, these advancements have established vacuum packaging as a critical component of contemporary food safety and distribution systems.

Keywords: Vacuum Packaging, Anaerobic Environment, External Sealers, Thermoforming and Rotary System.

Introduction:

Vacuum packaging is a preservation technique that removes air from a package before sealing, creating an oxygen-deficient environment that markedly reduces the growth of spoilage microorganisms and limits oxidative reactions. Initially developed for food preservation, its applications have extended to pharmaceuticals and electronics, where maintaining product integrity and increasing shelf life are essential. This technique utilizes specialized barrier materials in combination with vacuum sealing technology to extend freshness, ensure hygiene,

reduce packaging volume, and enhance product presentation. By preventing aerobic microbial growth and oxidation, vacuum packaging helps retain flavor, color, texture, and nutritional quality. Increasing consumer demand for safer, longer-lasting products has established vacuum packaging as a vital method in modern packaging. It offers benefits such as prolonging shelf life up to five times compared to conventional storage, preventing freezer burn, optimizing storage efficiency, and minimizing food waste. This method supports sustainability while maintaining product quality and safety across various industries.

History of Vacuum Packaging

In the early 19th century, the concept of preserving items by removing air was initially explored through experiments focusing on modified atmosphere packaging. However, the true advent of modern vacuum packaging, as it is known today, occurred primarily after World War II, driven by advancements in plastic technology. Before the war, rudimentary attempts in France aimed to extend the shelf life of frozen foods by removing air from rubber latex bags. The post-war period, marked by the commercialization and widespread availability of plastics, significantly enabled the practical application of vacuum packaging.

A landmark development occurred in the 1950s with the introduction of the Cryovac vacuum packing method, initially designed for packaging whole turkeys. This marked a major milestone in the commercial use of vacuum packaging for perishable foods. In the 1940s, German inventor Karl Busch developed vacuum sealing for domestic use, though widespread commercial adoption did not happen until the 1960s. The 1970s saw further progress with the integration of inert gases into vacuum packaging termed Modified Atmosphere Packaging (MAP) which extended product shelf life by controlling the internal gas composition.

The evolution of vacuum packaging has been driven by continuous improvements in materials, machinery, and techniques, including the development of advanced barrier films (such as NYLON/EVOH) for enhanced protection against oxygen and moisture, as well as innovations in sealing methods (hermetic sealing, vacuum skin packaging, thermoforming). The focus has shifted towards increasing efficiency, sustainability (through recyclable and biodegradable materials), and versatility, establishing vacuum packaging as an indispensable tool across diverse industries today.

Principles of Vacuum Packaging

Vacuum packaging is based on a number of fundamental principles, all of which are designed to preserve the quality of packaged products and extend their shelf life. This is achieved by regulating the surrounding atmosphere. These principles operate in tandem to establish an environment that is resistant to conventional decomposition mechanisms:

1. Deoxygenation (Oxygen Removal): This is the fundamental principle. Air is evacuated from the package during vacuum packaging, which significantly diminishes the oxygen concentration. Oxygen is a gas that is intensely reactive and accelerates:

- **Oxidation:** The presence of oxygen causes oxidative rancidity in a variety of food components, including lipids and oils, resulting in discolouration, odours, and off-flavours. Oxidation can also degrade vitamins (such as A and C). These chemical reactions are attenuated by the removal of oxygen.
- **Aerobic Microbial Growth:** The majority of spoilage microorganisms, including moulds, yeasts, and numerous common spoilage bacteria (e.g., *Pseudomonas* species), necessitate oxygen to flourish. Vacuum packaging significantly impedes the growth and reproduction of these organisms by depriving them of oxygen,

2. Setting up of an Anaerobic or Microaerobic Environment: Vacuum packaging generates an environment in which oxygen concentrations are exceedingly low (typically less than 1%), although a genuine 'perfect' vacuum is essentially unattainable. The activity of aerobic spoilage organisms is restricted by this reduced oxygen environment. However, it is imperative to acknowledge that certain pathogenic bacteria, including specific strains of *Clostridium botulinum* (which generate a lethal toxin), are anaerobic and can thrive in the absence of oxygen. Consequently, to guarantee food safety, vacuum packaging of specific foods (particularly those with high moisture or low acidity) must be complemented by other preservation methods, such as refrigeration or freezing, or specific processing (e.g., retorting).

3. Moisture Control (Prevention of Dehydration and Freezer Burn): Vacuum packaging prevents moisture from evaporating by establishing a tight barrier around the product. This is especially crucial for frozen foods, as it effectively prevents "freezer burn," a condition in which moisture evaporates from the food's surface, resulting in dry, discoloured, and unappealing regions. It safeguards dry products from moisture absorption, which can result in caking or staleness.

4. Physical Protection and Volume Reduction: The compact, firmly conforming design of the vacuum packaging offers physical protection against external contaminants such as dust, dirt and insects. It also diminishes the overall volume of many products, particularly those that are soft or irregularly shaped, which can result in more efficient storage and transportation.

5. Preservation of Organoleptic Qualities: Vacuum packaging assists in the preservation of the product's natural colour, aroma, flavour, and texture for extended periods by reducing oxidation and microbial growth. This is a substantial advantage, particularly for high-value food products.

The fundamental principle of vacuum packaging is to establish a controlled microenvironment within the container that reduces the factors that contribute to degradation, thereby extending the product's freshness and shelf life.

Types of Vacuum Packaging Machines

Vacuum packaging machines come in various types, each designed to meet specific needs in terms of volume, product type and automation level. Understanding these distinctions is crucial for selecting the appropriate equipment for a given application.

1. External Vacuum Sealers (Nozzle/Edge Type): These are the most prevalent and cost-effective form, frequently observed in small-scale operations or home kitchens. They operate by positioning the open end of a vacuum bag that has been specifically engineered (often featuring textured channels) over a suction nozzle or within a vacuum channel. The container is then heat-sealed after the machine draws air directly out of it. Although they are compact and user-friendly, they may not provide as deep a vacuum as chamber machines and are generally less suitable for liquids or extremely delicate items due to the direct suction, which can draw liquids or pulverise fragile products.

2. Chamber Vacuum Sealers: Chamber sealers are the workhorses of commercial vacuum packaging. They are made for larger volume and more flexibility. The whole bag, with the product inside, goes into a sealed chamber. The machine then removes all the air from the chamber, bringing the pressure inside and outside the bag to the same level. This makes the vacuum much stronger, which makes them perfect for packing liquids, marinades, or fragile things without worrying about breaking them or pulling out fluids. Chamber sealers come in a wide range of sizes, from small tabletop devices to big, floor-standing equipment with one or two chambers for higher throughput. This makes them good for restaurants, butcher shops, and medium-sized food processors.

3. Thermoforming Vacuum Packaging Machines (Rollstock Machines): These systems are widely employed in industrial production on a large scale and are highly automated. The first roll of film is heated and "thermoformed" into the shape of the tray or hole that is needed. The second roll of film is sealed over the filled cavities. The machine creates a vacuum-packed product by evacuating air and sealing the top film after the product is inserted in the formed cavities. Because they work quickly and efficiently, these machines are often built into production lines for meat, poultry, fish, and ready-to-eat meals. They can make different types of packages, such as rigid or flexible packs. In addition, they can offer Modified Atmosphere Packaging (MAP) or Vacuum Skin Packaging (VSP).

4. Rotary Vacuum Packaging Machines (Rotary Pick, Fill, Seal): Rotary vacuum packaging machines are high-speed, automated systems often used for granular, powdered, or liquid products that are pre-filled into pouches. These machines typically feature a rotating table with multiple stations for various operations: bag loading, filling, vacuuming, sealing, and discharge. They are designed for continuous operation and high output, making them suitable for large-scale production facilities in the food industry, especially for items like coffee, snacks, or prepared foods.

5. Belt Conveyor Vacuum Packaging Machines: These industrial-scale machines are intended for the continuous vacuum packaging of larger or bulkier products in high volume. A conveyor belt is utilised to transport products through a sequence of vacuum chambers and sealing stations. This continuous flow enables the efficient processing of large quantities of products, such as whole cuts, cheese blocks, or large industrial components, which are frequently observed in meat processing facilities. It is widely recognised that they possess high throughput capabilities and are robust.

6. Vacuum Skin Packaging (VSP) Machines: A specialized type of vacuum packaging, VSP machines create a "second skin" around the product. The product and a tray are covered with a heated, highly stretchable film, which is then pulled by a vacuum, causing the film to firmly conform to the product's precise shape. The outcome is a package that is visually appealing and leak-proof, which secures the product in position and prevents movement and purge. VSP is particularly popular for fresh meats, poultry, seafood, and ready meals, as it enhances product presentation, extends shelf life, and minimizes liquid migration.

Applications of Vacuum Packaging in Food Industry

Vacuum packaging has become an indispensable tool across nearly every segment of the food industry, fundamentally altering how food is processed, distributed, and consumed. Its applications are diverse, driven by the core benefits of extending shelf life, preserving quality, reducing waste, and enhancing food safety.

Meat and Poultry: This application is considered to be the most significant. The shelf life of fresh and processed meats is significantly extended by vacuum packaging, which prevents oxidative rancidity of fats and inhibits the development of aerobic spoilage bacteria. Although the initial vacuum process removes oxygen and darkens the colour of red meats (due to deoxymyoglobin), the meat will "bloom" back to its vibrant red colour upon exposure to air upon opening. Vacuum skin packaging (VSP) is particularly popular for fresh cuts, as it generates a compact, visually appealing seal that emphasises the product while simultaneously preventing

purge and preserving its freshness. It's widely used for beef, pork, poultry and both for raw cuts and processed products like sausages, ham and bacon.

Seafood: Similar to meat, seafood benefits immensely from vacuum packaging. It prevents spoilage and minimises bacterial growth, which is quick to occur in fish due to its delicate composition. Vacuum packaging is effective in preserving the fresh flavour, texture, and vibrant colour of fish and shellfish, regardless of whether they are pre-cooked, smoked, or fresh. This is essential for reducing spoilage losses and expanding market reach, particularly for high-value seafood products.

Dairy Products: To prevent mould growth, retain moisture, and maintain the unique flavours and fragrances of hard and semi-hard cheeses, they are extensively vacuum packaged. Surface oxidation and dehydration are prevented by the absence of oxygen. Vacuum packaging even enables the continued maturation of certain cheeses, which further enhances their qualities. While vacuum packaging is less prevalent for fresh milk, certain dairy products, such as paneer, butter, and processed cheese, also employ it to maintain their freshness for an extended period.

Fruits and Vegetables: The shelf life of fruits and vegetables can be extended by vacuum packaging, which is frequently used in conjunction with Modified Atmosphere Packaging (MAP), while fresh produce continues to respire (consume oxygen and eject carbon dioxide). Vacuum sealing retards decomposition and prevents dehydration in vegetables that are more resistant to moisture loss. MAP is essential for delicate leafy greens or sliced fruits, as it introduces specific gas mixtures after vacuuming to regulate respiration rates, prevent anaerobic spoilage, and maintain freshness while preventing crushing. This enables a more extensive distribution and a decrease in deterioration during transportation.

Processed Foods and Ready Meals: Vacuum packaging is advantageous for a wide variety of processed food items, such as pasta, sauces, soups, pre-cooked meals and treats such as nuts, dried fruits and coffee. It safeguards against microbial contamination, moisture absorption, and oxidation, thereby extending the utilisation of the product and ensuring its integrity. The vacuum pack is frequently employed in conjunction with other technologies, such as cook-in-bag or sous vide applications, to ensure safe and consistent cooking for ready dishes.

Bakery Products: While soft bakery items can be crushed by a strong vacuum, certain products like bread, rolls (especially par-baked), cookies, and dried cakes can be vacuum packaged to maintain freshness and prevent staleness or mold growth. Frequently, MAP is employed to control oxygen levels while providing a buffering effect for delicate items using inert gases such as nitrogen.

Other Applications: In addition to these categories, vacuum packaging is employed for a diverse array of other food items, including:

- **Coffee:** Preserves the aroma and flavour by inhibiting the oxidation of volatile compounds.
- **Dry Goods**: Legumes, cereals, and flour are safeguarded from spoilage, moisture, and insects.
- **Marinades:** The vacuum process can expedite the marinating of meats and poultry by allowing the marinade to penetrate into the product.

Advantages of Vacuum Packaging

- ✓ **Extended Shelf Life:** Vacuum packaging significantly retards oxidative reactions and impedes the proliferation of aerobic spoilage microorganisms (such as moulds, yeasts, and numerous bacteria) by eliminating oxygen, which are the primary causes of food spoilage. This can increase the shelf life of refrigerated products by 3-5 times or even longer for frozen commodities.
- ✓ **Preservation of Quality:** Vacuum packaging contributes to the preservation of the sensory attributes of food in addition to extending its shelf life. It prevents degradation caused by oxygen exposure, thereby preserving the natural colour, flavour, aroma, and texture. For example, it prevents the rapid wilting of fresh produce and prevents lipids from turning rancid.
- ✓ **Prevention of Freezer Burn:** Vacuum sealing freezes foods to prevent moisture sublimation from the food surface, which results in "freezer burn" - a condition marked by dry, discoloured, and tough areas. This is achieved by preventing direct contact with air.
- ✓ **Reduced Food Waste:** Vacuum packaging significantly reduces food degradation and waste at all levels of the supply chain, from producers to consumers, by extending freshness. This results in environmental benefits and economic savings.
- ✓ **Improved Food Safety (in conjunction with other methods):** Vacuum packaging, when in conjunction with appropriate refrigeration, chilling, or cooking, can improve food safety by preventing the growth of spoilage organisms that could otherwise obscure the presence of pathogens.
- ✓ **Space Optimization:** The package's volume is reduced by removing air, resulting in more efficient storage in refrigerators, freezers, and during transportation.
- ✓ **Faster Marination:** The vacuum can open up the pores of certain foods, enabling marinades to penetrate deeper and more quickly, resulting in more intensely flavoured products in a short time.
- ✓ **Protection from Contaminants:** The airtight seal serves as a physical barrier against external contaminants, including moisture, insects, grime, and dust.

- ✓ **No Need for Chemical Preservatives:** Vacuum packaging accomplishes preservation naturally by removing oxygen, which is appealing to consumers who are interested in products that are free of artificial additives.

Limitations of Vacuum Packaging

- ✓ **Anaerobic Pathogen Growth Risk:** The most critical limitation is that vacuum packaging creates an ideal anaerobic (oxygen-free) environment for certain dangerous pathogenic bacteria to flourish, most notably *Clostridium botulinum,* despite inhibiting aerobic spoilage organisms. This bacterium generates a lethal toxin that does not necessarily exhibit visible symptoms of spoilage, such as slime or off-odours. To guarantee safety, vacuum-packed low-acid, moist foods (e.g., fresh fish, meat, mushrooms, garlic, and certain prepared vegetables) must be either frozen, cooked, acidified, or retorted, or maintained at strict refrigeration temperatures (typically below 3.3°C / 38°F).
- ✓ **Not Suitable for All Foods:**
  - o **Soft/Delicate Foods:** Direct vacuum pressure has the potential to crush delicate items such as berries, soft cheeses (such as brie), certain leafy greens or soft baked products.
  - o **Gassy Vegetables:** Raw mushrooms, cabbage, cauliflower, and broccoli are known to emit gases naturally, even after they have been harvested. This can result in the bag inflating or the vegetables turning slimy or spoiling more quickly as a result of accelerated anaerobic respiration after vacuum encapsulation.
  - o **Raw Garlic and Onions:** These can promote the growth of *Clostridium botulinum* in an anaerobic environment, making them unsafe if not properly handled and refrigerated.
  - o **Fermented Foods:** The fermentation process in foods such as sauerkraut or kimchi can result in the burst of vacuum-sealed containers due to the continued production of gases.
- ✓ **Requires Specific Equipment and Materials:** Vacuum packaging is effective when specialised machines and multi-layer barrier coatings are used, which may require an initial investment.
- ✓ **Loss of Preservation Once Opened:** The shelf life of a vacuum-packed item is reduced to that of conventionally packaged food when the vacuum is ruptured.
- ✓ **Doesn't Improve Initial Quality:** Vacuum packaging is unable to enhance the quality of food that is already deteriorating; it merely preserves the quality of the food at the time of packaging. It is essential to commence with high-quality, fresh ingredients.
- ✓ **Potential for Crushing/Deformation:** The high vacuum pressure can result in undesirable compression or deformation for certain products, which can affect their aesthetic appeal or texture.

Conclusion:

Vacuum packaging, a modern preservation technique that is ubiquitous, fundamentally functions by removing air from a package, thereby establishing a low-oxygen or anaerobic environment. In the food industry, vacuum packaging significantly extends the shelf life of perishable products by significantly reducing the presence of oxygen. This process preserves the nutritional integrity, flavour, and texture of the product. Vacuum packaging's success is rooted in the synergy between specialised multi-layer barrier coatings and advanced vacuum machine technology, which has revolutionised food preservation and expanded the global reach of products. The technology's indispensable status as a safeguard for product quality and a means of expanding market reach has been established by its adaptability, economic benefits, and effectiveness.

References:

1. Birhanu, A. F. (2022). Assessment Available Meat Packaging Materials and Their Challenges at Ethiopian Private Abattoirs. *International Journal of Food Science and Agriculture*, *6*(3).
2. Czerwiński, K., Rydzkowski, T., Wróblewska-Krepsztul, J., & Thakur, V. K. (2021). Towards impact of modified atmosphere packaging (MAP) on shelf-life of polymer-film-packed food products: Challenges and sustainable developments. *Coatings*, *11*(12), 1504.
3. Devi, M. C. R. A. Influence of packaging material and storage temperature on the shelf life and quality of broccoli: A review.
4. Lechevalier, V. (2016). Packaging: principles and technology. Handbook of Food Science and Technology 2*: Food Process Engineering and Packaging*, 269-315.
5. Mahardika, B., & Andriani, E. (2022). Design of Vacuum Packaging Tools to Increase the Resistance of Processed Cook Fish Products. *Bulletin of Culinary Art and Hospitality*, *2*(2), 5.
6. Sivamma P., Mounika E., Naga Hari Sairam N., & Jagannadha Rao PVK (2021). Applications of vacuum technology in food processing. *The Pharma Innovation Journal,* 10(5): 914–918.

Bhumi Publishing, India
November 2025

METAL-DOPED TITANIUM DIOXIDE NANOPARTICLES (AG AND AU): SYNTHESIS, OPTICAL CHARACTERIZATION, AND PERFORMANCE ENHANCEMENT IN DYE-SENSITIZED SOLAR CELLS

Rupali S. Patil* and Hemant S. Suryawanshi

School of Chemical Sciences,

Kavayitri Bahinabai Chaudhari North Maharashtra University,

Jalgaon–425001, Maharashtra, India

*Corresponding author E-mail: rupalipatil2211@gmail.com

Abstract:

Titanium dioxide (TiO_2) is one of the most widely investigated semiconductor materials for dye-sensitized solar cells (DSSCs) owing to its chemical stability, suitable band edge positions, and low fabrication cost. However, its DSSC performance is often constrained by limited visible-light absorption and rapid electron–hole recombination. In this study, bare TiO_2 nanoparticles and metal-doped TiO_2 (Ag–TiO_2 and Au–TiO_2) were synthesized using a controlled sol–gel method and calcined at selected temperatures. Their structural and optical characteristics were analyzed using UV–Visible spectroscopy, Tauc bandgap estimation, and Fourier Transform Infrared (FTIR) spectroscopy. Metal incorporation induced notable modifications in optical absorption behavior and band-edge transition patterns. DSSCs were fabricated using both bare and doped TiO_2 photoanodes, and device performance was evaluated under illumination with and without electrolyte. The Ag–TiO_2 photoanode exhibited the highest photovoltage output (520 mV with electrolyte), followed by Au–TiO_2 (400.13 mV) and bare TiO_2. The performance enhancement is attributed to improved charge separation, reduced recombination losses, and plasmonic effects introduced by noble-metal dopants. Overall, the study demonstrates that Ag- and Au-modified TiO_2 nanostructures offer promising potential for enhanced DSSC photoanode applications.

Keywords: TiO_2; Ag@TiO_2; Au@TiO_2; sol–gel synthesis; FTIR; Dye-Sensitized Solar Cell; etc.

1. Introduction:

Nanostructured titanium dioxide (TiO_2) has emerged as a highly versatile semiconductor material due to its exceptional chemical stability, nontoxic nature, strong oxidizing capability, and wide applicability in solar cells, photocatalysis, sensors, and environmental remediation. However, pristine TiO_2 suffers from intrinsic limitations such as its wide band gap and rapid recombination of photogenerated electron–hole pairs, restricting its activity predominantly to the

UV region. To address these challenges, extensive research has focused on modifying TiO_2 through metal doping, surface functionalization, and controlled synthesis routes.

The synthesis conditions of TiO_2—particularly pH, temperature, and precursor chemistry—strongly influence its particle size, morphology, and crystalline phase. Mahshid *et al.* (2007) reported that hydrolysis of titanium isopropoxide under controlled pH conditions produces anatase TiO_2 nanoparticles with distinct morphological variations, demonstrating the crucial role of pH in tailoring TiO_2 characteristics. Similarly, the pyrolytic temperature significantly impacts the microstructure and crystallinity of TiO_2-based coatings. Raut *et al.* (2011) showed that increasing pyrolysis temperatures (400–900°C) in SiO_2/TiO_2 hybrid coatings leads to enhanced transparency, mechanical hardness, and structural homogeneity due to improved Ti–O bonding.

Environmentally friendly synthesis approaches are gaining prominence. Green synthesis routes using plant extracts provide a sustainable alternative to conventional chemical methods. Helen Rathi *et al.* (2023) demonstrated that TiO_2 nanoparticles produced via plant-mediated methods exhibit excellent photocatalytic activity toward dye degradation and antimicrobial performance, emphasizing the potential of green chemistry in nanomaterial production.

Advanced solution-phase and sol–gel syntheses remain the most frequently used methods for achieving homogeneous TiO_2 nanostructures with tunable morphology. Nematov *et al.* (2024) reviewed various solution-based synthetic strategies, demonstrating that precursor chemistry, reaction kinetics, and solvent environment dictate the formation of well-defined TiO_2 nanocrystals. Singh *et al.* (2019) further reported that nonhydrolytic sol–gel synthesis yields highly conductive TiO_2 nanoparticles suitable for photovoltaic applications.

Metal doping—especially with silver (Ag) and gold (Au)—has been widely studied to address TiO_2 intrinsic optical limitations. Ag nanoparticles improve visible-light absorption through surface plasmon resonance and enhance electron transfer, significantly boosting DSSC efficiency (Lim *et al.,* 2014). Au nanoparticles similarly enhance dye-sensitized solar cell performance by improving local electric fields and reducing charge recombination (Kabir *et al.,* 2021). Additionally, our prior work demonstrated that Ag-doped TiO_2 not only reduces particle size but also enhances light absorption and suppresses recombination, resulting in improved DSSC performance (Patil *et al.,* 2023).

The present chapter provides a comparative investigation into the synthesis, characterization, and DSSC performance of bare and metal-doped TiO_2 nanoparticles. TiO_2 was synthesized at different temperatures (400°C, 500°C, 600°C), and further modified through Ag and Au doping. Comprehensive characterization using XRD, FTIR, UV–Vis absorption

spectroscopy, and Tauc analysis was performed to evaluate structural and optical modifications. The materials were subsequently incorporated as photoanodes in dye-sensitized solar cells, and their photovoltage performance was measured with and without electrolyte. This integrated analysis highlights the influence of calcination temperature, noble-metal doping, and structural variations on the functional efficiency of TiO_2-based photoanodes.

2. Materials and Methods:

2.1 Materials

Titanium(IV) isopropoxide (TTIP, 97%), ethanol, and distilled water were used as precursors for TiO_2 synthesis. Silver nitrate ($AgNO_3$) and chloroauric acid ($HAuCl_4$) served as dopant sources for Ag–TiO_2 and Au–TiO_2, respectively.

Two natural plant dyes were used for photoanode sensitization:

- Plumeria rubra (Plumeria Dainea) pigment extract
- Opuntia ficus-indica (Opuntia Delhiniya) pigment extract

The electrolyte used in the DSSC assembly was a standard iodide/triiodide (I^-/I_3^-) redox electrolyte, prepared using KI and I_2 in ethylene carbonate–propylene carbonate solvent. All chemicals were analytical grade and used without further purification.

2.2 Synthesis of Bare TiO_2 Nanoparticles (Sol–Gel Route)

Step 1: Preparation of TTIP Solution: 15 ml of ethanol was taken in a beaker, and 2.97 ml of TTIP was added drop wise under continuous stirring. Ethanol was used as a solvent to control the hydrolysis rate of TTIP. The mixture was stirred for 10–15 min.

Step 2: Controlled Hydrolysis: In a separate beaker, 15 ml of distilled water was prepared and added drop wise to the TTIP–ethanol solution. Hydrolysis occurred according to:

$$Ti(OC_3H_7)_4 + 4H_2O \rightarrow Ti(OH)_4 + 4C_3H_7OH$$

A white $Ti(OH)_4$ precipitate formed, and the mixture was stirred for 30–60 min.

Step 3: pH Adjustment and Precipitation: A 0.1 M NH_3 or NaOH solution was added drop wise until the pH reached 8–10 to ensure complete precipitation. The slurry was stirred for an additional 1 hour.

Step 4: Aging: The mixture was aged for 12–24 hours at room temperature to promote uniform particle growth.

Step 5: Washing and Purification: The precipitate was centrifuged and washed 3–5 times with ethanol and distilled water to remove unreacted organics.

Step 6: Drying: The washed precipitate was dried at 80–120°C for 12–24 hours, yielding amorphous TiO_2.

Step 7: Calcination: Dried powder was calcined in a muffle furnace at 400°C, 500°C, and 600°C for 2–4 hours.

- ≤400°C → amorphous TiO_2
- 500°C → anatase TiO_2
- ≥600°C → partial anatase-to-rutile transformation

2.3 Synthesis of Ag@TiO_2 Nanoparticles

The initial procedure up to hydrolysis (Steps 1–2 above) was identical.

Step 3: Preparation of Ag-Doping Solution: 0.066 g of $AgNO_3$ was dissolved in 5 ml deionized water to obtain a uniform dopant solution.

Step 4: Incorporation of Dopant: After $Ti(OH)_4$ formation, the $AgNO_3$ solution was added drop wise under constant stirring while maintaining pH 8–10.

Steps 5–7: Aging, Washing, Drying, and Calcination: Procedures were identical to Section 2.2, with calcination at 500°C to obtain crystalline Ag@TiO_2.

2.4 Synthesis of Au–TiO_2 Nanoparticles

The procedure up to Step 2 was the same as the bare TiO_2 synthesis.

Step 3: Preparation of Au-Doping Solution: 0.06 mL of liquid gold chloride ($HAuCl_2$) was taken using a micropipette and diluted to 5 ml with triple distilled water.

Step 4: Incorporation of Dopant: The Au solution was added dropwise to the $Ti(OH)_4$ dispersion under constant stirring while maintaining pH 8–10.

Steps 5–7: Aging, Washing, Drying, and Calcination: Conditions identical to bare TiO_2 were followed, with calcination at **500°C** to obtain Au–TiO_2 nanoparticles.

2.5 Preparation of Plant Dye Sensitizers

Fresh petals of Plumeria rubra and fruits of Opuntia ficus-indica were washed, cut, and crushed in a mortar–pestle. The pulp was soaked in ethanol–water (70:30) and kept in the dark for 24 h. The extract was filtered and stored at 4°C until use.

2.6 Fabrication of DSSC Photoanodes

Calcined TiO_2 (bare and doped) was mixed with a few drops of acetic acid and ethanol to form a uniform slurry. This was coated on cleaned FTO glass by doctor-blade method and sintered at 450°C. The films were immersed in respective plant dyes for 24 h for sensitization.

2.7 Assembly of the DSSC

The dye-loaded TiO_2 electrode served as the working electrode. A platinum-coated FTO glass served as the counter electrode. The two electrodes were sandwiched using a Surlyn spacer, and the I^-/I_3^- electrolyte was injected between the electrodes.

2.8 Photovoltage Measurement

Photovoltage was measured using a multimeter under direct illumination. Output voltage values were recorded for:

- bare TiO_2
- TiO_2 + dye
- TiO_2 + dye + electrolyte
- Ag@TiO_2 + dye
- Au@TiO_2 + dye

3. Results and Discussion:

3.1 X-Ray Diffraction (XRD) Analysis

The XRD patterns of the synthesized TiO_2 samples—bare TiO_2 calcined at 400°C, 500°C, and 600°C, along with Ag-doped and Au-doped TiO_2 prepared at 500°C—display a series of sharp, well-defined diffraction peaks characteristic of the anatase crystal phase. All patterns show prominent reflections located near 25°, 37°, 48°, 54°, and 62° in the 2θ range. The strongest peak at approximately 25.3° corresponds to the (101) plane, which is the primary fingerprint peak of anatase TiO_2. Additional reflections at about 37.8° (004), 48.0° (200), 53.9° (105), and 62.7° (204) further confirm the presence of the anatase structure.

Across all samples, the absence of peaks belonging to rutile or brookite phases indicates that anatase TiO_2 remains the dominant and stable phase, even after high-temperature calcination and metal doping. Notably, the samples calcined at higher temperatures exhibit sharper and more intense diffraction peaks, suggesting improved crystallinity and increased crystallite size due to thermal growth.

Metal doping (Ag and Au) leads to a further enhancement in peak intensity without shifting the major peak positions. This indicates that the incorporation of Ag or Au does not alter the TiO_2 lattice structure but improves overall crystallinity and structural ordering. Any minor broadening observed in the doped samples may be attributed to lattice strain or defect formation introduced by dopant incorporation.

Overall, the XRD analysis confirms that all materials retain the pure anatase phase, while both temperature and metal doping significantly influence crystallite size and peak intensity—factors directly linked to the optical absorption and photovoltaic performance of the synthesized TiO_2 nanoparticles.

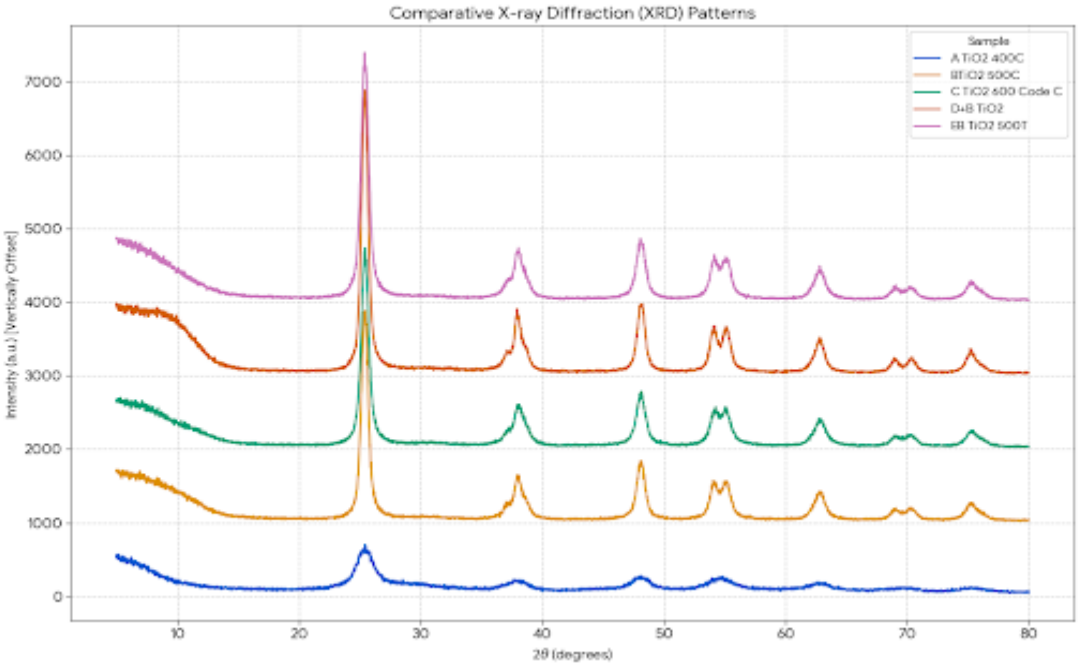

Figure 1: Comparative XRD patterns of bare TiO_2 nanoparticles calcined at 400°C, 500°C, and 600°C, and Ag- and Au-doped TiO_2 composites (D+B and EB).

3.2 FTIR Spectroscopy

The FTIR spectra of the synthesized TiO_2 samples provide important information regarding the presence of functional groups, metal–oxygen bonding, and the structural changes occurring due to calcination temperature and metal (Ag/Au) doping. All samples show a broad absorption band in the region of 3200–3600 cm^{-1}, which corresponds to the O–H stretching vibrations of surface-adsorbed water molecules and hydroxyl groups. This band is more pronounced in the sample calcined at 400°C, indicating the presence of a larger fraction of surface moisture and hydroxyl species due to its comparatively lower crystallization. As the calcination temperature increases to 500°C and 600°C, the intensity of the O–H band decreases, reflecting the removal of physisorbed water and improved structural consolidation.

A distinct band observed near 1620–1640 cm^{-1} is attributed to the bending vibrations of molecular water, further confirming the presence of adsorbed moisture on the TiO_2 surface. The most significant feature of the FTIR spectra is the strong, broad absorption band located in the range of 400–700 cm^{-1}, corresponding to Ti–O and Ti–O–Ti lattice vibrations. This band is characteristic of the anatase phase of TiO_2 and becomes sharper and more defined at higher temperatures due to improved crystallinity and growth of the TiO_2 lattice.

In the metal-doped samples, slight variations in the shape and intensity of the Ti–O stretching band are observed, which reflect subtle structural distortions introduced by Ag and Au incorporation. Although Ag and Au do not form separate FTIR-active phases, their interaction

with the TiO_2 lattice results in minor shifts or broadening of the metal–oxygen band, indicating successful doping. Importantly, no additional peaks corresponding to organic residues appear in the doped samples, suggesting complete removal of unreacted precursors during calcination.

Overall, the FTIR analysis confirms the formation of metal–oxygen lattice vibrations typical of anatase TiO_2, while also demonstrating the influence of calcination temperature and metal doping on the structural order, surface hydroxyl content, and degree of crystallinity of the synthesized nanoparticles.

TiO_2 at 400°C

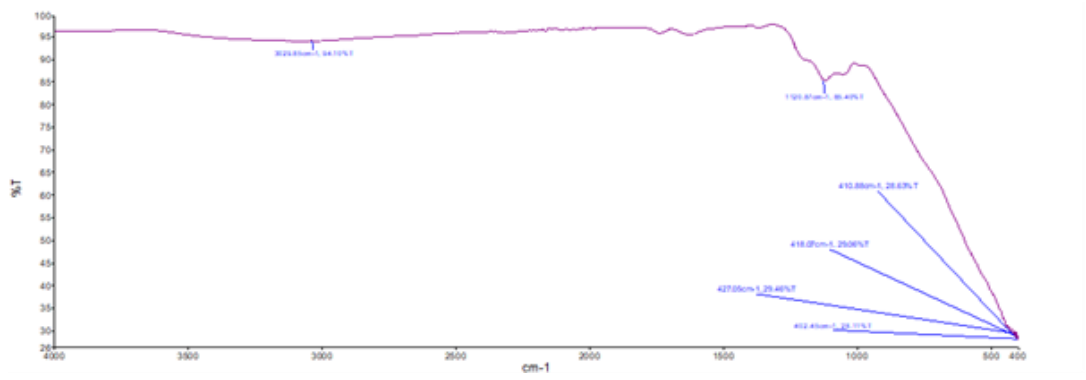

TiO_2 at 500°C

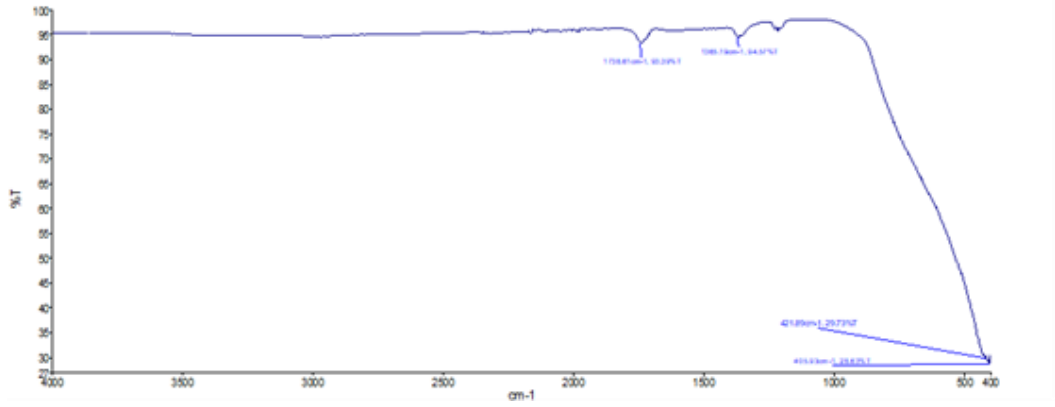

TiO_2 at 600°C

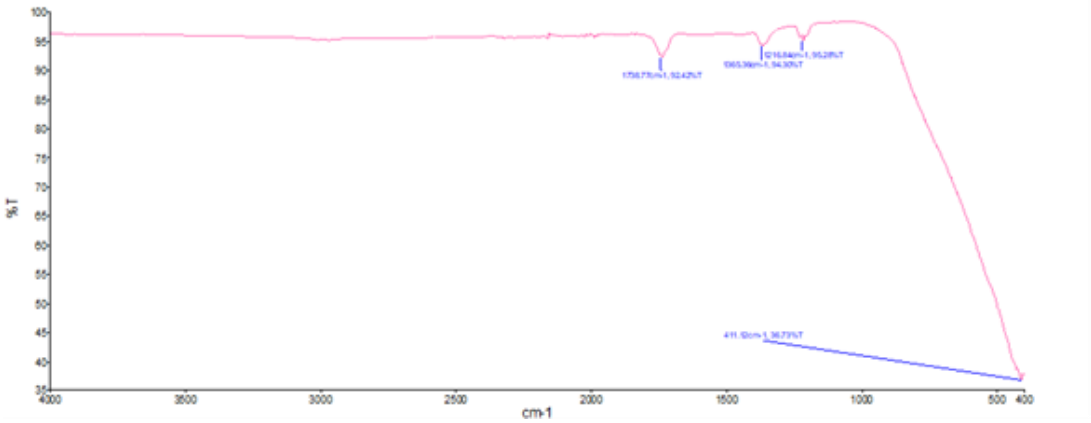

Ag@TiO_2 at 500°C

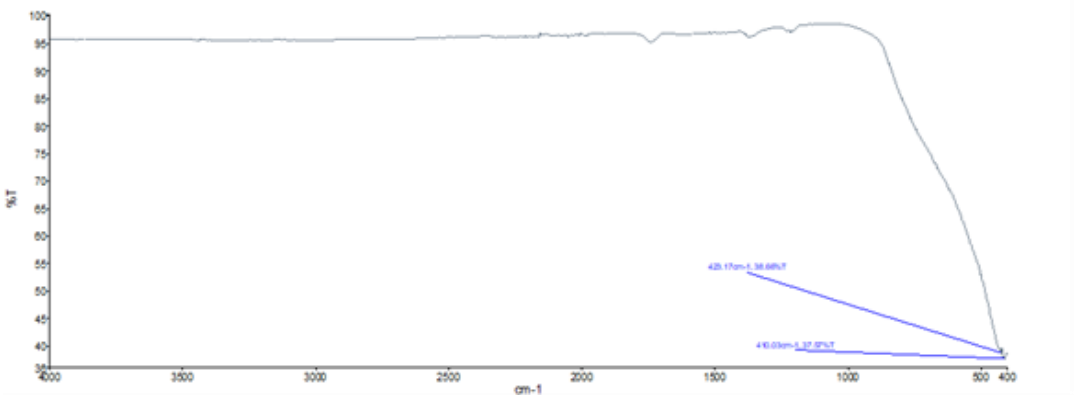

Au@TiO_2 at 500°C

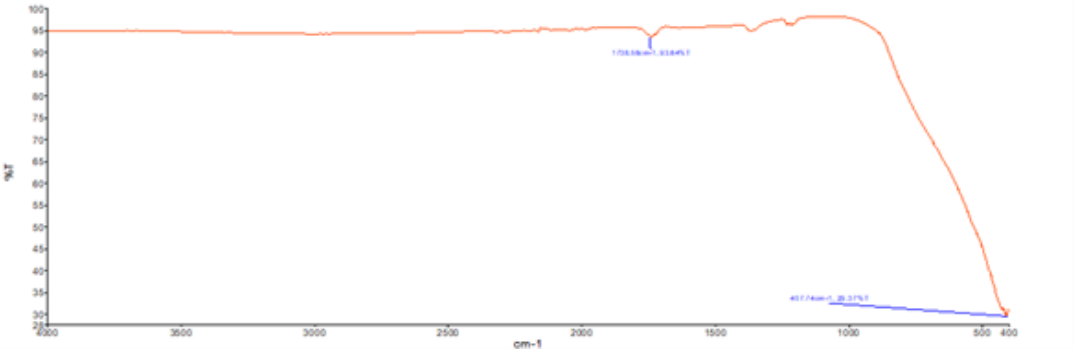

Figure 2: FTIR Spectra of bare TiO_2 nanoparticles calcined at 400°C, 500°C, and 600°C. Ag@TiO_2 and Au@TiO_2 at 500^0C.

3.3 UV–Visible Absorption and Bandgap (Tauc) Analysis

The UV–Visible absorption spectra of the TiO_2 nanoparticles calcined at 400°C, 500°C, and 600°C reveal the influence of temperature on the optical behaviour and electronic structure of the synthesized materials. All three samples exhibit a strong absorption band in the ultraviolet region, with a sharp absorption edge occurring below 400 nm, which is characteristic of the intrinsic band-to-band electronic transition in TiO_2. The sample calcined at 400°C shows a slightly higher absorption intensity in the UV region, indicating the presence of smaller and less crystalline nanoparticles with a greater density of surface defect sites. As the calcination temperature increases to 500°C, the absorption edge becomes more defined, reflecting improved crystallinity and reduction of defect states within the band structure. For the 600°C sample, the absorption intensity slightly decreases compared to the 500°C sample, which can be attributed to partial grain growth and reduced surface area at higher temperatures.

The position of the absorption edge provides insight into the bandgap energy of the materials. The Bandgap (Eg) values calculated from Tauc plots indicate energies of 3.0744 eV for TiO_2 calcined at 400°C, 3.2022 eV for the 500°C sample, and 3.1481 eV for the 600°C

sample. The slightly lower bandgap at 400°C is associated with amorphous or poorly crystalline TiO_2, where localized defect levels within the bandgap facilitate transitions at lower photon energies. The increase in bandgap at 500°C corresponds to the formation of well-defined anatase crystallites with fewer defect states, resulting in a sharper band edge and higher optical energy gap. The minor decrease in bandgap at 600°C suggests the onset of structural changes, such as initial growth of larger grains, slight reduction of quantum confinement, or early stages of anatase-to-rutile transformation that commonly begins above 600°C.

Overall, the UV–Vis and bandgap analysis confirm that calcination temperature plays a crucial role in tailoring the optical properties of TiO_2 nanoparticles. The 500°C sample exhibits the most desirable optical behaviour, with strong UV absorption, a well-defined absorption edge, and the highest bandgap value—attributes that enhance charge separation efficiency and make this sample particularly suitable for photocatalytic and photovoltaic applications such as DSSCs.

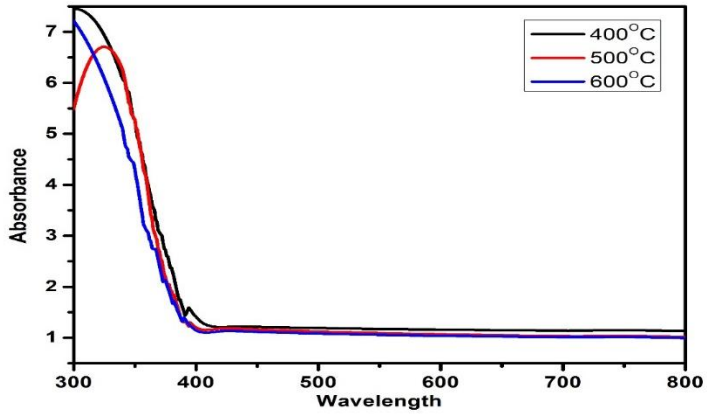

Figure 3: UV–Visible absorption spectra of TiO_2 nanoparticles calcined at 400°C, 500°C, and 600°C

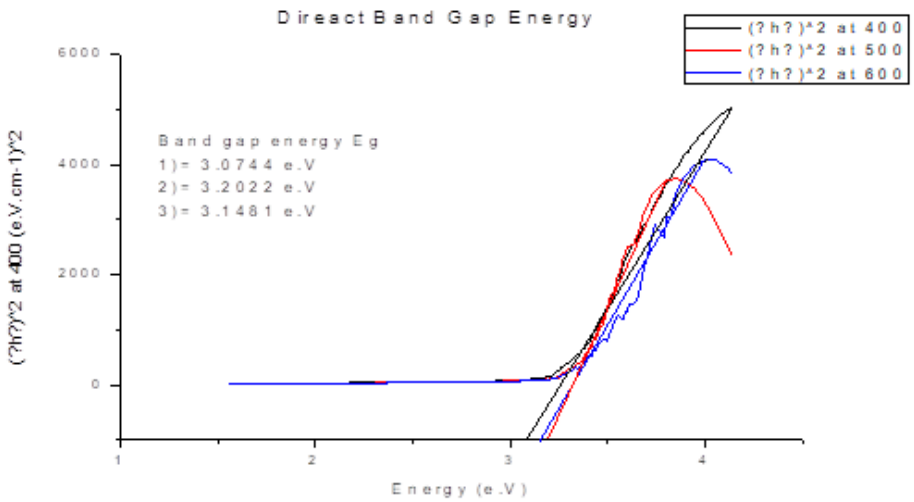

Figure 4: Tauc plots for TiO_2 nanoparticles (400°C, 500°C, 600°C) used for bandgap estimation

3.4 Photovoltaic Performance of DSSCs (Photovoltage Output)

The photovoltage output (mV) under illumination was measured for all DSSC assemblies (with and without electrolyte). The raw results are collated and summarized in Table 1 (reproduced from your data). For clarity, the "with electrolyte" column corresponds to cells where a standard iodide/triiodide electrolyte was present; "without electrolyte" measurements correspond to the same cell geometry but without the redox electrolyte (intended to probe the intrinsic photoresponse of the dye–TiO_2 interface and metal doping effects).

Table 1: Photovoltage output (mV) for bare and metal-doped TiO_2 DSSCs under illumination

Sr. No.	Bare TiO_2 at T°C	Composite of Nano particle with dye	With electrolyte	Without electrolyte	Photovoltage (mV)
1	400	TiO_2 + Plant dye		✓	78.90
2	400	TiO_2 + Plant dye	✓		136.021
3	500	TiO_2 + Plant dye		✓	91.31
4	500	TiO_2 + Plant dye	✓		391.31
5	600	TiO_2 + Plant dye		✓	51.591
6	600	TiO_2 + Plant dye	✓		151.431
7	500	TiO_2 +Ag + Plant dye		✓	500.00
8	500	TiO_2 +Ag + Plant dye	✓		520.00
9	500	TiO_2 +Au + Plant dye		✓	313.01
10	500	TiO_2 +Au + Plant dye	✓		400.13

The photovoltaic response of the fabricated dye-sensitized solar cells (DSSCs) was evaluated by measuring the photovoltage (mV) under illumination for both bare TiO_2, Ag-doped TiO_2, Au-doped TiO_2, and their dye-sensitized photoanodes in the presence and absence of electrolyte. The results clearly show that both calcination temperature and metal doping significantly influence the charge generation and electron transport behaviour of the photoanodes.

For bare TiO_2, the photovoltage values increase when the material is sensitized with plant dye, indicating successful photon absorption by the natural pigment and effective electron injection into the TiO_2 conduction band. Among the bare samples, TiO_2 calcined at 500°C

exhibits the highest photovoltage (391.31 mV with electrolyte), which correlates well with its superior crystallinity and optimized bandgap as observed in UV–Vis and XRD analyses. The improvement from 400°C (136.02 mV) to 500°C reflects enhanced charge transport due to reduced surface defects. However, the photovoltage decreases at 600°C (151.43 mV), suggesting that higher calcination temperatures lead to excessive grain growth and reduction in active surface area, which limits dye adsorption and electron injection.

In contrast, metal-doped TiO_2 photoanodes exhibit a substantial enhancement in photovoltage compared to undoped TiO_2. The Ag-doped TiO_2 sample shows the highest performance, reaching 520.00 mV with electrolyte and 500.00 mV without electrolyte. This enhancement is attributed to the surface plasmon resonance (SPR) effect of Ag nanoparticles, which improves visible-light absorption and facilitates rapid electron transfer by acting as electron sinks. Ag doping also reduces recombination by trapping electrons temporarily and facilitating their movement toward the external circuit.

The Au-doped TiO_2 sample also exhibits improved photovoltage outputs, with 400.13 mV in the presence of electrolyte and 313.01 mV without electrolyte. Although Au enhances the absorption of light through plasmonic behaviour similar to Ag, the slightly lower performance compared to Ag-doping may be due to differences in particle size, dispersion, or charge-transfer dynamics, as observed in previous studies.

The role of electrolyte is also evident across all samples. The presence of the I^-/I_3^- redox couple consistently increases photovoltage output because the electrolyte efficiently regenerates the dye molecules after electron injection and maintains continuous charge flow within the cell.

Overall, the DSSC performance follows the trend: Ag–TiO_2 > Au–TiO_2 > Bare TiO_2 (500°C) > Bare TiO_2 (600°C) > Bare TiO_2 (400°C) This demonstrates that metal doping, particularly with Ag nanoparticles, significantly enhances the photovoltaic behaviour, primarily through plasmonic effects, improved charge separation, and reduced recombination.

Conclusion:

In this study, bare and metal-doped TiO_2 nanoparticles were successfully synthesized using a controlled sol–gel route, and the influence of calcination temperature and noble-metal doping (Ag and Au) on their structural, optical, and photovoltaic performance was systematically investigated. XRD analysis confirmed that all synthesized samples retained the anatase crystalline phase, with increasing calcination temperature leading to sharper and more intense diffraction peaks, indicative of enhanced crystallinity. Ag and Au doping further increased peak

intensity without shifting the anatase reflections, demonstrating that the dopant atoms were incorporated without altering the underlying TiO_2 crystal lattice.

UV–Vis absorption studies revealed strong UV activity for all samples, with the most defined absorption edge and highest bandgap observed for TiO_2 calcined at 500°C, reflecting optimal crystallinity and minimal defect states. Bandgap values (3.07–3.20 eV) showed a clear dependence on calcination temperature, with the 500°C sample displaying the most suitable optical characteristics for photoactive applications. FTIR spectroscopy further supported these findings by confirming the presence of characteristic Ti–O and Ti–O–Ti lattice vibrations, along with a reduction in hydroxyl-related bands at higher calcination temperatures.

The DSSC performance evaluation demonstrated a significant enhancement in photovoltage upon metal doping. Among all samples, Ag–TiO_2 exhibited the highest photovoltage output (520 mV), attributed to its strong plasmonic resonance and efficient electron-trapping capability, which reduce recombination and promote effective charge transport. Au–TiO_2 also improved cell performance compared to undoped TiO_2, although to a lesser extent than Ag. Bare TiO_2 showed optimal performance at 500°C, consistent with its superior crystallinity and bandgap characteristics. The presence of the I^-/I_3^- electrolyte further enhanced photovoltage output by promoting efficient dye regeneration and continuous charge flow within the cell.

Overall, this chapter demonstrates that calcination temperature and noble-metal doping play critical roles in tailoring the structural and electronic properties of TiO_2, directly influencing its suitability for dye-sensitized solar cell applications. Among all investigated materials, Ag-doped TiO_2 synthesized at 500°C exhibited the best synergy of crystallinity, optical activity, and photovoltaic performance, establishing it as a promising candidate for high-efficiency DSSCs. This work provides a comprehensive understanding of how controlled synthesis and targeted modification of TiO_2 can optimize its functionality in solar-energy-conversion technologies.

References:

1. Mahshid, S., Askari, M., & Sasani Ghamsari, M. (2007). Synthesis of TiO_2 nanoparticles by hydrolysis and peptization of titanium isopropoxide solution. *Journal of Materials Processing Technology, 189*(1–3), 296–300. https://doi.org/10.1016/j.jmatprotec.2007.01.040
2. Helen Rathi, V., & Rejo Jeice, A. (2023). Green fabrication of titanium dioxide nanoparticles and their applications in photocatalytic dye degradation and microbial activities. *Chemical Physics Impact, 6*, 100197. https://doi.org/10.1016/j.chphi.2023.100197

3. Singh, R., Ryu, I., Yadav, H. M., Park, J., Jo, J. W., Yim, S., & Lee, J.-J. (2019). Non-hydrolytic sol-gel route to synthesize TiO_2 nanoparticles under ambient condition for highly efficient and stable perovskite solar cells. *Solar Energy*. https://api.semanticscholar.org/CorpusID:155699237
4. Cargnello, M., Gordon, T. R., & Murray, C. B. (2014). Solution-phase synthesis of titanium dioxide nanoparticles and nanocrystals. *Chemical Reviews, 114*(19), 9319–9345. https://doi.org/10.1021/cr500170p
5. Lim, S. P., Pandikumar, A., Huang, N. M., & Lim, H. N. (2014). Enhanced photovoltaic performance of silver@titania plasmonic photoanode in dye-sensitized solar cells. *RSC Advances, 4*, 38111–38118. https://doi.org/10.1039/C4RA05689B
6. Patil, R. S., Sangtani, N., Patil, K., Salunke, R. S., & Uddhage, V. (2023). Facile synthesis of TiO_2 and $Ag@TiO_2$ nanoparticles and its application as a photoanode in dye-sensitized solar cells. *International Research Fellows Association's Research Journal, 333*, 49–60. (e-ISSN: 2348-7143).
7. Raut, N. C., Mathews, T., Palogi, C., Srinivasan, M. P., Dash, S., & Tyagi, A. (2011). Effect of temperature on the growth of TiO_2 thin films synthesized by spray pyrolysis: Structural, compositional and optical properties. *Materials Research Bulletin, 46*, 2057–2063. https://doi.org/10.1016/j.materresbull.2011.06.043
8. Nematov, D. (2024). Titanium dioxide and photocatalysis: A detailed overview of the synthesis, applications, challenges, advances and prospects for sustainable development. *Journal of Modern Green Energy, 3*, 6. https://doi.org/10.53964/jmge.2024006

Innovations and Research in Science and Technology Volume I
(ISBN: 978-93-48620-73-6)

About Editors

Dr. P. Gajalakshmi, M.E., Ph.D., is an Assistant Professor in the Department of Electrical and Electronics Engineering at the University College of Engineering, Tindivanam, a constituent college of Anna University. She obtained her B.E. in Electrical and Electronics Engineering from the University of Madras and completed her M.E. in Power Electronics and Drives from Government College of Technology, Coimbatore. She earned her Ph.D. from Anna University, Chennai, and has 20 years of teaching and research experience. Dr. Gajalakshmi has published more than 15 papers in SCI, Scopus-indexed, UGC, and peer-reviewed journals. Her research interests include power electronics, converters, and FACTS devices, and she is currently working in emerging areas such as IoT and blockchain, contributing to interdisciplinary technological advancements.

Dr. Poonam Panaskar is an Assistant Professor in the Department of Botany at Dapoli Urban Bank Senior Science College, Dapoli. She earned her Ph.D. in Botany from Shivaji University, Kolhapur, in 2017. Her research interests include ethnobotany, pharmacognosy, nutraceutical studies, and pharmacology. Dr. Panaskar has published fourteen research papers in reputed national and international journals. She is the author of two books, editor of three books, and has contributed two book chapters. She also holds three patents and one copyright to her credit, reflecting her innovative work. Additionally, she has served as a member of the Board of Studies (BoS) at Mahaveer Mahavidyalaya, Kolhapur, affiliated with Shivaji University. Dr. Panaskar continues to advance botanical research and academic development through her scholarly contributions.

Dr. R. Elavarasi, M.E., Ph.D., is an Associate Professor in the Department of Electrical and Electronics Engineering at AMET Deemed to be University. She obtained her B.E. in Electrical and Electronics Engineering and M.E. from the University of Madras, Chennai, and her Ph.D. from AMET University, securing the 3rd rank in her M.E. program. With 25 years of teaching and research experience, she has published over 30 papers in SCI, Scopus-indexed, UGC, and peer-reviewed journals. Dr. Elavarasi is a lifetime member of ISTE, IAENG, and SCIEI, and has received a funded project from the Tamil Nadu State Council for Science and Technology. She holds three patent publications and focuses her research on power converters, special machines, and renewable energy sources.

Mrs. N. Priya, M.E., is an Assistant Professor in the Department of Electrical and Electronics Engineering at Easwari Engineering College. She earned her B.E. in Electrical and Electronics Engineering from the University of Madras and her M.E. from Anna University, Chennai, and is currently pursuing her Ph.D. at Anna University. With 20 years of teaching and research experience across reputed institutions, she has published over 25 papers in SCI, Scopus-indexed, UGC, and peer-reviewed journals. Mrs. Priya is a lifetime member of the Indian Society for Technical Education (ISTE) and holds eight patent publications. Her research interests focus on power converters, electric vehicles, renewable energy sources, and artificial intelligence, reflecting her commitment to advancing innovative technologies in electrical engineering.

Bhumi Publishing

ISBN 978-93-48620-73-6
9 789348 620736